2002-11-08

Development and Design of Constant-Force Mechanisms

Brent Lewis Weight
Brigham Young University - Provo

DEVELOPMENT AND DESIGN OF CONSTANT-FORCE MECHANISMS

by

Brent L. Weight

A thesis submitted to the faculty of

Brigham Young University

in partial fulfillment of the requirements for the degree of

Master of Science

Department of Mechanical Engineering

Brigham Young University

December 2001

BRIGHAM YOUNG UNIVERSITY

GRADUATE COMMITTEE APPROVAL

of a thesis submitted by

Brent L. Weight

This thesis has been read by each member of the following graduate committee and by majority vote has been found to be satisfactory.

Date	Larry L. Howell, Chair
Date	Spencer P. Magleby
Date	Mark S. Evans

BRIGHAM YOUNG UNIVERSITY

As chair of the candidate's graduate committee, I have read the thesis of Brent L. Weight in its final form and have found that (1) its format, citations, and bibliographical style are consistent and acceptable and fulfill university and department style requirements; (2) its illustrative materials including figures, tables, and charts are in place; and (3) the final manuscript is satisfactory to the graduate committee and is ready for submission to the university library.

Date

Larry L. Howell
Chair, Graduate Committee

Accepted for the Department

Brent L. Adams
Graduate Coordinator

Accepted for the College

Douglas M. Chabries
Dean, College of Engineering and Technology

ABSTRACT

DEVELOPMENT AND DESIGN OF

CONSTANT-FORCE MECHANISMS

Brent L. Weight

Department of Mechanical Engineering

Master of Science

This thesis adds to the knowledge base of constant-force mechanisms (CFMs). It begins by reviewing past work done in the area of CFMs and then develops new non-dimensionalized parameters that are used to simplify the calculations required to design a CFM. Comparison techniques are then developed that utilize these non-dimensionalized parameters to compare mechanisms based on stiffnesses, percent constant-force, actual lengths, normal displacements, and feasible design orientations. These comparison techniques are then combined with optimization to define new mechanisms with improved performance and range of capabilities. This thesis also outlines a design process, methods to identify mechanisms that are suitable for a given design problem, and relationships and trends between variables. The thesis concludes by discussing the adaptation of CFMs for use in electrical contacts and presenting the results of a design case study which successfully developed a constant-force electrical contact (CFEC).

ACKNOWLEDGEMENTS

This research was supported by funding from the Utah Center of Excellence Program and the National Science Foundation through grant No. DMI-9624574. These foundations are gratefully acknowledged for their help.

I would like to acknowledge the continuous help and support of Dr. Larry Howell. He has dedicated countless hours to training, guiding, and teaching me. His impact on me extends beyond the engineering classroom and laboratory.

I would also like to acknowledge the help of the Mechanical Engineering Faculty and staff. They have been an immense help to me and have always been there. Especially the help of Dr. Spencer Magleby and Dr. Mark Evans for their support and direction with regards to this work.

The help of Christopher Mattson, Dan Carroll, and Ryan Weight in development and testing of the constant-force electrical contact and Cameron Boyle for his efforts in discovering the affects of friction on constant-force mechanisms is appreciated and acknowledged.

Most of all, I would like to thank my wonderful wife. She is truly a pillar of strength in my life. I am thankful for her patience with long, odd hours, for her genuine interest in my research, her playful teasing, and her efforts to motivate me through to the end.

TABLE OF CONTENTS

LIST OF FIGURES

LIST OF TABLES

CHAPTER 1

INTRODUCTION AND BACKGROUND

1.1 Thesis Problem

Many efforts have been made to design systems that produce constant force. Some of these systems use complex control loops and algorithms that result in costly systems or operate only in tension. There still exists the need for inexpensive compression constant-force mechanisms.

Through the effort of others and in correlation with other research projects, compliant constant-force mechanisms have been developed. However, despite the many recent advances in these mechanisms, there is still a lack of understanding of these configurations. This includes their design, their limits, and how to improve their performance. Additionally, there exists new configurations that have yet to be explored. Once a better understanding of constant-force mechanisms has been achieved, there is an opportunity to develop mechanisms for specific applications.

This work attempts to further develop the understanding of compliant constant-force mechanisms. Using the results of prior research efforts as a starting point, this work first seeks to understand compliant constant-force mechanism behavior from both a stress and force viewpoint. This work then examines different ways of comparing constant-force mechanisms and then use these comparison methods to define mechanisms with improved performance. Finally, this work attempts to outline a design method that can be used independent of the pseudo-rigid-body model. In parallel with this theoretical work, an attempt to incorporate constant-force behavior into electrical contacts is made.

Before new work is done on compliant constant-force mechanisms, general background information is given on constant-force mechanisms and compliant mechanisms. Additionally, a literature review in these areas is presented. Next, an entire chapter is devoted to a review of the work on compliant constant-force mechanisms done prior to this research. This includes the behavioral model developed for these mechanisms and other important background information. After the review, the new research of this thesis is presented, after which conclusions and recommendations are given.

1.2 Background

1.2.1 Constant-Force Mechanisms

Constant-force mechanisms (CFMs) can be rigid-body mechanisms with linear and/or torsional springs or they can be compliant mechanisms. In general, they use the principles of mechanical advantage and stored strain energy to produce a near-constant output force over a large range of input displacement. This is accomplished by determining specific geometric ratios that allow for equal increases in stored strain energy and mechanical advantage. In this way, the output remains constant throughout the displacement.

1.2.2 Compliant Mechanisms

A compliant mechanism is one in which the mechanism's motion comes from deflection of one or more of its members. Compliant mechanisms offer several advantages over rigid-body mechanisms. The deflection characteristics of compliant mechanisms allow energy storage directly within a flexible member, eliminating the need for additional energy storage devices (i.e. springs) found in rigid-body mechanisms. The member deflection also allows for the replacement of pin joints with small-length flexural pivots, or living hinges, thereby reducing part count and assembly time. In fact, one of the most significant advantages of compliant mechanisms is their ability to be fabricated from fewer pieces of material providing savings in both production time and manufacturing cost. This increase in performance with lower maintenance makes them better suited for harsh environments. Due to these advantages, compliant mechanisms are replacing many rigid-body mechanisms.

1.2.3 The Pseudo-Rigid-Body Model (PRBM)

The pseudo-rigid-body model is used to help model and design compliant mechanisms. With this design technique, compliant mechanisms can be converted into functionally equivalent, rigid-link mechanisms on which standard kinematics and force-deflection analysis can be performed. Once designed and analyzed, the resulting rigid mechanism can then be easily converted back into a compliant mechanism.

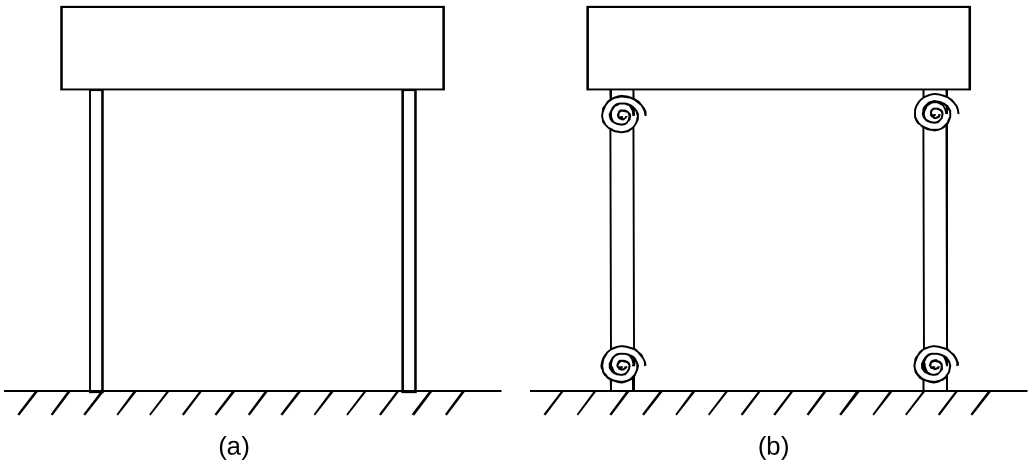

Figure 1.1 (a) A compliant parallel mechanism and (b) its PRBM counter part

The conversion between rigid-body and compliant mechanisms is done by representing compliant members as rigid links with torsional springs at the pin joints to account for the moments at the pin joints due to compliant member deflection. An example of this can be seen in Figure 1.1. The compliant parallel mechanism in Figure 1.1a has the same motion and force characteristics as the rigid mechanism in Figure 1.1b. The PRBM works well for both small and large deflections as well as with a variety of compliant member types (i.e. small length flexural pivots, living hinges, and fixed guided beams). For more information on the pseudo-rigid-body model see Appendix A.

1.3 Literature Review

1.3.1 Constant-Force Systems

For many years, there has been a search for reliable mechanical methods that produce a constant force. The first real success in this endeavor was the development of constant-force tension springs. These springs, also known as “Neg’ator” springs, consist of a coil of flat spring material which has been given a heavy forming operation. When unstressed, the material tends to form a tight coil. These springs exhibit little change in load with deflection (Wahl, 1963). Constant-force tension springs have been around for many years and can be found in many common applications such as inertia reel seat belts, tape measures, and pull starts (Williman, 1995). They have even been used in creating constant-torque spring motors which are capable of producing 50 revolutions on one winding (Wahl, 1963).

Much work has also been given to develop drive units that produce a constant force. These include electrical, hydraulic, and pneumatic systems (Nathan, 1985). Many of these drive systems use complex algorithms and feed-back loops to achieve the desired goal. Bossert et al. (1996) developed a complex algorithm for following unknown surfaces with a robotic arm. As part of the method, the robot kept a constant normal force on the surface. In other work (Chang and Fu, 1997), a complex deburring model was used to produce a drive system that maintained a constant normal force on the workpiece while following a prescribed path. Successful drive systems have been developed and demonstrated.

1.3.2 Constant-Force Mechanisms

Recently, much effort has been made to design mechanisms that produce a constant output force. Nathan (1985) proposed a rigid-link constant-force generator. His work resulted in the creation of a hinged lever that produces a constant unidirectional force for any position. This work was extended resulting in a chain of parallel mechanisms that

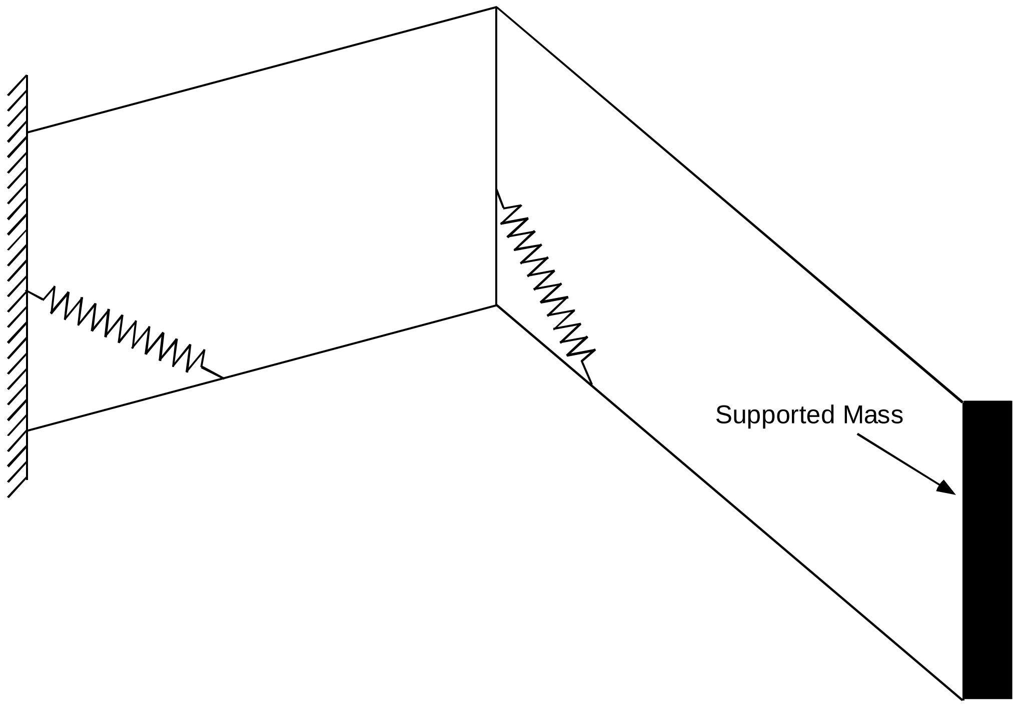

Figure 1.2 Two element chain of constant-force generator mechanisms developed by Nathan (1985)

would support a mass when moved to any position. A diagram of this mechanism can be seen in Figure 1.2. This mechanism can be seen in applications such as desk lamp stands (Nathan, 1985). Jenuwine and Midha (1994) have proposed a rigid-link CFM. This mechanism, as seen in Figure 1.3, uses rigid-links and linear springs to achieve a constant-force and has been successfully implemented in concrete testing equipment.

Compression slider-crank compliant CFMs have been proposed (Murphy et al., 1994, Howell et al., 1994, Midha et al., 1995). Millar et al. (1996) developed non-dimensionalized parameters to facilitate their design and tested several mechanisms. Murphy et al. (1994) used type synthesis on the compression CFM to develop 28 configurations while Howell et al. (1994) performed dimensional synthesis of several of these configurations. Most recently, Evans and Howell (1999) implemented the compliant CFM into a

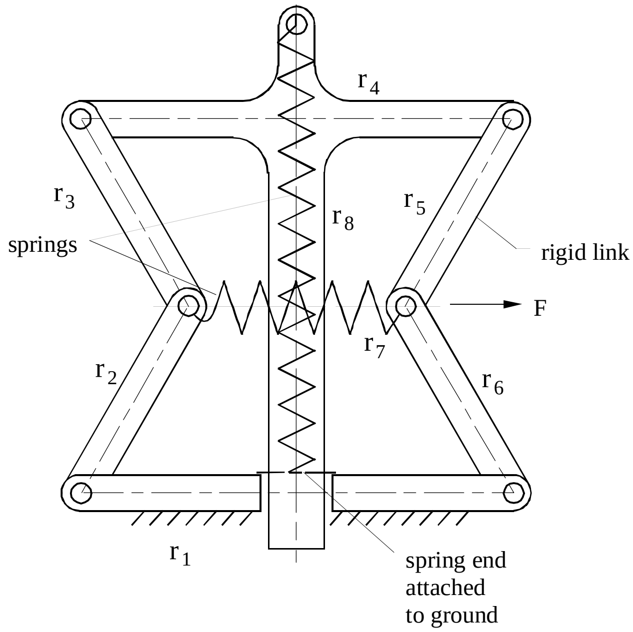

Figure 1.3 Rigid-body CFM developed by Jenuwine and Midha (1994)

robot end-effector that successfully demonstrated constant-force behavior while cutting glass.

Parkinson et al. (1997) used a parametric optimization approach to develop compliant mechanisms. In one study, they examined a fully compliant constant-force mechanism that was developed through optimization techniques.

Herder and Tuijthof (2000), have developed 4 and 6 degrees-of-freedom spatial gravity equilibrators. These mechanisms are similar to the work done by Nathan (1985), who developed the constant-force generator commonly found in desk lamps, but have a larger range of motion. Additionally, Herder and Berg (2000) developed a statically balanced compliant mechanism. This system consisted of a compliant gripper on the output end and a balancing mechanism on the input end. In this fashion, the force required by the user to deflect the gripper is offset by the balance mechanism, and the user only feels the force generated at the output.

Chapter 2 reviews in detail the work done on the compliant slider-crank CFMs. The chapter provides valuable information and a foundation for the proposed research. The notation developed, equations derived, and the optimization problem used are presented and discussed.

1.3.3 Compliant Mechanisms

Compliant mechanisms get their motion and energy from the deflection of their members. The PRBM uses links and springs to model motion and compliance (Howell, 2001).

The PRBM allows for easy design and synthesis of compliant mechanisms. Compliant mechanism synthesis can be divided into rigid-body replacement synthesis and synthesis for compliance. Rigid-body replacement synthesis deals only with the motion and path of the mechanisms, while synthesis for compliance takes into account both the motion and the force/torque characteristics (Howell and Midha, 1996).

To determine the force/torque characteristics, several different methods can be used. Conventional Newtonian methods require free-body diagrams of each link and result in forces for the entire mechanism. A second method, the principle of virtual work, also works well with the PRBM. This method looks at the whole mechanism and accounts easily for the springs (Howell and Midha, 1994).

The PRBM also allows for the determination of the degrees of freedom of a compliant mechanism. While traditional methods predict many compliant mechanisms are structures, consideration must be made for the movement made possible by the compliant sections. Methods have been developed that take this into consideration allowing for accurate calculation of the degrees of freedom (Howell and Midha, 1995).

CHAPTER 2 BEHAVIORAL MODEL DEVELOPMENT AND PREVIOUS RESULTS

Work was done prior to this thesis on the development of a behavioral model for compliant constant-force mechanisms (CFMs). This behavioral model is used extensively in this work and is used as the basis for further development. All other equations developed in this thesis are derived from this behavioral model or the PRBM and thus have the same accuracy as these two models.

This chapter summarizes the derivation of the behavioral model, the extend of its development, and the validity of the model. The following is summarized from Howell (2001) unless otherwise noted.

2.1 Constant-Force Behavioral Model

The compliant constant-force behavioral model is developed from a compliant slider-crank model using the PRBM and the principal of virtual work. Several non-dimensional parameters can be developed and the model simplified. This next section discusses in detail each of these aspects of the behavioral model.

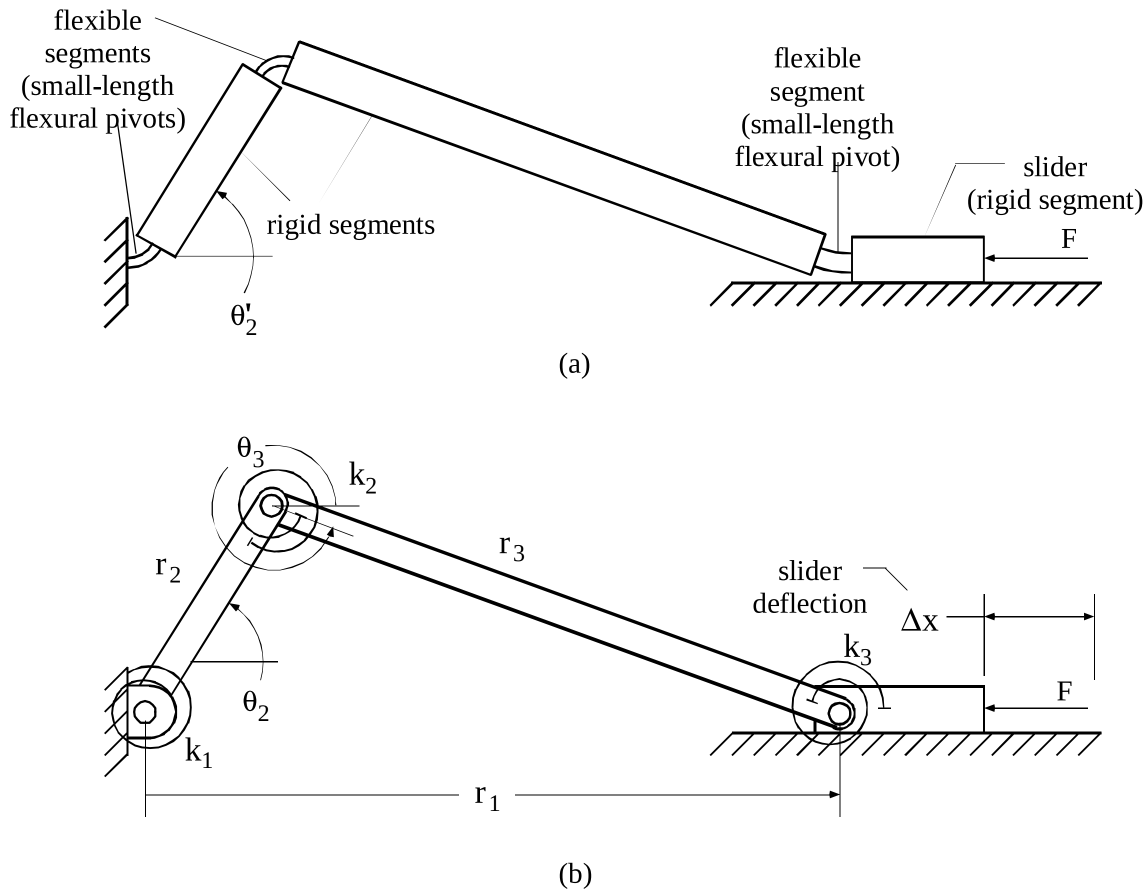

Figure 2.1 Compliant and rigid-body slider crank model and parameters

2.1.1 Slider-Crank Model

The original behavioral model is based upon a simple compliant slider crank mechanism. The PRBM and standard kinematic equations are used to solve for the position of the slider crank given a deflection. The variables used in the equations and the mechanism orientation is shown in Figure 2.1b. The known variables for the problem are r_2, r_3, and Δx. The angles θ_2 and θ_3 and length r_1 can be determined from

$$\theta_2 = \operatorname{acos}\frac{r_1^2 + r_2^2 - r_3^2}{2r_1r_2} \tag{2.1}$$

$$\theta_3 = \operatorname{asin}\frac{-r_2\sin\theta_2}{r_3} \tag{2.2}$$

$$r_1 = r_2\cos\theta_2 + r_3\cos\theta_3 \tag{2.3}$$

These equations allow for all unknown variables to be determined.

Figure 2.1a shows one configuration of the compliant version of the slider crank. The appropriate lengths of the flexible segments can be determined using the PRBM as discussed in Appendix A.

2.1.2 Principle of Virtual Work

The principle of virtual work and the PRBM can be used to determine the static force for a given deflection. It can be assumed that all force references throughout this work refer to the static force unless otherwise noted.

To determine the static force for a given deflection, equations must be developed relating displacement, compliant member deflection, and static input force. Using the principle of virtual work and the PRBM, a fictitious or virtual displacement ($\delta\vec{z}$) can be made from which the virtual work (δW) can be calculated from

$$\delta W = \vec{F} \cdot \delta\vec{z} \tag{2.4}$$

Similarly, virtual work due to a moment can be calculated from

$$\delta W = \vec{M} \cdot \delta\vec{\theta} \tag{2.5}$$

where δW is the virtual work due to the moment, $\vec{M}$, and virtual angular displacement, $\delta\vec{\theta}$. A good equation for conservative forces is found by taking the derivative of potential energy, (V), with respect to the generalized coordinate, (q). This results in

$$\delta W = -\frac{dV}{dq}\delta q \tag{2.6}$$

Summing the virtual works in Equation (2.4) to Equation (2.6) results in

$$\delta W = \sum_i \vec{F}_i \cdot \delta\vec{z}_i + \sum_j \vec{M}_j \cdot \delta\vec{\theta}_j - \sum \frac{dV_k}{dq_k}\delta q_k \tag{2.7}$$

Having established equations for virtual work, the principle of virtual work can be applied. The principle of virtual work can be stated as (Paul, 1979):

> The net virtual work of all active forces is zero if and only if an ideal mechanical system is in equilibrium.

This principle allows equation (2.7) to be set equal to zero. If all virtual displacements are written in terms of the generalized coordinate, equation (2.7) reduces to

$$\left(\sum_i \vec{F}_i \cdot A + \sum_j \vec{M}_j \cdot B - \sum_k \frac{dV_k}{dq_k}\right)(\delta q_k) = 0 \tag{2.8}$$

where A and B are vectors that change the linear and angular displacements into terms of the generalized coordinate. If δq_k is assumed to be zero (hence the fictitious displacement), then the remaining equation can be solved for the unknown force or moment.

The method of virtual work was applied to the slider crank. The variable θ_2 was chosen to be the generalized coordinate. Equations for the virtual work associated with each torsional spring were developed. A fourth equation was developed relating an unknown static input force applied to the slider in the horizontal direction. These equations were summed, and the principle of virtual work was applied. The force, F, was solved for resulting in

$$F = \frac{r_3 \cos\theta_3[k_1\theta_2 + k_2(2\pi + \theta_2 - \theta_3)] + r_2 \cos\theta_2[k_2(2\pi + \theta_2 - \theta_3) + k_3(2\pi - \theta_3)]}{r_2 r_3(\sin\theta_2 \cos\theta_3 - \sin\theta_3 \cos\theta_2)} \tag{2.9}$$

This equation tells how the force, F, is related to the link lengths, spring constants, and angles of the mechanism as defined in Figure 2.1b.

2.1.3 Non-Dimmensionalization

Inspection of the model shows that it relies on many independent variables. It is beneficial to generalize the model to simplify its use. One method to do this is to try and remove all the independent variables replacing them with dimensionless parameters. In the complimentary work done by Millar et al. (1996), three non-dimensionalized parameters were chosen. They were

$$R = \frac{r_3}{r_2} \tag{2.10}$$

$$K_1 = \frac{k_2}{k_1} \tag{2.11}$$

$$_2 = \frac{K_3}{k_1} \tag{2.12}$$

These parameters where substituted into equation (2.9). Furthermore, the trigonometric identity $\sin(\alpha - \beta) = \sin\alpha\cos\beta - \cos\alpha\sin\beta$ was used to simplify the denominator of equation (2.9). This results in

$$F = \frac{k_1}{r_2}\Phi \tag{2.13}$$

where

$$\Phi = \frac{(R\cos\theta_3[\theta_2 + K_1(2\pi + \theta_2 - \theta_3)] + \cos\theta_2[K_1(2\pi + \theta_2 - \theta_3) + K_2(2\pi - \theta_3)])}{R\sin(\theta_2 - \theta_3)} \tag{2.14}$$

Close examination shows that equation (2.14) is dimensionless. Therefore, F depends only on the non-dimensional parameter Φ and the spring constant k_1 and link length r_2. The spring constant is considered to be the stiffness parameter, while the link length is known as the geometric parameter. Thus, the creation of non-dimmensionalized parameters reduces the number of independent variables in the model, making the model easier to use.

2.2 Type Synthesis

Murphy et al. (1994) performed type synthesis on the slider-crank model. This work resulted in the development of 28 configurations for the CFM. The 28 configurations consist of different arrangements of pin joints and flexible segments. These 28 configurations were reduced to 15 viable configurations and are divided into 5 classifications based

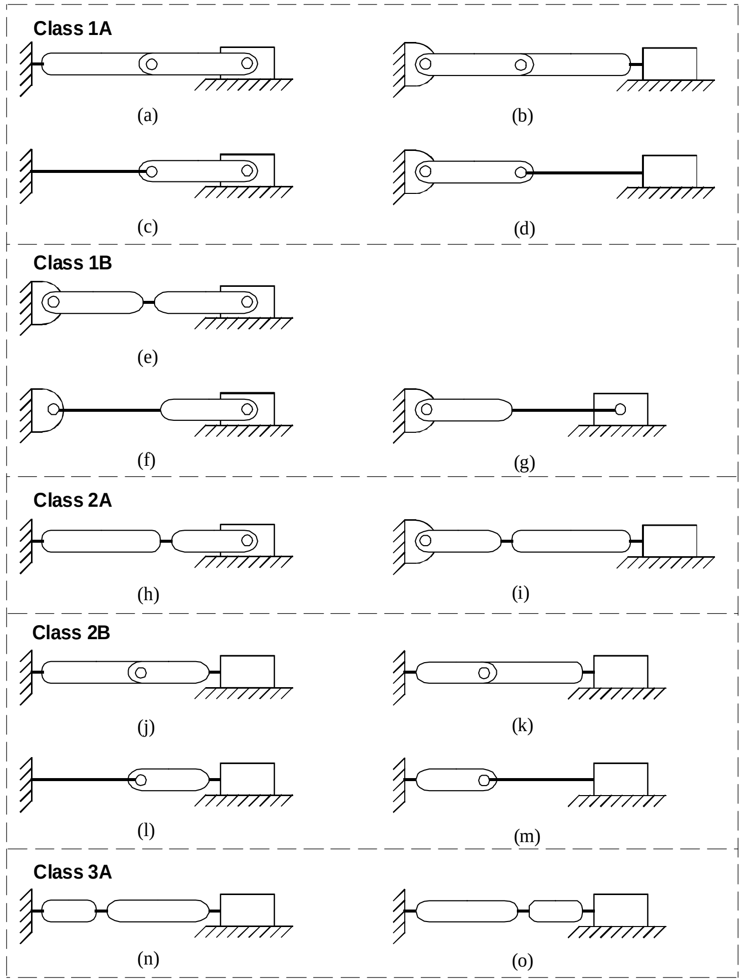

Figure 2.2 Fifteen original configurations

on the number of flexible segments and their location in each configuration. These classifications and configurations can be seen in Figure 2.2.

2.3 Original Optimization Problem

The objective of the original project was to find combinations of the non-dimmenionalized parameters that allow the slider-crank mechanism to experience a constant-force over the entire displacement. To determine these combinations of parameters, an optimization problem must be established and solved.

2.3.1 Displacement Vector

To perform the optimization, a vector $\vec{r}_1$ such that

$$\vec{r}_1 = (r_2 + r_3) - \Delta\vec{x} \tag{2.15}$$

where

$$0 \le \Delta x < \frac{d}{100}(r_2 + r_3) \tag{2.16}$$

was created where d is the deflection parameter and the vector Δx contains 50 points (an arbitrary number). For example, if the mechanism is 10 inches long and d is 40, then the total Δx would be 4 inches. Originally, two deflection parameters, d, were chosen, 16 (16%) and 40 (40%) deflection.

The vector $\vec{r}_1$ was then used to calculate the angles θ_2 and θ_3 for the 50 positions using equations (2.1) and (2.2). Subsequently, these values were then used to calculate the force from equation (2.13). The result of this process is a force vector, $\vec{F}$ which corresponds to the vector $\vec{r}_1$.

2.3.2 Objective Function

An objective function was needed for the optimization routine. This was accomplished by developing a parameter Ξ such that

$$\Xi = \frac{max(\vec{F})}{min(\vec{F})} \tag{2.17}$$

This parameter shows how constant the static force is for the mechanism throughout the slider displacement. As defined, a perfectly constant-force mechanism would have a level of constant-force equal to 1. Due to the definition in (2.17), Ξ is always greater than or equal to 1. Therefore, the optimization objective can be stated

$$\text{Minimize } \Xi \tag{2.18}$$

2.3.3 Other Variables

The design variables for this problem vary depending upon the configuration. The design variables are taken from the non-dimensionalized parameters R, K_1, and K_2. The parameter R is always included as a design variable while K_1 and K_2 are added when there is a k_2 and k_3 respectively. The analysis variables are the displacement vectors, k_1, r_2, and the angles θ_2 and θ_3.

2.4 Original Results

Each of the five classes of configuration found in Figure 2.2 were run through the optimization code to find ideal values for the parameters R, K_1, and K_2. The values for K_1 and K_2 were set to zero for configurations in which pin joints were present at the respective joints. The results of the original work are summarized in Table 2.1

This table shows that a set of viable non-dimensionalized parameters were found for all 5 CFM classifications with deflections (d) of both 16 and 40. These configurations have a percent constant-force close to one. However, these solutions are not the only set of unique solutions to the problems, but represent what was felt to be the best combinations that provided the minimum Ξ value.

2.5 Model Verification

The validity of the behavioral model was verified through prototyping and testing of mechanisms from each of the classes of CFMs. Millar et al. (1996) describe some of these tests and their results. Mechanisms from different classifications were prototyped from various materials and tested using a compression testing machine. The mechanisms displayed a constant output force for a large range of deflection. However, it was noted that the initial deflection of the mechanism resulted in a large force spike. This was attributed to internal friction (for partially compliant mechanisms) and polymer re-alignment. However, after the initial deflection, the results were very reliable.

.

Table 2.1 Original results

Class	d	R	K_1	K_2	Ξ	Φ
1A	16	0.8274	-	-	1.0030	0.4537
	40	0.8853	-	-	1.0241	0.4773
1B	16	1.0000	1.0000	-	1.0564	2.0563
	40	1.0000	1.0000	-	1.1576	2.1513
2A	16	0.3945	0.1906	-	1.0015	0.9575
	40	0.4323	0.2237	-	1.0058	1.0466
2B	16	0.7591	-	0.1208	1.0029	0.5230
	40	0.8441	-	0.1208	1.0235	0.5438
3A	16	2.6633	1.0000	12.6704	1.0002	3.4016
	40	2.0821	1.0000	9.3816	1.0049	3.6286

2.6 Model Exceptions

Close examination of previous work reveals some exceptions and alterations to the behavioral model. These exceptions are important to the general understanding of past work and will be re-examined in future work. For this purpose, they are briefly explained at this point.

2.6.1 Eccentricity

Close examination of the slider-crank in Figure 2.1 on page 12 reveals that when the model is fully extended, the mechanism is horizontal. This shows that eccentricity, or an offset from the slider in the vertical direction, is omitted. In fact, eccentricity is omitted from all equations in the behavioral model.

2.6.2 Class 1B Mechanisms

The PRBM of the class 1B mechanism consists of a torsional spring in the center of the mechanisms with pin joints on either side. This requires that k_1 equal 0. However, according to equation (2.13), this results in F equal to 0 while K_1 and K_2 would go to infinity. To solve this problem, K_1 is set equal to 1, which allows k_1 to equal k_2. Since k_3 equals 0, K_2 becomes 0. However, as a result of k_1 not being equal to zero, Equation (2.14) must be modified to

$$\Phi' = \frac{(R\cos\theta_3[K_1(2\pi+\theta_2-\theta_3)] + \cos\theta_2[K_1(2\pi+\theta_2-\theta_3)+K_2(2\pi-\theta_3)])}{R\sin(\theta_2-\theta_3)} \tag{2.19}$$

It should be noted that Equation (2.19) is used exclusively with the Class 1B mechanisms. With these modifications, the force equation becomes

$$F_{in} = \frac{k_2}{r_2}\Phi' \tag{2.20}$$

This configuration was then run through the optimization routine and the results can be found in Table 2.1.

2.7 Outstanding Issues

The work summarized above develops several non-dimmensionalized equations and a classification system for CFMs. Although these equations and classification system work, there are several challenges to using them in the exploration and design of CFMs.

First, the equations developed rely heavily upon the PRBM making the design of CFMs difficult for engineers with little experience with the PRBM. Additionally, although the equations are non-dimensionalized, they require that a full model be developed for each configuration to determine the stresses in the flexible segments and the mechanism output force.

Second, the classification system developed identifies only large groups of mechanisms and provides no way of identifying smaller groups of mechanisms or specific mechanisms.

Third, the prior work used only one method for comparing mechanisms, the parameter Ξ. No attempt was made to determine other methods of comparison or other areas in which improved performance could be achieved.

Finally, a methodical approach to design was not developed. The basic design steps and issues are not discussed and the advantages and disadvantages of each configuration of mechanisms are not known, making the selection of an appropriate configuration for a given application difficult. The following chapters address these issues.

CHAPTER 3

CLASSIFICATION REFINEMENT

To improve the performance of CFMs and better understand how to design them, it becomes necessary to look more closely at specific mechanisms. This will allow for comparison and differentiation between the mechanisms, and eventually lead to an ability to design CFMs for a wide variety of situations.

The original classification system, presented in Section 2.2, does not differentiate between specific, single mechanisms. For this reason, the rest of this chapter is devoted to the presentation of a refined classification system based upon the original system. With this refined classification, groups of mechanisms or individual mechanism can be referred to quickly and easily.

3.1 Original Classification

The original classification system developed by Millar et al., 1996, is first presented in Section 2.2. The system, seen in Figure 3.1, is based first upon the number of

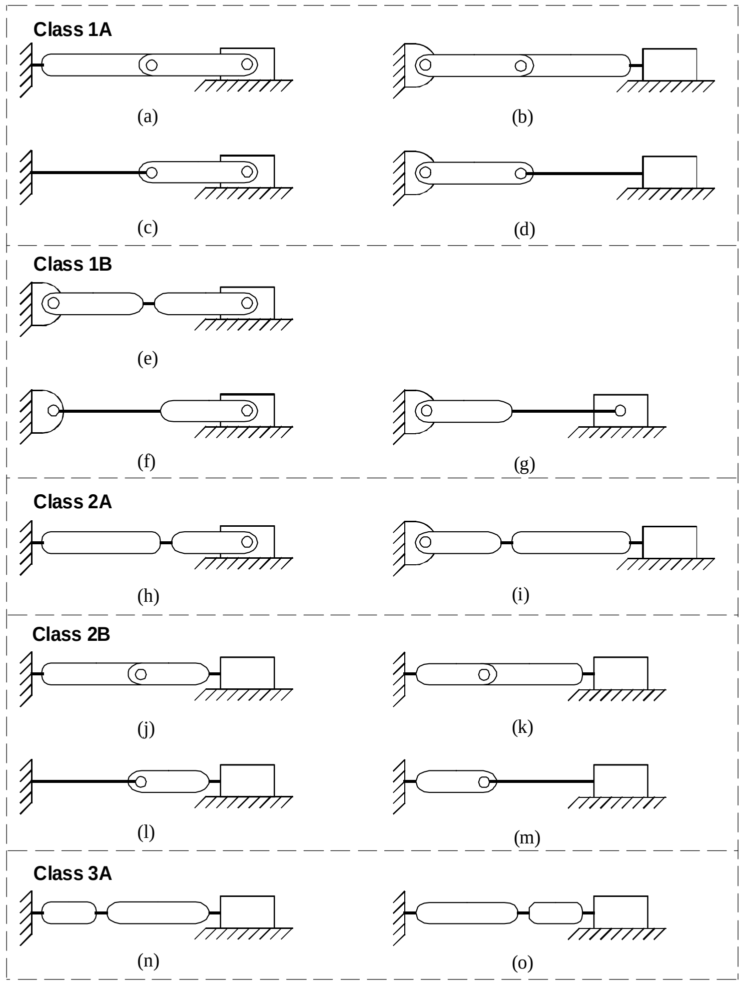

Figure 3.1 Fifteen original configurations

flexible members in each mechanism, and then upon the arrangements of those flexible segments. It can be seen that mechanisms that have one flexible segment located at the first pivot fall into Class 1A while mechanisms with three flexible segments fall into Class 3A. Additionally, specific constant-force parameters (R, K_1, K_2, Φ, and Ξ) are associated with each class of mechanism. These parameters are valid for every mechanism in that class.

Therefore, the original classification refers not only to the physical arrangement of flexible segments and pin-joints, but also to the specific parameter set.

3.2 Classification Refinement

The original classification system is simple and easy to use. Therefore, the new system simply adds a method to distinguish between mechanisms within a class that have the same pseudo-rigid-body model (PRBM) but have different constant-force parameters and/or flexible segment types. This refinement allows for various levels of classification. Each level corresponds to various sets of parameters and groups of mechanisms. At the most refined level, a specific mechanism can be identified along with a specific set of parameters associated with it.

3.2.1 Flexible Segment Configuration

The first refinement to the original classification system is a method to distinguish between possible flexible segment configurations within each class. This configuration is denoted by a string of letters representing the order and type of pivots used. The letter "*s*" will be used for small-length flexural pivots, the letter "*l*" will be used for long flexible segments, and the letter "*p*" will be used for pin joints. Figure 3.2 shows the refined classification system using the original classes. For each mechanism, a flexible segment configuration has been added and can be seen under the corresponding mechanism.

When writing the classification, the configuration is added after the class. For example, a Class 2A-*ssp* is a mechanism that has two small-length flexural pivots located at the first and second pivot points, and a pin joint at the third pivot point. A Class 1A-*lpp* is a mechanism that has a single fixed-pinned beam at the first pivot, and pin joints at the

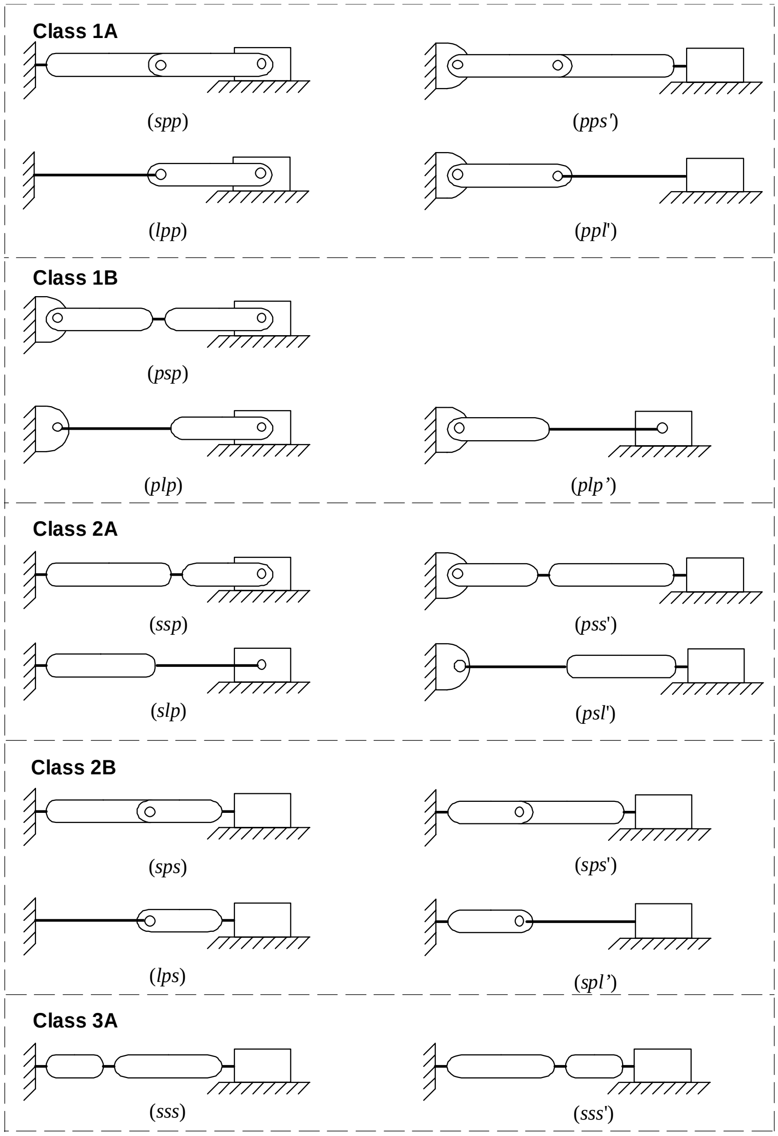

Figure 3.2 Refined classification system which identifies flexible segment configurations

last two pivots. However, notice that the specific set of parameters to be used with the mechanisms has not yet been identified.

3.2.2 Sub-Classes

Sub-classes will be used to distinguish between different sets of constant-force parameters within a given class and configuration. Each sub-class within a given class will have the same PRBM, but will lead to different CFMs. These new sub-classes will be denoted using a string of lower case letters and numbers. The first letter will denote the maximum percent deflection for which the sub-class was designed. The other letters and numbers will be explained later in this work as other parameters are developed and new mechanisms are defined.

The original work performed actually resulted in different sub-classes even though they were not thought of in this manner. These sub-classes were distinguished by the percentage of deflection for which they worked. They are commonly referred to as 16% and 40% deflection mechanisms. In the new classification system, these sub-classes will be distinguished as sub-class “a” for the 16% deflection mechanisms and sub-class “b” for the 40% deflection mechanisms.

When specifying a specific sub-class, the identifying string of letters and numbers is added after the configuration. For example, if a new Class 2B-*lps* mechanism is defined with a maximum deflection of 25% and a unique set of parameters, then the new classification will be Class 2B-*lps*-c.

3.2.3 Classification Summary

A classification consists of a mechanism class, configuration, and sub-class. Each class refers to a group of mechanisms that share a common PRBM, each configuration refers to a mechanism with specific flexible segment types, and each sub-class identifies a specific set of parameters. The naming scheme is summarized in Figure 3.3.

A configuration contains all of the following:

3A-*sss*-b

Level	Class	Configuration	Sub-Class
Common Elements	PRBM	Flexible Segments	Parameters
Applicable	Group of Mechanisms	Family of Mechanisms	Specific Mechanism

Figure 3.3 Summary of classification scheme

3.2.4 Mechanism Inversions

In some cases, mechanisms are simply inversions of other mechanisms. The slider is fixed, while the fixed end is allowed to slide. These mechanisms are easily accounted for. In Figure 3.2, these inversions are shown next to their counterparts and have the same flexible segment arrangement followed by a prime. It should be noted that all parameter values that have been given are valid for both mechanisms. It is only necessary to apply the nomenclature in the same way in either instance. For example, in a 1A-*spp*, the link length r_2 is always associated with the link with the flexible segment and k_1 is always associated with the flexible segment regardless of which end of the mechanism is grounded.

CHAPTER 4 STRESS AND FORCE FEASIBILITIES

To overcome the challenges associated with CFM design and analysis, it is desirable to develop a method that would allow for the quick and simple determination of the stress and force feasibility for a particular application. This would greatly reduce the amount of work required to determine which, if any, of the CFM configurations is viable for a given application. Additionally, a method is needed that will be simple to use and require only a limited understanding of the PRBM. Finally, the new method should aid in the comparison of different configurations revealing strengths and weaknesses of each.

This chapter adds to the work presented in Chapter 2. It begins by deriving several new parameters which can be used to help analyze the stress and force feasibilities. These derivations and design techniques are based upon the pseudo-rigid-body model and the behavioral model. The steps to the derivation are outlined, the end parameters are defined and further developed, and parameter values are summarized for the sub-classes and configurations of the original results as presented in Chapter 2. The derivations and results are then followed up with examples that show how the derivation works and its usefulness.

The parameters and methods established in this chapter will be used later in this work to make comparisons between different configurations, helping to develop a better understanding of their strengths and weaknesses. Additionally, values for the parameters developed in this chapter will be summarized and tabulated for new configurations developed as part of this work.

4.1 Stress Feasibility

4.1.1 Stress Derivation

To analyze the stresses in the CFMs, it is necessary to first look at the stress in one of the links of the mechanisms. The critical stress, σ_c, in a flexible beam under bending can be determined from

$$\sigma_c = \frac{Mc}{I} \tag{4.1}$$

where M is the bending moment in the flexible segment, c is the distance from the neutral plane to the top/bottom plane, and I is the moment of inertia of the cross section of the flexible segment. Using the pseudo-rigid-body model, the bending moment M is found to be

$$M = K\Delta\theta \tag{4.2}$$

where K is the PRBM spring constant and $\Delta\theta$ is the actual angle of deflection of the beam. The values for $\Delta\theta$ for each pivot in the slider-crank are defined in Figure 4.1.

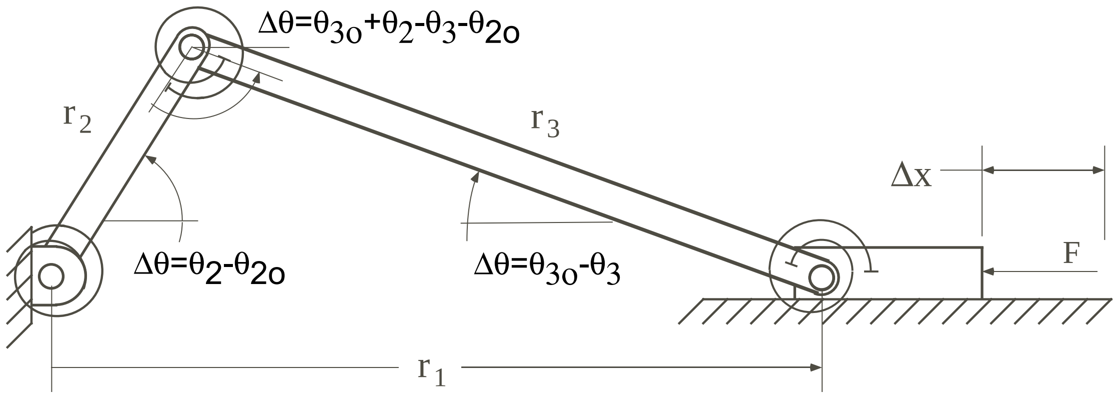

Figure 4.1 Values of Δθ for each pivot point

The general spring constant K is

$$K = \gamma K_{\theta} \frac{EI}{l} \tag{4.3}$$

where γ is the PRBM characteristic radius factor, K_{θ} is the stiffness coefficient, E is the material's modulus of elasticity, I is the moment of inertia, and l is the length of the flexible segment.

Constant-force mechanism configurations use two different types of flexible segments, small-length flexural pivots, and fixed-pinned beams. There are some assumptions associated with each of these flexible beams.

For fixed-pinned beams, the assumptions are:

1. The length of the flexible segment, l, is

$$l = \frac{r_i}{\gamma} \tag{4.4}$$

where γ is the PRBM characteristic radius factor and r_i is an effective link length associated with the flexible segment. For fixed-pinned beams, r_i can be either r_2 or r_3.

2. γ is typically assumed to be 0.85.

3. K_θ is approximated as 2.65

For small-length flexural pivots, the following assumptions are made:

1. The flexural pivot length (l) is much smaller than the corresponding PRBM link length. Mathematically,

$$l = \mu r_i \tag{4.5}$$

where μ is the ratio of l over r_i and r_i will be either one of the two PRBM link lengths, or an average link length, r_{ave}, defined below.

2. Commonly, the value for μ is 0.10. This value will be used unless stated otherwise.

3. The values for K_θ and γ in Equation (4.3) are 1. This is consistent with the PRBM.

4. The link length r_i used for k_2 (middle pivot) is taken to be the average (r_{ave}) of r_2 and r_3. Thus, r_i used to find l in Equation (4.5) for k_2 is

$$r_i = r_{ave} = \frac{r_2 + r_3}{2} \tag{4.6}$$

Equations (4.4) and (4.5) can be generalized to

$$l = \rho r \tag{4.7}$$

where ρ is either $\frac{1}{\gamma}$ for fixed-pinned beams or μ for small-length flexural pivots.

Furthermore, the link length or average link length, r_i, depends upon the configuration of the mechanism. With this in mind, a new parameter, ζ, can be developed where

$$\zeta = \frac{r_{tot}}{r_i} \tag{4.8}$$

and

$$r_{tot} = r_2 + r_3 \tag{4.9}$$

This new parameter defines the ratio between the total PRBM length r_{tot} of the CFM and the link length of interest. The values for ζ for the different link lengths encountered in a CFM are:

$$r_2 \ldots \quad \zeta = R + 1 \tag{4.10}$$

$$\mathrm{r}_3 \ldots \quad \zeta = \frac{1}{R} + 1 \tag{4.11}$$

$$r_{ave} \ldots \zeta = 2 \tag{4.12}$$

Rearranging Equation (4.8) and substituting Equations (4.2), (4.3), (4.7), and (4.8) into equation (4.1) yields

$$\sigma_c = \frac{\gamma \zeta K_\theta E \Delta\theta c}{\rho r_{tot}} \tag{4.13}$$

Equation (4.13) gives the stress in a flexible beam according to the PRBM. The values for γ, K_θ, and ρ depend upon the assumptions for each type of flexible beam used, ζ depends on the configuration, E depends on the material selected, $\Delta\theta$ is based upon the deflection and the sub-class as defined in Figure 4.1, and c and r_{tot} depend on the geometry of the flexible segment.

The stress can be related to the safety factor, *SF*, and the yield strength, S_y, as

$$\sigma_c \cdot SF = S_y \tag{4.14}$$

Substituting equation (4.13) into equation (4.14) and rearranging, results in

$$\frac{\gamma\zeta K_\theta \Delta\theta c}{\rho r_{tot}} = \frac{S_y}{E} \cdot \frac{1}{SF} \tag{4.15}$$

Equation (4.15) can then be separated into a non-dimensionalized stress factor, α, a geometric parameter, A, and a material parameter, Ω, where

$$\alpha = \frac{\gamma\zeta K_\theta \Delta\theta}{\rho} \tag{4.16}$$

$$A = \frac{c}{r_{tot}} \tag{4.17}$$

$$\Omega = \frac{S_y}{E} \tag{4.18}$$

and equation (4.15) becomes

$$\alpha A = \frac{\Omega}{SF} \tag{4.19}$$

The parameter α is determined by the configuration and sub-class, A is based upon the geometry, Ω is determined by the material, and *SF* is a design parameter. The following section will develop and refine these parameters so that they are easy to use.

4.1.2 Stress Parameters Development

Inspection of the parameter α, or *stress parameter*, shows that it is a direct measure of the stress in the specified flexible segment at a given deflection. It is dependent upon the type of flexible segment, the amount of deflection, and the constant-force parameter *R*. The actual size and material of the flexible segment have no affect on this parameter.

Using Equation (4.16) and the assumptions for each flexible segment as stated in Section 4.1.1, for a small-length flexural pivot,

$$\alpha = 10\zeta\Delta\theta \tag{4.20}$$

while for a fixed-pinned beam, the parameter α is

$$\alpha = 1.91\zeta\Delta\theta \tag{4.21}$$

Equations (4.20) and (4.21) show that small-length flexible pivots have an α approximately 5 times larger than fixed-pinned beams if $\zeta\Delta\theta$ is held constant. According to the relationship defined in equation (4.19), small-length flexural pivots are much higher in stress than long flexible segments. This is consistent with what would be expected.

The change in angular deflection, $\Delta\theta$, in equation (4.16) does not depend upon the flexible segment type. It depends on the mechanism displacement and the parameter R.

The second parameter, A, is a geometric parameter. This parameter depends upon the distance c, and the PRBM length of the mechanism.

In determining the stress feasibility of a mechanism, it is necessary to look only at the flexible segment that has the highest stress, or the *primary pivot*. Table 4.1 shows the primary pivot for each configuration. This table holds true provided the inequality

$$c_o \le C c_p \tag{4.22}$$

remains true where c_p is the value for c for the primary pivot, c_o is the value(s) for the other flexible segment in the mechanism, and C is a parameter that is mechanism dependent. In the case of the fully compliant mechanism (*sss* configuration), two C values are given. The first one is for the second pivot, the second value is for the third pivot.

As an example, take a Class 2A-*ssp*-a mechanism. The second flexible segment has the highest stress and therefore, the c value for this flexible segment is c_p. Addition-

Table 4.1 Primary pivot and parameter C for each configuration

Configuration	Primary Pivot	C sub-class a	C sub-class b
Class 1A-*spp*	1	-	-
Class 1A-*lpp*	1	-	-
Class 1B-*psp*	2	-	-
Class 1B-*plp*	2	-	-
Class 2A-*ssp*	2	5.090	4.647
Class 2A-*slp*	2	1.721	1.474
Class 2B-*sps*	3	1.739	1.405
Class 2B-*lps*	3	9.081	7.339
Class 3A-*sss*	1	1.384 8.258	1.043 4.359

ally, the c value for the first flexible pivot is c_o. If c_p is 0.2, then c_o must satisfy Equation (4.22). Therefore,

$$c_o < 1.739 c_p \tag{4.23}$$

or

$$c_o < 0.3478 \tag{4.24}$$

Equation (4.24) indicates that if c_o becomes larger than this value, then the flexible segment with the highest stress changes and a new value for α must be calculated. Values for C for each configuration and sub-class can also be found in Table 4.1.

Once the primary pivot has been identified, α can be calculated for each classification for a percent deflection, d. Figure 4.2 shows a graph of α vs. d for the 1A-*spp*-a mechanism. Additionally, the curve has been fitted with a power function. This allows α to be quickly calculated using

$$\alpha = M d^n \tag{4.25}$$

where M is the multiplier of the power function and n is the exponent.

This procedure was repeated for all of the configurations in both sub-classes and similar functions were determined. The values for the parameters M and n in the α power function for each configuration and sub-class are listed in Table 4.2. This table also restates the information from Table 4.1. From this table, a value for α can be quickly calculated for each classification at any displacement. It should be remembered that the val-

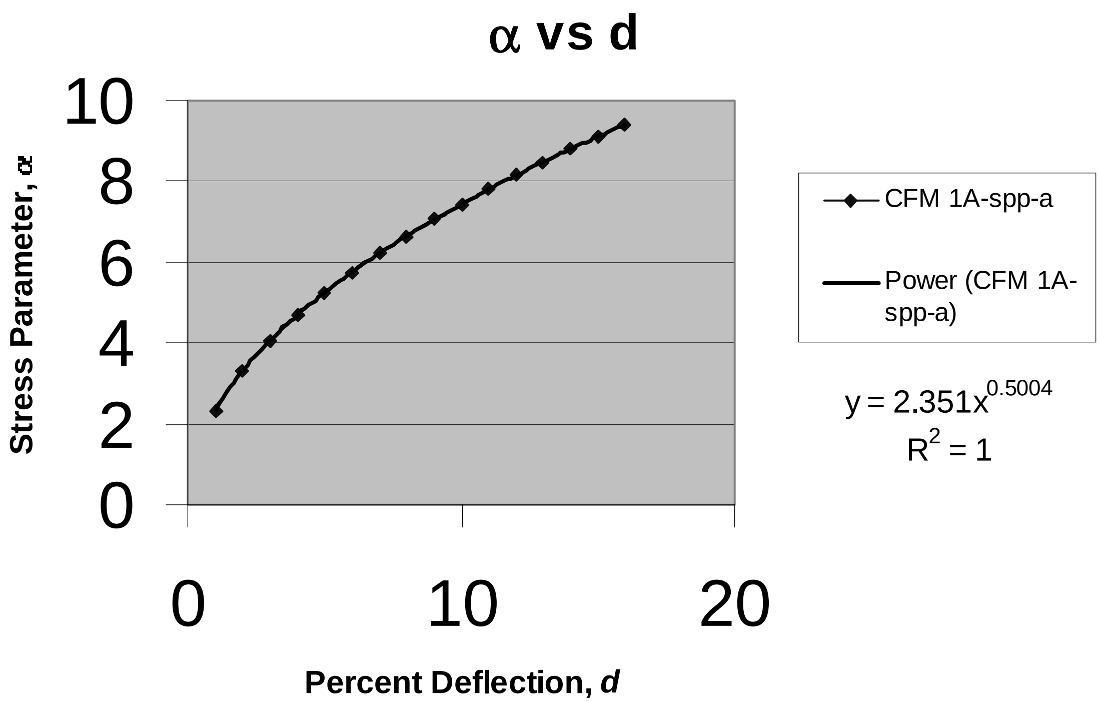

Figure 4.2 Graph of α vs. *d* for Class 1A-*spp*-a

ues for α are good for all deflection percentages, d, up to the maximum percent deflection of the sub-class. The α value, along with other known parameters, can then be used with Equations (4.17) to (4.19) to validate the stress feasibility of a design given cer-

Table 4.2 Power function values for all classifications

Configuration	Primary Pivot	Sub-class a: *C*	Sub-class a: *M*	Sub-class a: *n*	Sub-class a: α_{max}	Sub-class b: *C*	Sub-class b: *M*	Sub-class b: *n*	Sub-class b: α_{max}
Class 1A-*spp*	1	-	2.351	0.500	9.414	-	2.504	0.503	16.004
Class 1A-*lpp*	1	-	0.450	0.500	1.802	-	0.479	0.503	3.065
Class 1B-*psp*	2	-	5.645	0.505	22.889	-	5.588	0.511	36.806
Class 1B-*pl p*	2	-	1.081	0.505	4.382	-	1.070	0.511	7.047
Class 2A-*ssp*	2	5.090	6.250	0.510	25.718	4.647	5.984	0.524	41.352
Class 2A-*slp*	2	1.721	2.113	0.510	8.692	1.474	1.898	0.524	13.116
Class 2B-*sps*	3	1.739	3.743	0.511	15.420	1.405	3.280	0.521	22.422
Class 2B-*lps*	3	9.081	3.743	0.511	15.420	7.339	3.280	0.521	22.422
Class 3A-*sss*	1	1.384 8.258	8.356	0.525	35.784	1.043 4.359	5.892	0.553	45.280

tain parameters. The next section demonstrates the usefulness and practicality of this method.

4.1.3 Stress Feasibility Example

Suppose that a CFM is needed in an application where the overall PRBM length can not be larger than 5 inches and a deflection of 0.6 inches is needed. The mechanism is to be made with a single rectangular cross section ($c = h/2$) under the constraints that $h \geq 0.001$ inches. The mechanism must use the Class 2B-*lps*-a configuration, and must be made from either 1010 Steel ($Sy/E = 0.00087$) or Beryllium Copper ($Sy/E = 0.0092$). Assume $SF = 1.5$. Using the information in Table 4.2, determine if the mechanism is feasible from a stress stand point.

This problem calls for the use of the Class 2B-*lps*-a mechanism. This mechanism consists of a long flexible beam at the first pivot, a pin joint at the second, and a small-length flexural pivot at the third. Table 4.2 indicates that the third pivot has the highest stress. To solve this problem, it is necessary to determine the value of the parameter α. First, the percent deflection or *d* of the problem is determined. This is done by dividing the desired displacement by the overall length and multiplying by 100, or

$$d = \frac{0.6}{5}(100) = 12 \tag{4.26}$$

Therefore, the percent deflection or d for this problem is 12. From Table 4.2, M and n are found to be

$$M = 3.743 \tag{4.27}$$

$$n = 0.511 \tag{4.28}$$

The parameter α can be calculated using equation (4.25) and is

$$\alpha = 3.743(12^{0.511}) = 13.31 \tag{4.29}$$

Using the value of $c = h/2$ for a rectangular cross section, the maximum thickness, h_{max}, can be calculated by combining and rearranging Equations (4.17) and (4.19)

$$h_{max} < \frac{2\Omega r_{tot}}{\alpha SF} \tag{4.30}$$

For 1010 Steel, Equation (4.30) becomes

$$h_{max} < \frac{2(0.00087)5}{13.31(1.5)} \tag{4.31}$$

or

$$h_{max} < 0.00043 \quad inches \tag{4.32}$$

and for Beryllium Copper

$$h_{max} < \frac{2(0.0092)5}{13.31(1.5)} \tag{4.33}$$

or

$$h_{max} < 0.0046 \quad inches \tag{4.34}$$

Equation (4.32) shows that the thickness for the flexible segment at the third pivot must be less than 0.00043 inches when using 1010 Steel to keep the stress below the maximum level. This thickness is below the minimum thickness value defined in the problem, and therefore, 1010 Steel can not be used for this situation. However, Equation (4.34) shows that using Beryllium Copper up to a thickness of 0.0046 inches will satisfy the stress requirements for the problem. Therefore, the flexible segment can have any thickness between 0.001 inches and 0.0046 inches, and still satisfy the requirements.

Also, using Equation (4.22), it is possible to determine the maximum thickness for the flexible segment on the first pivot in the configuration. From Table 4.2, the value for C for this configuration is 9.08. Using the value for C, the equation $c = h/2$, and the value for h_{max} in Equation (4.34), Equation (4.22) becomes

$$h_1 < 9.08(0.0046) = 0.0418 \tag{4.35}$$

This indicates that the width of the first flexible pivot must be less than 0.0418 when the thickness 0.0046 inches is used for the flexible segment of the third pivot. Any value above 0.0418 will cause the stress parameter equation to become invalid as the flexible segment with the maximum stress shifts from one segment to the other. At this point, new values for the exponential relationship for α would have to be generated.

4.2 Force Feasibility

The force feasibility equations are similar in purpose to the stress feasibility equations developed above. These equations contain a set of unique parameters that help in determining if a given mechanism can meet the force demands of a given situation while still satisfying all the constraints. In many cases, the information used and determined in the stress feasibility calculations can be applied to the force feasibility calculations.

The derivation for the force feasibility will be presented, results for the original configurations will be shown, and the example started above will be continued.

4.2.1 Force Derivation

The static force equation for the CFMs is given in equation (2.13) as

$$F = \frac{k_1}{r_2}\Phi \tag{4.36}$$

where k_1 is the PRBM spring constant for the first pivot, r_2 is a PRBM link length, and Φ is one of the non-dimensionalized CFM parameters.

The equation for the PRBM spring constant is

$$k_1 = \gamma K_\theta \frac{EI_1}{l} \tag{4.37}$$

where the parameters are the same as defined in the above sections.

Following the assumptions explained in Section 4.1.1 for l, and substituting equation (4.7) into equation (4.37), results in

$$k_1 = \gamma K_\theta \frac{EI_1}{\rho r_2} \tag{4.38}$$

In turn, this is combined with equation (4.36) to give

$$F = \frac{\gamma K_\theta E I_1 \Phi}{\rho r_2^2} \tag{4.39}$$

Using the parameter ζ presented in Equation (4.8), Equation (4.39) can be further generalized to

$$F = \frac{\gamma \zeta^2 K_\theta E I_1 \Phi}{\rho r_{tot}^2} \tag{4.40}$$

where

$$\zeta = R + 1 \tag{4.41}$$

for r_2. Therefore, substituting Equation (4.41) into Equation (4.40) results in

$$F = \frac{\gamma K_\theta E I_1 \Phi (R+1)^2}{\rho r_{tot}^2} \tag{4.42}$$

4.2.2 Force Parameter Development

In Equation (4.42), γ, K_θ, Φ, R, and ρ are dependent upon the configuration and sub-class, E depends upon the material, and r_{tot} and I_1 depend upon the geometry. The variables that are dependent upon configuration and sub-class can be combined to form a nondimensionalized parameter β such that

$$\beta = \frac{\gamma K_\theta (R+1)^2 \Phi}{\rho} \tag{4.43}$$

and

$$F = \frac{\beta E I_1}{r_{tot}^2} \tag{4.44}$$

The first moment of inertia, I_1, is associated with the flexible segment of the first pivot (k_1). The parameter β is easily calculated for each specific configuration (with an exception for Class 1B, discussed in Section 4.2.4). The results of these calculations can be found in Table 4.3. Equation (4.44) is used to determine if a specific configuration, material, length, and cross sectional geometry are suitable to achieve a desired force. This equation can be readily used without a complex model to run a simple feasibility check or to determine an unknown parameter.

4.2.3 Relating Moments of Inertia

In order to use the force equation with the stress equation, it becomes important to relate the moment of inertia of the first flexible segment, I_1, with the moment of inertia of the flexible segment with the maximum stress. This moment of inertia will be denoted as

Table 4.3 β for each configuration and sub-class

Configuration	sub-class a		sub-class b	
	Φ	β	Φ	β
Class 1A-*spp*	0.4537	15.1508	0.4773	16.9649
Class 1A-*lpp*	0.4537	2.9008	0.4773	3.2482
Class 1B-*psp*	2.0563	82.2520	2.1500	86.0000
Class 1B-*pl p*	2.0563	15.7482	2.1500	16.4658
Class 2A-*ssp*	0.9575	18.6332	1.0466	21.4708
Class 2A-*slp*	0.9575	18.6332	1.0466	21.4708
Class 2B-*sps*	1.2259	37.9347	1.2154	41.3322
Class 2B-*lps*	1.2259	7.2631	1.2154	7.9136
Class 3A-*sss*	3.4016	456.4868	3.6286	344.6931

I_x where x is the primary pivot as defined in Table 4.1. To relate the moments of inertia, the general spring constant equation

$$k = \frac{\gamma K_\theta E I}{l} \tag{4.45}$$

will be used. Rearranging this equation and substituting values according to the methods above, Equation (4.45) becomes

$$k = \frac{\gamma \zeta K_\theta E I}{\rho r_{tot}} \tag{4.46}$$

The constant-force parameters K_1 and K_2, where

$$K_1 = \frac{k_2}{k_1} \tag{4.47}$$

$$K_2 = \frac{k_3}{k_1} \tag{4.48}$$

can now be used to relate the spring constants for the first flexible pivot and any other flexible pivot. If i is used to represent any of the flexible segments, then the spring constant of any flexible segment can be related to I_1 through Equation (4.47) and (4.48). Generalizing, these equations become

$$\frac{K_{i-1}\gamma_1 \zeta_1 K_{\theta_1} E_1 I_1}{\rho_1 r_{tot}} = \frac{\gamma_i \zeta_i K_{\theta_i} E_i I_i}{\rho_i r_{tot}} \tag{4.49}$$

If it is assumed that the flexible segments are made from the same material and that r_{tot} is the same for each, then the equation reduces to

$$\frac{K_{i-1}\gamma_1\zeta_1 K_{\theta_1} I_1}{\rho_1} = \frac{\gamma_i\zeta_i K_{\theta_i} I_i}{\rho_i} \qquad \textbf{(4.50)}$$

At this point, a new parameter, κ, is introduced where

$$\kappa_i = \frac{\gamma_i\zeta_i K_{\theta_i}}{\rho_i} \qquad \textbf{(4.51)}$$

This parameter depends upon the sub-class and the configuration. Table 4.4 gives the values for κ_i for each flexible segment in each configuration. Substituting Equation (4.51) into Equation (4.50) and rearranging for I_1, the equation of interest becomes

$$I_1 = \frac{\kappa_i I_i}{\kappa_1 K_{i-1}} \qquad \textbf{(4.52)}$$

This equation relates the two moments of inertia together allowing quick calculations of any moment of inertia within the mechanism and can be used in connection with the force and stress equations developed to determine feasibilities.

Table 4.4 Values for $K_{x\text{-}1}$ and κ_x for each sub-class and configuration

Configuration	Primary Pivot	Sub-class a					Sub-class b				
		K_1	K_2	κ_1	κ_2	κ_3	K_1	K_2	κ_1	κ_2	κ_3
Class 1A-*spp*	1	0	0	18.274	-	-	0	0	18.853	-	-
Class 1A-*lpp*	1	0	0	3.499	-	-	0	0	3.610	-	-
Class 1B-*psp*	2	1.000	0	-	20.000	-	1.000	0	-	20.000	-
Class 1B-*plp*	2	1.000	0	-	3.829	-	1.000	0	-	3.829	-
Class 2A-*ssp*	2	0.191	0	13.950	20.000	-	0.224	0	14.323	20.000	-
Class 2A-*slp*	2	0.191	0	13.950	6.762	-	0.224	0	14.323	6.344	-
Class 2B-*sps*	3	0	1.003	17.591	-	23.173	0	1.024	18.441	-	21.847
Class 2B-*lps*	3	0	1.003	3.368	-	23.173	0	1.024	4.183	-	21.847
Class 3A-*sss*	1	1.000	12.670	36.633	20.000	13.755	1.000	9.382	30.821	20.000	14.803

4.2.4 Exceptions in the Force Parameter β

In the above derivation, Equations (4.41) and (4.42) are true for all configurations except the Class 1B mechanisms. From Chapter 2, the force equation for Class 1B mechanisms is defined as

$$F = \frac{k_2}{r_2}\Phi \tag{4.53}$$

where

$$k_2 = \gamma K_\theta \frac{EI_2}{l} \tag{4.54}$$

In this case, k_2 depends upon the length of the flexible segment which is no longer guaranteed to be related to r_2. Therefore, the value for ζ is different depending upon the specific mechanism used and the equation for the parameter β becomes

$$\beta = \frac{\gamma K_\theta (R+1)\zeta\Phi}{\rho} \tag{4.55}$$

where ζ has the values as defined by Equations (4.10) to (4.12) and Equation (4.53) becomes

$$F = \frac{\beta EI_2}{r_{tot}^2} \tag{4.56}$$

where I_2 is the first moment of inertia of the flexible segment associated with pivot two (k_2) and β is found from Table 4.3.

4.2.5 Force Feasibility Example

This example is a continuation of the example found in Section 4.1.3. The mechanism is required to have a force of 0.1 pounds and the width of the flexible segments can be no more than 1.0 inch. If Beryllium Copper is chosen as the material (E=18.5 Mpsi), is the mechanism feasible? The stress feasibility calculations were performed in a previous example.

We know that the stress is feasible when Beryllium Copper is used. Therefore, the question is whether or not the mechanism can generate the required force with the limitations on the width of the material.

First, β must be determined for the mechanism. This is accomplished my looking at Table 4.3. The value for β on a Class 2B-*lps*-a mechanism with k_1 coming from a small-length flexural pivot is

$$\beta = 7.263 \tag{4.57}$$

Now, the moments of inertia between the third flexible segment and the first must be related. This is done by using Equation (4.52) and looking up the values for each parameter in Table 4.4. The equation becomes

$$I_1 = \frac{23.17}{3.368(1.003)} I_3 = 6.86 I_3 \tag{4.58}$$

Substituting the formula for a rectangular cross section and Equation (4.58) into Equation (4.56) and rearranging for b results in

$$b = \frac{12Fr_{tot}^2}{6.86\beta Eh^3} \tag{4.59}$$

If the original thickness restriction of $h > 0.001$ inches is used, then the minimum width (b_{min}) can be found from

$$b_{min} > \frac{12Fr_{tot}^2}{6.86\beta Eh^3} \tag{4.60}$$

Plugging values into Equation (4.60) results in

$$b_{min} > \frac{12(0.1)5^2}{6.86(7.263)(18.5e6)0.001^3} \tag{4.61}$$

or

$$b_{min} > 32.54 \text{ inches} \tag{4.62}$$

This exceeds the acceptable width and therefore is not an acceptable design. However, if the maximum value for h_{max} (0.0046) given in equation (4.34) is used, then b_{min} becomes

$$b_{min} > \frac{12(0.1)5^2}{6.86(3.0987)(18.5e6)0.0046^3} \tag{4.63}$$

or

$$b_{min} > 0.334 \text{ inches} \tag{4.64}$$

The stress feasibility equation indicates that this combination of b and h allows for the mechanism to meet the force requirement without violating the width requirements. It should also be noted that there are several combinations of h and b that will satisfy both the h_{max} and b_{min} inequalities. Assuming that the maximum b (1.0 in) is used, then the h to be used with it for the third flexible pivot becomes 0.0032. This combination will also give an acceptable value as will any values between these two sets.

The final part of the design process is to find the width and thickness of the first flexible segment. Depending upon the constraints, it is an easy matter to use Equation (4.58) and pick a value for one of the dimensions while solving for the other. In this manner, the complete geometry of all of the flexible segments can be found while still satisfying the constraints of the problem. This example demonstrates the usefulness and ease with which force feasibility checks can be performed.

CHAPTER 5

MECHANISM COMPARISONS

To effectively use the CFMs, it is necessary to understand the advantages and disadvantages of each configuration. One way to understand this is to compare the mechanisms with each other to determine which ones are best suited under given circumstances. This chapter presents several different comparisons that can be made to help better understand each configuration including comparisons of:

- Actual lengths
- Maximum stiffness
- Percent constant-force
- Manufacturing orientations
- Normal displacement

5.1 Length Comparison

The equations developed in Chapter 4 are in terms of the total PRBM length r_{tot}. However, it is often desirable to express the equations for CFMs in terms of the actual length of the mechanism, l_{tot}. This can be done by using the following equation:

$$l_{tot} = \lambda r_{tot} \tag{5.1}$$

where λ is a length parameter. A value for λ for each mechanism can be found by examining them individually. The calculation of the value for the parameter λ for the class 1A-*lpp* mechanism is presented as an example. Following which, the general equations and values for λ of all configurations will be presented.

5.1.1 Length Parameter for class 1A-*lpp*

The total length of the mechanism is found by adding the actual length of each link as expressed in

$$l_{tot} = l_2 + l_3 \tag{5.2}$$

where l_2 and l_3 are the actual link lengths. In this configuration, the first link is a long flexible beam. The length of the beam is found by dividing the PRBM link length by γ or

$$l_2 = \frac{r_2}{\gamma} \tag{5.3}$$

The second beam is a rigid link with two pin joints and its length is expressed as

$$l_3 = r_3 \tag{5.4}$$

Combination of Equations (5.2) to (5.4) results in

$$l_{tot} = \frac{r_2}{\gamma} + r_3 \tag{5.5}$$

To find the value for the parameter L, Equation (5.5) can be substituted into Equation (5.1) and solved for λ. This results in

$$\lambda = \frac{\frac{r_2}{\gamma} + r_3}{r_{tot}} \tag{5.6}$$

where

$$r_{tot} = r_2 + r_3 \tag{5.7}$$

Once again, Equation (4.8) can be used to express the PRBM link lengths in terms of the overall PRBM length. Substituting Equation (4.8) and the corresponding ζ values into Equation (5.6) and rearranging results in

$$\lambda = \frac{R\gamma + 1}{(R+1)\gamma} \tag{5.8}$$

Equation (5.8) expresses λ in terms of R and γ. Substituting the values for R and γ that correspond to the class 1Aa-*lpp* mechanism results in

$$\lambda = \frac{0.8274(0.85) + 1}{(0.8274 + 1)0.85} = 1.027 \tag{5.9}$$

This indicates that the actual length of the mechanism is 1.027 times longer than the PRBM length of the mechanism.

The length parameter is valuable in that it allows any equations that are expressed in terms of r_{tot} to be easily expressed in terms of l_{tot}. This is done by substituting Equation (5.1) into the equation and using the appropriate λ value. This allows the actual mechanism length to be used throughout the design process. This parameter also allows for comparisons of the actual lengths of mechanisms that have the same PRBM length.

5.1.2 General λ values

The technique described above can be used for all of the different configurations and corresponding λ values can be found. Table 5.1 presents the general equation and value of λ for each mechanism. Two mechanisms can be compared by comparing λ values. The mechanism with the higher λ value will have a larger actual length assuming that the mechanisms have identical PRBM lengths.

5.2 Stiffness Comparisons

A valuable comparison between the configurations can be made by examining the stiffness of each configuration under identical sets of circumstances. By making this comparison, the mechanisms that provide the most force are identified, allowing them to be used in design situations to achieve the desired forces.

5.2.1 Stiffness Comparison Issues

The stiffness referred to in this work is a measure of the maximum force that can be generated for a given mechanism size and stress level. To make this comparison, it is necessary to derive a method to hold conditions such as size and stress constant while comparing the output force. The force equation, Equation (4.44), is

$$F = \frac{\beta E I_1}{r_{tot}^2} \tag{5.10}$$

where β is configuration dependent, I_1 and r_{tot}^2 are geometry dependent, and E is material dependent. Equation (5.10) can be written in terms of l_{tot} by using Equation (5.1), resulting in

$$F = \frac{\beta E L^2 I_1}{l_{tot}^2} \tag{5.11}$$

Table 5.1 Length parameter formulas and values

Configuration	λ Formula	λ Value	
		sub-class a	sub-class b
Class 1A-*spp*	$\frac{R + 1.05}{R + 1}$	1.027	1.027
Class 1A-*lpp*	$\frac{R\gamma + 1}{\gamma(R + 1)}$	1.097	1.094
Class 1B-*psp*	1	1.0	1.0
Class 1B-*plp*	$\frac{R\gamma + 1}{\gamma(R + 1)}$	1.088	1.088
Class 2A-*ssp*	$\frac{R + 1.05}{R + 1}$	1.036	1.035
Class 2A-*slp*	$\frac{R + 1.05\gamma}{\gamma(R + 1)}$	1.086	1.088
Class 2B-*sps*	$\frac{1.05R + 1.05}{(R + 1)}$	1.050	1.050
Class 2B-*lps*	$\frac{1.05R\gamma + 1}{\gamma(R + 1)}$	1.122	1.119
Class 3A-*sss*	$\frac{1.05R + 1.05}{(R + 1)}$	1.050	1.050

A method could be pursued that would fix I_1, l_{tot}, and E to form a common set of parameters. This would allow for comparison of the configuration based on F, which would be directly proportional to β. Although this method would be valid, there are some underlying issues that have not been addressed.

By making the assumptions listed above, the amount of stress found in each configuration at the total displacement has not been taken into account. By holding I_1 constant, the maximum stress in each mechanism is not equivalent with the maximum stress in the other mechanisms. Therefore, it would be ideal to compare the forces of each configuration at the same stress value. This can be done by holding E, l_{tot}, and the width b constant for each mechanism while adjusting the height of the flexible segments until a predetermined stress level is reached.

5.2.2 Comparison Derivation

To equate the stress levels it is necessary to change the focus of the force equation from the first flexible segment to the primary pivot, after which, the stresses can be equated.

Equation (4.52) from Chapter 4 is

$$I_1 = \frac{\kappa_i I_i}{\kappa_1 K_{i-1}} \tag{5.12}$$

Substituting Equation (5.12) into Equation (5.11), and setting i to the primary pivot, the force equation becomes

$$F = \frac{\beta L^2 E \kappa_p I_p}{\kappa_1 K_{p-1} l_{tot}^2} \tag{5.13}$$

where κ_p, κ_1, and K_{p-1} are configuration dependent, and I_p is geometry dependent.

The stress parameter developed in Chapter 4 can be used to equate the stress in each mechanism to some maximum allowable stress value. The basic stress equation found in Chapter 4 is

$$\alpha A \le \frac{\Omega}{SF} \tag{5.14}$$

To make the comparison, the right hand side of the side of Equation (5.14) is set equal to 1 and the inequality is removed. This results in

$$\alpha A = 1 \tag{5.15}$$

Equation (5.15) assumes that the same material and safety factor are used for each mechanism and that the stress level in each mechanism is the same. Furthermore,

$$A = \frac{cL}{l_{tot}} = \frac{hL}{2l_{tot}} \tag{5.16}$$

To equate the stresses, either h or l_{tot} can be adjusted to give the maximum stress. However, if l_{tot} is assumed to be constant as described above, then the comparison of the maximum stresses in two configurations, i and j, can be expressed as

$$\alpha_i h_i L_i = \alpha_j h_j L_j \tag{5.17}$$

Equation (5.17) can be used to maximize the stress in each configuration. Using the general equation for a rectangular cross section, rearranging Equation (5.17), and substituting it into Equation (5.13) gives

$$F_i = \frac{\beta_i E \kappa_{p_i} \lambda_i^2 b_i \left(\frac{\alpha_j \lambda_j}{\alpha_i \lambda_i} h_j\right)^3}{12 \kappa_{1_i} K_{(p-1)_i} l_{tot}^2} \tag{5.18}$$

Equation (5.18) gives the force in configuration i at a stress level equal to the stress in configuration j given identical material properties (Ω), safety factor (SF), overall length (l_{tot}), and width (b).

Equation (5.18) can be used to make comparisons between two configurations. Ultimately, comparisons between all of the configurations, not just two, are to be made. This is accomplished by setting all of the configuration b parameters, as well as E, l_{tot}, and b_a to 1, and removing the 12. This results in a stiffness intensity parameter ψ where

$$\psi = \frac{\beta \kappa_p \left(\frac{1}{\alpha}\right)^3}{\lambda \kappa_1 K_{p-1}} \tag{5.19}$$

Equation (5.19) no longer results in a force value, but is a dimensionless parameter that describes the stiffness of the mechanism related to stress. This parameter can be used to compare all of the configurations assuming identical lengths, materials, widths, and stresses.

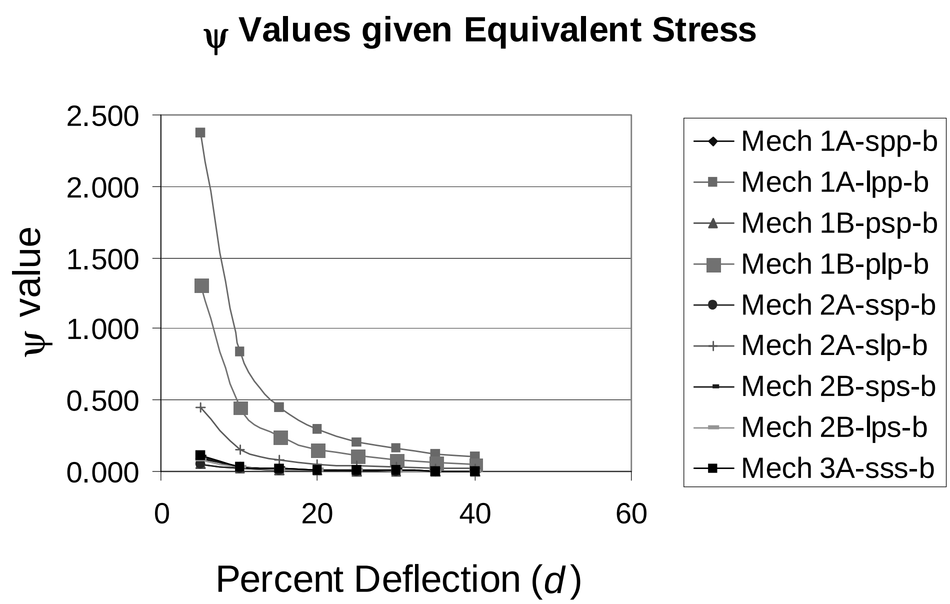

Figure 5.1 Ψ values for sub-class b

5.2.3 Stiffness Comparisons Results

Examination of Equation (5.19) shows that for a given configuration, ψ varies only as a function of α, which varies as a function of displacement. Values for ψ as a function of displacement have been calculated for all of the configurations and sub-classes as introduced in Chapter 3. Figure 5.1 shows a graph of the ψ values for the mechanisms in sub-class b versus the percent displacement. This graph shows that the Mech 1A-*lpp*-b has the highest value for the parameter ψ. The graph also shows how the available force decreases as percent deflection increases. This is consistent with expectations. As deflections increase, stresses will increase, limiting the height of the flexible segment. This in turn decreases the moment of inertia, the corresponding spring constant, and ultimately, the output force.

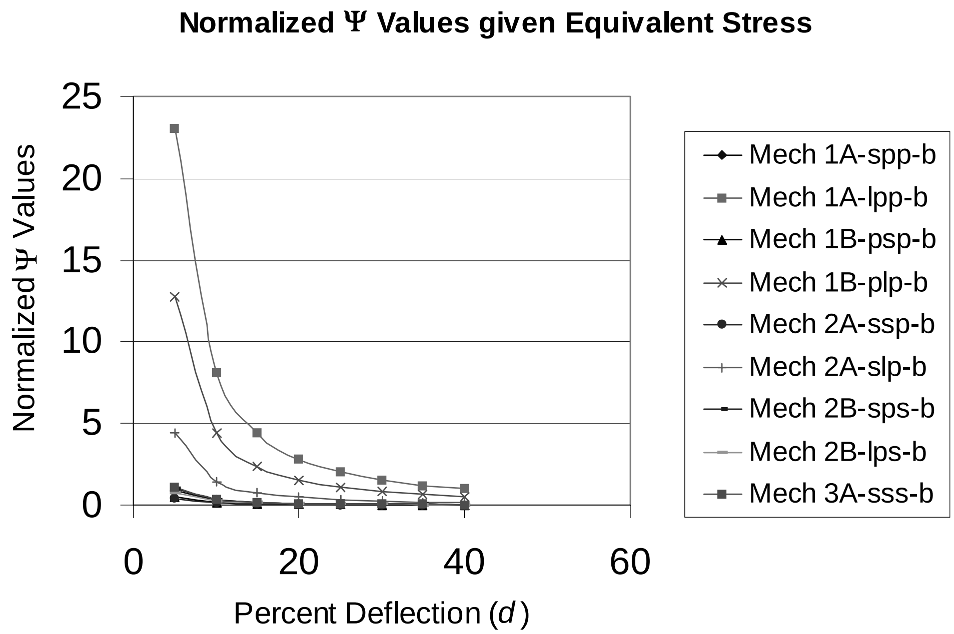

Figure 5.2 Normalized Ψ values for sub-class b

The data in Figure 5.1 can be normalized using the maximum value at maximum deflection, ψ_c. That is, a normalized parameter value Ψ is expressed as

$$\Psi = \frac{\psi}{\psi_c} \tag{5.20}$$

Figure 5.2 shows a graph of the same data, but in normalized form. This graph shows the values as percentages of the maximum value at full displacement, giving a better understanding of the force behavior. For example, the graph shows that the force output rises from a value of 1 at 16% deflection to 22 at 2% deflection, an increase of 2200%. This information helps show the trade off between deflection and stiffness of the mechanisms, helping to indicate in which deflection ranges a mechanism must operate to obtain a desired force. Additionally, Figure 5.2 shows the relationship between mechanisms. For

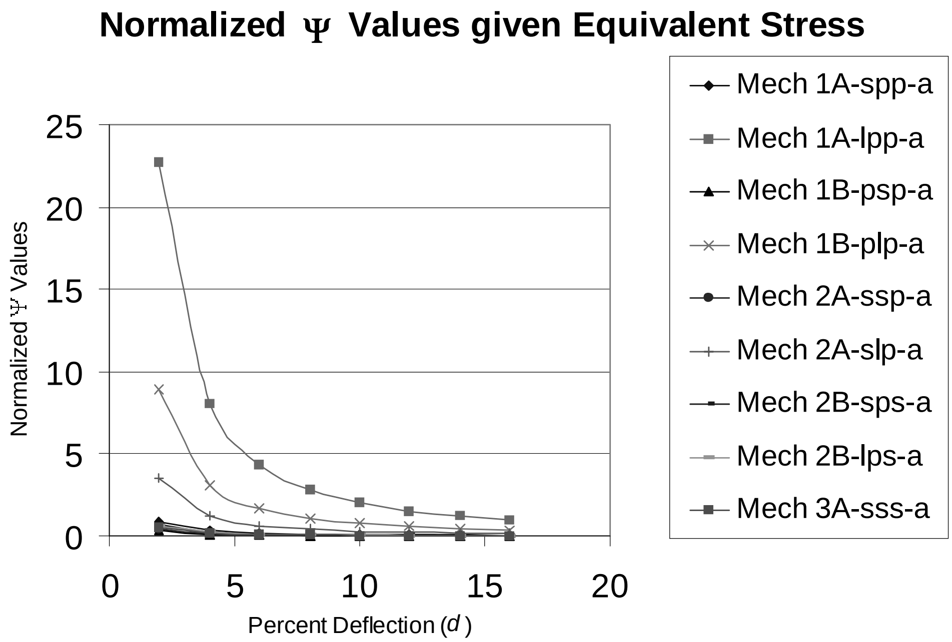

Figure 5.3 Normalized Ψ values for sub-class a

example, mechanism 1B-*plp*-b has only 40% of the force or stiffness of mechanism 1A-*lpp*-b when stress levels and deflections are equivalent.

The same procedures were followed for the mechanisms in sub-class a. The normalized results can be found in Figure 5.3. Comparison of Figure 5.2 and Figure 5.3 shows that the order of the mechanisms is the same for both sub-classes.

To illustrate the importance of equating the stresses, normalized Ψ values when stresses are not equated are graphed in Figure 5.4. This graph shows that when the stresses are not equated, mechanism 3A-*sss*-b is the stiffest mechanism, while mech 1A-*lpp*-b is not even in the top three. It also indicates that the maximum stiffness is not a function of

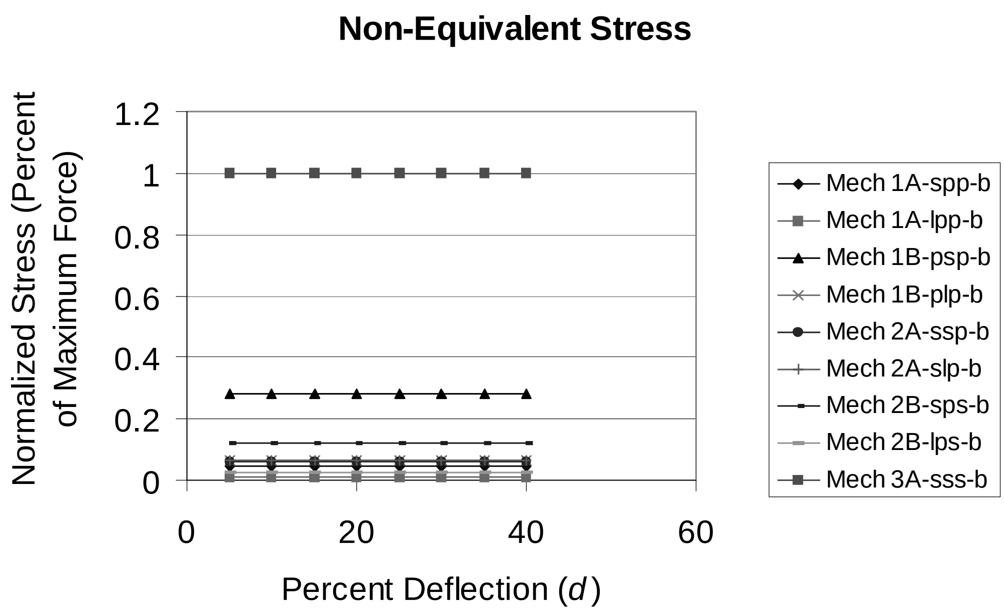

Figure 5.4 Normalized Ψ values for sub-class b without stress equalization

maximum deflection. However, this information is misleading because the stresses in the mechanism are not considered.

5.2.4 Stiffness Comparison Conclusions

Based on the results from above, the stiffness of each mechanism can be determined relative to all of the other mechanisms. The results indicate that the three stiffest mechanisms are, in descending order, 1A-*lpp*, 1B-*plp*, and 2A-*slp*. When large output forces are needed, these mechanisms should be the first ones considered. The rest of the mechanisms are similar to one another in stiffness.

The parameter Ψ also adds a valuable tool in looking for new classes of mechanisms. With the parameter, optimization routines can be designed to look only for mechanisms that are stiffer than the mechanisms currently defined. The parameter Ψ also makes it quick to determine if a mechanism is stiffer than another.

The parameter Ψ is also beneficial because, when values are standardized, the effect of percent deflection on the force can be determined quickly. This aids in design by indicating what deflection range must be used to obtain a desired force.

5.3 Percent Constant-Force Comparison

A second parameter that can be used for comparing configurations is the percent constant-force parameter, Ξ. However, to ensure that this parameter is beneficial, several issues must first be discussed.

5.3.1 Percent Constant-Force Inversion

In Chapter 2, the parameter that measures percent constant-force was introduced as

$$\Xi = \frac{max(\vec{F})}{min(\vec{F})} \tag{5.21}$$

To help this parameter be more intuitive, it can be inverted and multiplied by 100, resulting in

$$\Xi' = 100\frac{min(\vec{F})}{max(\vec{F})} \tag{5.22}$$

Multiplying this parameter by a hundred gives the percent constant-force as a percentage with 100% being perfectly constant. Redefining this parameter make it more intuitive and easier to understand. It measures the amount of variation between the minimum and maximum output force of a CFM.

5.3.2 Percent Constant-Force Comparison

To use this parameter, it is important to ensure that the values are used in a consistent manner. The maximum force, as defined in Equation (5.21), is taken to be the maximum force throughout the percent displacement specified for the sub-class. Due to the nature of CFMs, this force is usually located at the maximum deflection. The minimum force is defined similarly to the maximum force, and can generally be found at the smallest deflection.

One way to help guarantee a good comparison is to calculate an extrapolated Ξ' across the full range of displacement of the mechanism. This value will be termed Ξ'_{ex} and is

$$\Xi'_{ex} = \frac{F_0}{F_{max}} \tag{5.23}$$

where F_0 is the force at zero deflection.

Often, Ξ'_{ex} can not be calculated directly due to limitations in the models. These limitations may include inflection points at zero displacement or limitations in step size. For example, in a finite-element model (FEA), it may only be feasible to calculate the force at five points along the deflection. In this case, d_{min} may be some distance from the zero displacement. Additionally, results from experimental testing often have a small range at the beginning in which friction and other factors distort the output force. In these cases, to ensure comparability, Ξ'_{ex} must be determined through another method.

A value for Ξ'_{ex} can be determined by curve fitting a line through the maximum force at the total displacement and the minimum force at the smallest known deflection. The y-intercept of this line can be used as the force at zero deflection (F_0).

Using the basic slope-intercept equation of a line, the maximum force is found to be

$$F_{max} = d_{max}\left(\frac{F_{max} - F_{min}}{d_{max} - d_{min}}\right) + F_0 \quad \textbf{(5.24)}$$

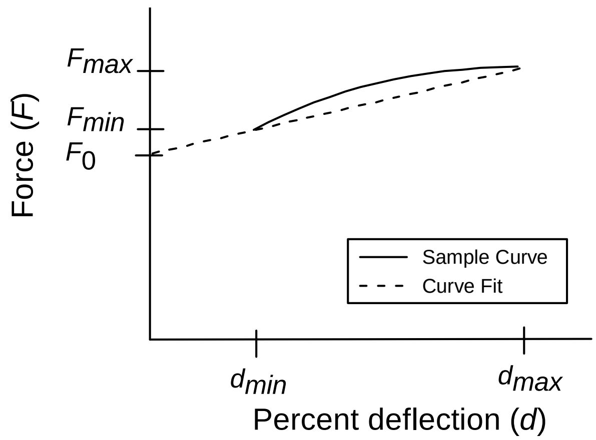

Figure 5.5 Parameters for Ξ'_{abs} calculation

where F_{max} is the force calculated at displacement d_{max} (percent or actual displacement) and F_{min} is the force at the displacement d_{min}. Figure 5.5 shows the parameters used to calculated Ξ'_{ex}. Rearranging for F_0 and factoring d_{max} out of the denominator gives

$$F_0 = F_{max} - \left(\frac{F_{max} - F_{min}}{1 - \frac{d_{min}}{d_{max}}}\right) \quad \textbf{(5.25)}$$

Factoring F_{max} from the numerator and collecting terms results in

$$F_0 = F_{max}\left(1 - \left(\frac{1 - \frac{F_{min}}{F_{max}}}{1 - \frac{d_{min}}{d_{max}}}\right)\right) \quad \textbf{(5.26)}$$

Finally, dividing F_0 by F_{max} gives

$$\Xi'_{ex} = 100 \cdot \frac{F_0}{F_{max}} = 1 - \left(\frac{1 - \frac{F_{min}}{F_{max}}}{1 - \frac{d_{min}}{d_{max}}} \right) \tag{5.27}$$

This equation gives a level of constant-force for the entire deflection of the mechanism. If the minimum force (F_{min}) is already on the y-axis, then Equation (5.27) reduces to Equation (5.22).

5.3.3 Percent Constant-Force Results

For the configurations presented in Chapter 2, the slider-crank model is very robust. It is assumed

$$F_{min} \cong F_0 \tag{5.28}$$

and therefore, it is reasonable to suggest

$$\Xi' \cong \Xi'_{ex} \tag{5.29}$$

The original values for Ξ from Chapter 2 are shown in Table 5.2. These values were calculated using the method illustrated in Equation (5.21). The values for the new method, the inverse of the original, can be seen next to the old values. Examination of these values show that the percent constant-force can now be referred to in a more intuitive way as 99% constant rather than the value 1.0030.

From Table 5.2, it can be seen that the class 1B mechanisms have a smaller percent constant-force than the other mechanisms. This indicates that these mechanisms will have a greater variation in force than the other mechanisms. This knowledge will allow designers to pick a mechanism suitable for the application. Additionally, as new sub-classes are found, a method has been established to help identify which mechanisms exhibit a higher percentage of constant-force.

The parameter Ξ'_{ex} is useful in establishing a consistent manner to measure percent constant-force. For the new mechanisms presented in this work, Ξ' is calculated and presented as Ξ'_{ex} since it can be assumed that inequality in Equation (5.29) is satisfied. In the cases in which this inequality does not hold true, the extrapolated percent constant-force Ξ'_{ex} will be presented. This will help ensure the comparability of this parameter, allowing for useful and accurate conclusions to be drawn. Additionally, the further usefulness of this parameter to determine the percent constant-force from experimental data will be exhibited as testing results are explored.

Table 5.2 Percent constant-force values for the original mechanisms.

Sub-Class	Class	Ξ	Ξ'_{ex}
a	1A	1.0030	99.70
	1B	1.0564	94.66
	2A	1.0015	99.85
	2B	1.0721	93.27
	3A	1.0002	99.98
b	1A	1.0241	97.65
	1B	1.1576	86.39
	2A	1.0058	99.42
	2B	1.1914	83.93
	3A	1.0049	99.51

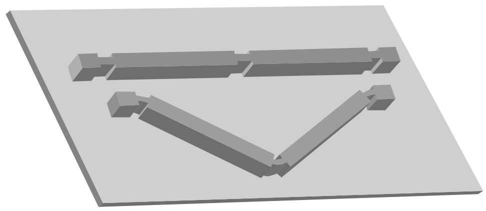

(a)

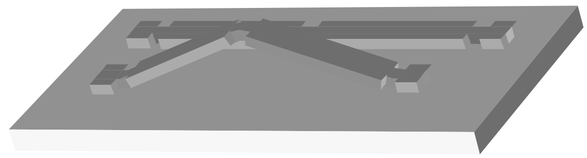

(b)

Figure 5.6 (a) In-plane and (b) out-of-plane manufacturing orientations

5.4 Manufacturing Orientations

CFMs can be fabricated in many ways. The special case orientations are discussed in this section.

5.4.1 In-plane Orientation

The first special case CFM orientation is an in-plane orientation. In this orientation, all motion takes place in the plane of manufacturing. To simplify the manufacturing of CFMs in an in-plane orientation, the widths of the flexible segments must be equal to one another and to the thickness of the work material. This is shown graphically in Figure 5.6a.

5.4.2 Out-of-plane Orientation

The second orientation is the out-of-plane orientation–the orientation in which part of the mechanism displaces normal to the manufacturing plane, as illustrated in Figure 5.6b. In this case, to simplify manufacturing, the thicknesses of the flexible segments must be equal to one another and to the thickness of the material. This allows the mechanism to be fabricated from a uniform piece of material with either simple milling or stamping type operations.

5.4.3 Orientation Comparison

Different mechanisms can be compared based on suitable fabrication orientations. A mechanism that is suitable for both types of fabrication orientations may be preferable over a mechanism that is not suitable for either one of these fabrication orientations, all other things being equal.

5.5 Flexible Segment Design Space Comparison

When comparing different CFMs, the design space surrounding the flexible segments in the mechanisms should be compared. The moment of inertia value is set by the spring constants requirements and can not be changed. However, there are many different combinations of flexible segment thicknesses and widths that can give the correct moment of inertia. It is advantageous to have combinations of thicknesses and widths that meet the design requirements and manufacturing limitations faced by designers. Therefore comparison of these flexible segment design spaces is essential.

5.5.1 Thickness Limits

The thicknesses of the primary pivot is limited by the stress constraint. However, as presented in Chapter 4, if the primary pivot is used during design, the other flexible segments in the mechanism must be limited to values that will maintain a stress level equal to or lower than the stress in the primary pivot.

The relationship above is defined mathematically in Equation (4.22) as

$$c_i \leq C'c_p \qquad \textbf{(5.30)}$$

where c_p is half the thickness of the primary pivot, c_i is half the thickness of the other pivots in the mechanism, and C' is a parameter for each specific mechanism.

The parameter C' varies with displacement. For simplicity, and to ensure that the inequality in Equation (5.30) is always satisfied, only the minimum values for C' are presented in this work. These minimum values, C, can be determined as

$$C = \text{minimum of } \frac{\alpha_p}{\alpha_o} = \text{minimum of } \frac{M_p d^{n_p}}{M_o d^{n_o}} = \frac{M_p}{M_o} d^{(n_p - n_o)} \qquad \textbf{(5.31)}$$

By selecting the minimum values, the inequality in Equation (5.30) will be satisfied at any displacement, ensuring that the primary pivot will always have the maximum stress. The values for C for each mechanism are repeated in Table 5.3.

The other limitation on the design space for the thicknesses of the flexible segments is the minimum thickness of the mechanism. This limitation is defined by the limitations of the manufacturing process and materials.

Table 5.3 Maximum thickness and minimum width constants

Configuration	Primary Pivot	C	D_{equal}	D_{min}	C	D_{equal}	D_{min}
Class 1A-*spp*	1	-	-	-	-	-	-
Class 1A-*lpp*	1	-	-	-	-	-	-
Class 1B-*psp*	2	-	-	-	-	-	-
Class 1B-*plp*	2	-	-	-	-	-	-
Class 2A-*ssp*	2	5.090	7.522	0.057	4.647	6.242	0.062
Class 2A-*slp*	2	1.721	2.543	0.499	1.474	1.980	0.618
Class 2B-*sps*	3	1.739	1.314	0.250	1.405	1.157	0.417
Class 2B-*lps*	3	9.081	6.861	0.009	7.339	5.103	0.013
Class 3A-*sss*	1	1.384 8.258	1.832 33.745	0.691 0.060	1.043 4.359	1.541 19.533	1.359 0.236

5.5.2 Width Limits

The limitations on the width of the flexible segments are also important in determining the design space of a flexible segment. According to the first moment of inertia, the width of the beam is inversely related to the thickness of the flexible segment where

$$I_o = \frac{b_o h_o^3}{12} \tag{5.32}$$

for rectangular cross-sections. As for the thicknesses, the moment of inertia of any given flexible pivot is related to the moment of inertia of the primary pivot. Generalizing Equation (4.52), this relationship can be defined as

$$I_i = \frac{K_{i-1}\kappa_p}{K_{p-1}\kappa_i} I_p \tag{5.33}$$

Furthermore, using Equation (5.32), Equation (5.33) can be expanded to

$$b_i h_i^3 = \frac{K_{i-1}\kappa_p}{K_{p-1}\kappa_i} b_p h_p^3 \tag{5.34}$$

Equation (5.34) shows that the combinations of thickness and width are defined by the geometry of the primary pivot. The maximum thickness for any pivot is limited first by the minimum thickness, and second by the design constraints of the problem. Because general manufacturing limitations for thicknesses vary for different processes, the upper limit for widths is difficult to define. However, it is known that the limit can be relatively large.

The minimum width is also controlled by limitations on the thicknesses and, in some cases, perhaps even design constraints. There are two important width ratios limits that limit the width of a flexible segment and the width of the primary pivot. The first is the minimum ratio, D_{min}, which occurs when the thicknesses of the flexible segments are set at their highest value. The second is the width ratio that occurs when the thicknesses are all equal, D_{equal}.

The minimum width ratio can be calculated by combining the equality portion of Equation (5.30) and Equation (5.34) and solving for b_i / b_p. This results in

$$\frac{b_i}{b_p} = \frac{K_{i-1}\kappa_p}{K_{p-1}\kappa_i C^3} = D_{min} \tag{5.35}$$

Values for the parameter D_{min} are tabulated in Table 5.3. These values represent the lowest possible ratio between the width of a flexible segment and the width of the primary flexible segment.

The second ratio, D_{equal}, is important in cases when the mechanism needs to be manufactured using an out-of-plane orientation. This ratio is similar to the one above and is derived from Equation (5.34). Setting the thicknesses equal and solving for the ratio of the thicknesses, Equation (5.34) becomes

$$\frac{b_i}{b_p} = \frac{K_{i-1}\kappa_p}{K_{p-1}\kappa_i} = D_{equal} \tag{5.36}$$

This ratio indicates what ratio the widths of the flexible segments must be when the thicknesses are equal for all flexible segments.

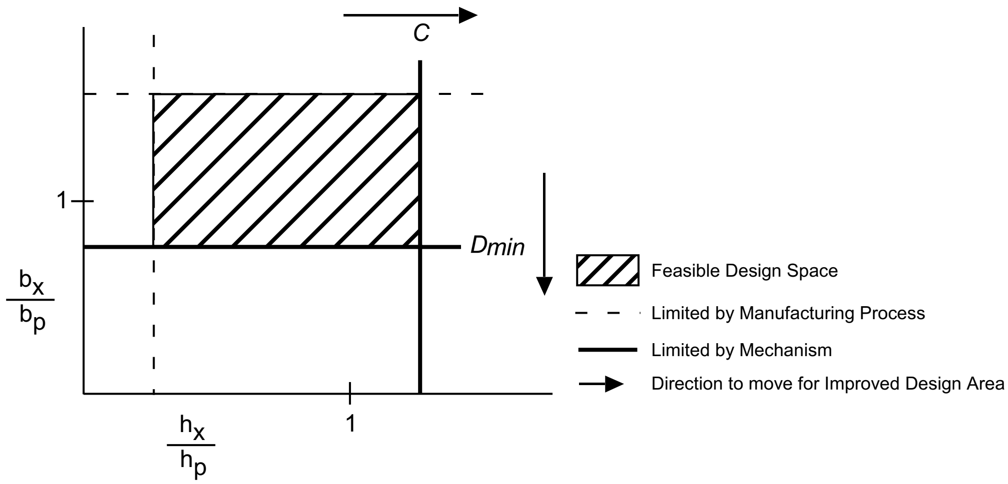

Figure 5.7 Graphical representation of flexible segment design area

5.5.3 Flexible Segment Design Area

The design area for the flexible segments that are not the primary pivot are partially defined by the parameters C and D_{min}. The rest of the area is defined by manufacturing limitations. A graphical representation of this design area can be seen in Figure 5.7.

The design area is bounded on the upper left corner by manufacturing limitations. The limitations on the lower and right side are due to stress limitations. The mechanism with the largest area, assuming the same limitations in manufacturing, will have the most valid combinations of thickness and width.

To improve the design area, the constants C and D_{min} must move according to the arrows in Figure 5.7. This provides for more suitable combinations of widths and thicknesses.

5.5.4 Determining Fabrication Orientations

The width and thickness ratios can also be used to determine suitable fabrication orientations. For in-plane orientation, the parameter D_{min} must be less than or equal to 1. This ensures that the flexible segments can have the same width as the material, a necessary trait for in-plane orientation. The magnitude of C in this case is not significant.

For out-of-plane orientation, is necessary that the parameter C be greater than or equal to 1 while D_{equal} is greater than or equal to 0.5 and less than or equal to 2. This allows the thicknesses to be the same width as the material while the ratio between the different widths is not larger than double. The magnitude of D_{min} is not significant in this orientation.

In some cases, mechanisms may be suitable for out-of-plane orientation in terms of thickness ($C \geq 1$), but the width ratio is smaller than 0.5 or larger than 2. In these cases, if D_{equal} is greater than 0.10 and less than 10, the mechanism is considered possibly suitable for out-of-plane orientation. The final decision is left to the designer.

The different types of fabrication orientations mentioned above, along with the required values for the thickness and width ratios, are summarized in Table 5.4.

Table 5.4 Summary of manufacturing orientation possibilities

Orientation	C	D_{equal}	D_{min}
In-plane	NA	NA	≤ 1
Out-of-plane	≥ 1	≤ 2 (0.5)	NA
Possibly out-of-plane	≥ 1	> 2 (0.5), ≤ 10 (0.1)	NA

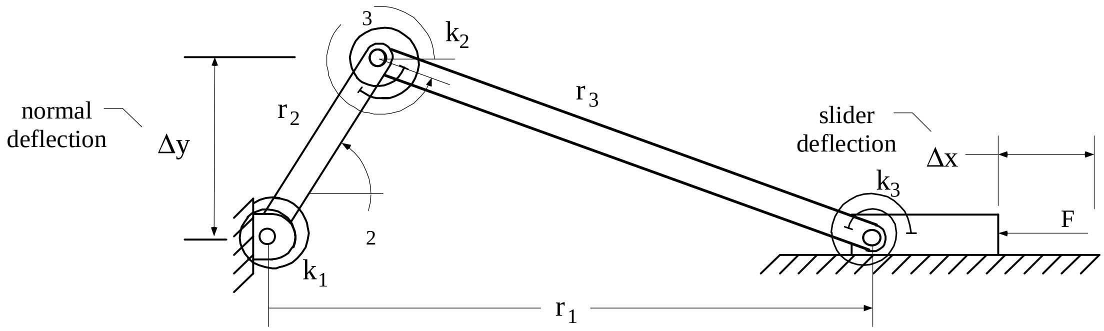

Figure 5.8 Normal displacement definition

5.6 Normal Displacement Comparison

In many applications, it is necessary to maintain a minimum normal displacement. This indicates that a method is needed to compare the normal displacement of different configurations.

5.6.1 Normal Displacement Derivation

The normal deflection, Δy, can be defined as the deflection normal to the input deflection resulting from the outward deflection of one slider-crank mechanism. Figure 5.8 shows a graphical definition of this deflection. The normal displacement, d_N, is the ratio between the normal deflection (Δy) at displacement d and the total undeflected length (r_{tot}) of the mechanism. More precisely,

$$d_N = 100 \cdot \frac{\Delta y}{r_{tot}} \quad (5.37)$$

Multiplying by 100 changes the ratio to a percentage.

It is important to calculate d_N at a displacement corresponding to the sub-class maximum deflection percentage (16 for sub-class a, 40 for sub-class b). This value is known as d_{Nmax}. To determine d_{Nmax} it is first necessary to develop an equation that will determine the normal displacement d_N in terms of r_{tot} and d. First, the normal deflection can be described in terms of θ_2 as

$$\Delta y = r_2 \sin\theta_2 \tag{5.38}$$

where, by using the law of cosines,

$$\theta_2 = \operatorname{acos}\left(\frac{r_1^2 + r_2^2 - r_3^2}{2 r_1 r_2}\right) \tag{5.39}$$

Using Equations (4.8), (4.10), and (4.11), r_2 and r_3 can be related to r_{tot} by

$$r_2 = \frac{r_{tot}}{R + 1} \tag{5.40}$$

$$r_3 = \frac{r_{tot}}{1 + \frac{1}{R}} \tag{5.41}$$

Furthermore, r_1 can be written in terms of r_{tot} by

$$r_1 = r_{tot}\left(1 - \frac{d}{100}\right) \tag{5.42}$$

where d is the displacement percentage.

Substituting Equations (5.40), (5.41), and (5.42) into Equation (5.39), and rearranging, results in

$$\theta_2 = \operatorname{acos}\left(\left(-\frac{1}{200}\right)\left(\frac{d^2R - 200dR - 200d + 20000 + d^2}{d - 100}\right)\right) \tag{5.43}$$

where r_{tot} drops out of the equation. Substituting Equations (5.40) and (5.43) into Equation (5.38) gives

$$\Delta y = \frac{r_{tot}}{R+1}\sin\left(\operatorname{acos}\left(\left(-\frac{1}{200}\right)\left(\frac{d^2R - 200dR - 200d + 20000 + d^2}{d - 100}\right)\right)\right) \tag{5.44}$$

Finally, Equation (5.44) can be substituted into Equation (5.37) resulting in

$$d_N = 100\frac{1}{R+1}\sin\left(\operatorname{acos}\left(\left(-\frac{1}{200}\right)\left(\frac{d^2R - 200dR - 200d + 20000 + d^2}{d - 100}\right)\right)\right) \tag{5.45}$$

Equation (5.45) gives the normal displacement as a percentage of the total displacement and in terms of R and d. This equation will allow a comparison of the normal displacement of each of the mechanisms. As mentioned before, not only will this parameter help compare different mechanisms, but it can be used during optimization to look for better mechanisms.

5.6.2 Normal Displacement Results

The R values for the original mechanisms were used to calculate the normal displacement at the sub-class maximum displacement percentage. The values calculated for d_{Nmax} are summarized in Table 5.5. These values represent the percent of the total length that the mechanisms will displace at the maximum sub-class displacement. These values can be used to help determine the space required for a particular design using a single CFM. If the total displacement for a sub-class is not utilized, the normal displacement d_N for any d can be found using Equation (5.45).

5.6.3 Normal Displacement Behavior

By observing a general slider crank, it can be seen that the normal deflection Δy can never be larger than the smallest link, either r_2 or r_3. Since the smallest link can never be larger than 50% of the mechanism, the normal displacement can never be greater than 50%.

Table 5.5 Summary of d_{Nmax} values

Mechanism	sub-class a		sub-class b	
	R	d_{Nmax}	R	d_{Nmax}
1a	0.8853	26.96	0.8853	39.79
1b	1.0000	27.13	1.0000	40.00
2a	0.4323	23.23	0.4323	30.03
2b	0.8441	26.77	0.8441	39.60
3a	2.0821	22.82	2.0821	32.44

CHAPTER 6

Model and Optimization

The development and improvement of CFMs is partially based upon the ability to model the mechanisms and optimize for the correct parameters. It is through the model and optimization that new sub-classes of constant-force parameters can be found. This chapter describes the key features and important issues of the modeling and optimization of CFMs connected with this research.

6.1 CFM Model

There are several directions from which to approach the construction of the CFM model to be linked with the optimization software. Since the optimization will alter key parameters rather than the mechanism geometries, which is opposite of a design approach, the model to be used at this point in this research will be constructed differently from a model used principally for design.

Although the model has the ability to produce valid designs, it was not developed for primary design of CFMs. Modeling methods and tips for use in design are presented in Chapter 8.

The CFM model is based on the behavioral model presented in Chapter 2, but has been adapted to include more general modeling abilities and the parameters developed in previous chapters.

6.1.1 General Model

The modeling methods presented in Chapter 2 are used as a starting point for the modeling of CFMs in this research. However, some generalization of the model was made to improve the capabilities of the model.

The model was programmed in Matlab, a mathematical software package. This software allows for easy use, quick alterations, data file manipulation, and linking with the optimization software. Detailed information and a copy of the code used in Matlab can be found APPENDIX B.

The model is based around the non-dimensionalized constant-force equation, Equation (2.13) (or Equation (2.20) for Class 1B). It is

$$F = \frac{k_1}{r_2}\Phi \tag{6.1}$$

where

$$\Phi = \frac{(R\cos\theta_3[\theta_2 + K_1(2\pi + \theta_2 - \theta_3)] + \cos\theta_2[K_1(2\pi + \theta_2 - \theta_3) + K_2(2\pi - \theta_3)])}{R\sin(\theta_2 - \theta_3)} \qquad \textbf{(6.2)}$$

or

$$F = \frac{k_2}{r_2}\Phi' \qquad \textbf{(6.3)}$$

where

$$\Phi' = \frac{(R\cos\theta_3[K_1(2\pi + \theta_2 - \theta_3)] + \cos\theta_2[K_1(2\pi + \theta_2 - \theta_3) + K_2(2\pi - \theta_3)])}{R\sin(\theta_2 - \theta_3)} \qquad \textbf{(6.4)}$$

for Class 1B mechanisms.

As before, a displacement vector is generated from zero displacement to the maximum deflection, dr_{tot}.

6.1.2 Model Inputs

The inputs for the CFM were selected specifically to aid in the search for new sub-classes. Some of the input parameters allow the optimization routine to alter the parameters that most directly affect the sub-classes. The other input parameters are parameters that have no direct impact on sub-classes, and in fact are often set at arbitrary values such as 1. They are included merely to allow the model to be used for calculations.

The inputs that directly affect the configurations are:

- Constant-Force Parameters: R, K_1, K_2

- Flexible pivot types: pin, small-length, or long flexible
- Percent deflection: d
- Associated link for Class 1-B mechanisms

The inputs that have no direct affect on the configurations, but are required to analyze actual designs are:

- Material Properties: E, S_y
- Spring Constant for the first flexible pivot: k_1
- Total Length: l_{tot}
- Width of Flexible segments: b

These inputs allow the optimization software to have the best access to modifying the mechanism and also allow the model to be used to generate real designs.

6.1.3 Model Outputs

The CFM model determines all the important parameters needed to define a new configuration. For a couple of these parameters, values are calculated at each point of the deflection, but only the average value of the parameter is reported - as is done with the parameter Φ in the prior work.

Actual parameter values returned:

- Link Lengths: r_2, r_3
- Stress Parameters: A, C, M, n, κ
- Comparison Parameters: λ, D
- Stiffness Parameter: Ψ

- Primary Pivot
- Normal Displacement Parameter: d_N
- Level of Constant-Force, Ξ'

Average parameter values returned:

- Θ
- Force Parameter: β

6.1.4 Model Verification

The original constant-force parameters were used to develop a simple design spread sheet, which in turn was used to verify the output of the model. All 6 classes of mechanisms were used at both sub-classes *a* and *b*. In all 12 cases, the model agreed with the spread sheet and correctly calculated the parameter values presented in Chapters 4 and 5.

6.2 Optimization

The optimization is performed to determine the best combination of constant-force parameters that provides the most desirable CFM performance. The performance is measured based on the comparison methods described in Chapter 5.

6.2.1 Objective Functions

The prior work was concerned with finding mechanisms that have the highest percent constant-force. For this research, several different objectives are possible depending on the desired output. Different optimization problems are defined below, at which point the objective functions are clearly stated.

In several cases, dual objective functions could be used. However, the use of dual objective functions complicates the optimization process. Where possible, dual objective functions are reduced to a single objective function with the other objective function becoming a constraint.

6.2.2 Variables

The analytical variables for the optimization are all of the model inputs described above. In the search for new configurations, all comparisons are made so that material properties and mechanism size are not important. Therefore, these variables are set equal to 1. The variables that control the mechanism type and sub-class are set to the respective values for the desired mechanism.

The only variables that are used as design variables are the constant-force parameters. These parameters allow the optimization to modify the link length ratio, R, and the spring constant ratios, K, in search of mechanisms with more desirable performance.

6.2.3 Functions

The analytical functions for the optimization problem include all of the model outputs described above. The selection of analytical functions as design functions depends upon the objective of the optimization problem. For each optimization problem described below, the design functions are clearly outlined.

6.2.4 Optimization Problem - Stiffer Mechanisms

To develop mechanisms that are stiffer, thus allowing for higher forces with the same stress limits, it is important to maximize the stiffness parameter Ψ. In this case, to eliminate the dual objective functions, the parameter Ξ' can be established as a design function and constrained above a certain value.

Formally, this optimization problem is written as:

$$\text{Maximize } \Psi \tag{6.5}$$

subject to

$$\Xi' > \Xi'_c \tag{6.6}$$

6.2.5 Optimization Problem - Smaller Normal Displacement

The optimization program can look for mechanisms that have a smaller normal displacement by minimizing the normal displacement parameter. Once again, the percent constant-force parameter becomes a design function. Formally, the problem is written:

$$\text{Minimize } d_N \tag{6.7}$$

subject to

$$\Xi' > \Xi'_c \tag{6.8}$$

6.2.6 Optimization Problem - In-plane/Out-of-plane

To determine the best configurations that are suitable for in-plane and out-of-plane manufacturing orientations, it is necessary that the width and thickness ratios satisfy the criteria defined in Section 5.5.4 and tabulated in Table 5.4. Formally, the optimization problem is written as:

$$\text{Maximize } \Xi' \tag{6.9}$$

subject to

$$C \geq 1 \quad \text{and/or} \quad D_{min} \leq 1 \tag{6.10}$$

$$0.5 \leq D_{equeal} \leq 2 \tag{6.11}$$

6.2.7 Combinations of Optimization Problems

The optimization problems described above are summarized in Table 6.1. Not all of the possible optimization problems that can be examined for improvements in CFMs are represented in the table. In fact, the problems presented above can be combined in many different ways. One such way is shown in Table 6.1 under the title “Best Method”. This problem defines an optimization problem that searches for the stiffest mechanism that is suitable for in-plane and out-of-plane orientation, as well as a certain percent constant-force value.

Table 6.1 Summary of different possible optimization problems

Objective	Stiffness	Normal Displacement	Stamping	Milling	Best Overall
Objective Function	Maximize Ψ	Minimize d_N	Maximize Ξ'	Maximize Ξ'	Maximize Ψ
Design Functions	$\Xi' \geq \Xi'_c$	$\Xi' \geq \Xi'_c$	$C \geq 1$ $D_{equal} \leq 2$	$D_{min} \leq 2$	$\Xi' \geq \Xi'_c$ $C \geq 1$ $D_{equal} \leq 2$ $D_{min} \leq 1$

The optimization problems presented in the chapter are presented as examples and guidelines. The optimization problems used may not be suitable for all mechanism types, thereby requiring some alterations in the problems. The next chapter, Chapter 7, will identify the particular problems used in the search for better mechanisms within each configuration, as well as the results achieved.

CHAPTER 7 NEW MECHANISMS

This chapter presents the results of the optimization, including explore plots and optimum plots, increases in stiffness, and summarization of parameters.

7.1 New Mechanisms

One of the main objectives of this research is to find new and improved CFMs, principally CFMs stiffer than the original mechanisms. To accomplish this, each configuration was examined through optimization for new mechanisms which were evaluated by the criteria outlined in Chapter 5.

Two main objectives existed for the optimization: find the stiffest mechanisms for three different levels of constant-force (90, 95, and 99 percent constant-force), and find the stiffest mechanisms for the same four levels of constant-force that are suitable for fabrication in in-plane and out-of-plane orientations.

In many cases, suitable mechanisms could not be found for several of these objectives, and the objectives were altered.

7.1.1 Sub-class Expansion

Further definitions to the sub-class nomenclature presented earlier must be added to help distinguish between new mechanisms defined through optimization.

Two new additions to the sub-class definition are needed. First, the limit for the level of constant-force used in the optimization is added after the percent displacement letter. This number identifies the mechanism and the constraint used. The number does not give the actual percent constant-force value of the mechanism, only the constraint value used.

The second addition identifies the mechanism as suitable for fabrication in an in-plane orientation, “I”, an out-of-plane orientation, “O”, and/or possibly suitable for out-of-plane orientation, “o”. These letters, when added after the percent deflection letter and percent constant-force limit, identify the mechanism as suitable for these orientations, allowing the designer to know the options available.

As an example, if a new Class 2A-*ssp*-a mechanism were identified using a percent constant-force limit of 90 and could be oriented either in-plane or possibly out-of-plane, the classification for the mechanism would be Class 2A-*ssp*-a90Io. This name summarizes important information and provides a unique naming method for the mechanisms.

7.2 Class 1A

Class 1A was the first class of mechanisms examined. This class consists of both the *lpp* and *spp* mechanisms.

7.2.1 Optimization Details

The mechanisms that make up this class only have one flexible segment, thus making it the primary pivot. Additionally, with only one pivot, the mechanism is suitable for both the in-plane and out-of-plane orientations.

The constant-force parameters K_1 and K_2 are both zero, leaving only the parameter R to be a design variable. This makes the optimization very straightforward. Optimization was performed to find the stiffest mechanisms for each of the three new sub-classes with Ψ being the objective function.

7.2.2 Optimization Observations

An explore plot with R as the variable was generated for both configurations and deflection ranges. The constant-force parameter R was allowed to vary from 0.5 to 3.0. Once the explore plot was generated, graphs of the relationship of Ξ'_{ex} and Ψ with respect to R were generated. These plots are shown in Figure 7.1a. In both configurations, Ξ'_{ex} peaks where R is about 0.8 while Ψ decreases as R increases.

A visual representation of these relationships helps to understand where to focus the optimization and shows that the highest percent constant-force occurs around an R value of 0.8. This is consistent with the findings of the prior work. The graphs in Figure 7.1 also shows that in order to increase Ψ, R must be decreased, sacrificing the level of constant-force.

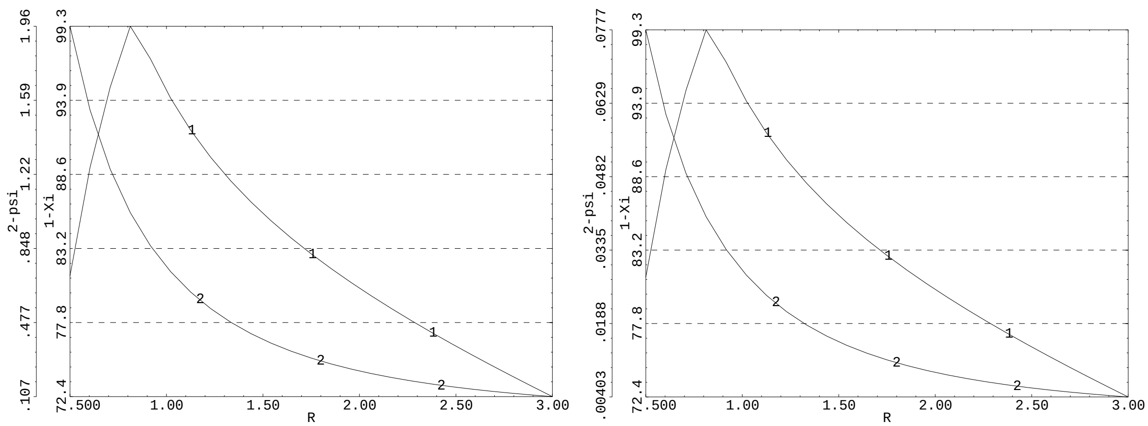

(a) (b)

Figure 7.1 Explore plot of R versus Ξ'_{ex} and Ψ for (a) Class 1A-*lpp*-a and (b) Class 1A-*spp*-a

7.2.3 Optimization Results

The optimization was able to improve the stiffness of both configurations within Class 1A for both deflection ranges. The results of the optimization are given in Table 7.1. The Class 1A-*lpp*-a and Class 1A-*spp*-a mechanisms both showed a 50% increase in stiff-

Table 7.1 Optimization results

Configuration	Sub-Class	Ξ'_{ex}	Ψ	R	$\%\Delta\Psi$	$\%\Delta\Xi'_{ex}$
lpp	a	99.7	1.000	0.8274	-	-
	a99	99	1.046	0.8018	4.6%	-0.7%
	a95	95	1.239	0.7106	23.9%	-4.7%
	a90	90	1.490	0.6185	49.0%	-9.7%
lpp	b	97.6	1.000	0.8853	-	-
	b99	N/A	N/A	N/A		
	b95	95	1.052	0.8595	5.2%	-4.7%
	b90	90	1.129	0.8226	12.9%	-9.7%
spp	a	99.7	0.039	0.8274	-	-
	a99	99	0.041	0.8018	4.9%	-0.7%
	a95	95	0.049	0.7104	24.9%	-4.7%
	a90	90	0.059	0.6187	50.8%	-9.7%
spp	b	97.6	0.039	0.8853	-	-
	b99	N/A	N/A	N/A		
	b95	95	0.041	0.8595	5.1%	-2.7%
	b90	90	0.044	0.8226	13.0%	-7.8%

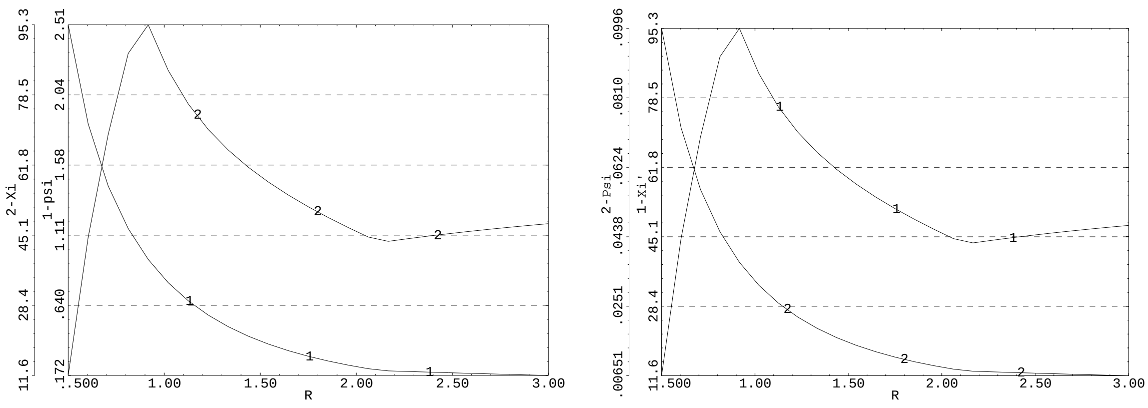

(a) (b)

Figure 7.2 Explore plot for (a) Class 1A-*lpp*-b and (b) Class 1A-*spp*-b

ness when Ξ'_{ex} was allowed to drop to 90. However, the *spp*-a configuration still only has about 4% of the total stiffness of the *lpp*-a.

The Class 1A-*lpp*-b and Class 1A-*spp*-b mechanisms had similar trends as the sub-class a mechanisms. However, at 90% constant, these mechanisms only showed a 13% increase in stiffness. Additionally, no feasible mechanism was found for both configurations at 99 percent constant-force. This is supported by the explore graph generated for these mechanisms. As seen in Figure 7.2, the highest Ξ'_{ex} value is around 95, the same as the prior work.

The optimization has defined stiffer mechanisms for three new sub-classes with 16% deflection and two new sub-classes with 40% deflection. If the design does not prevent the level of constant-force from being sacrificed, these new sub-classes can be used to obtain a higher stiffness in the mechanism. Table 7.2 summarizes the important design parameters for the Class 1A CFMs which can be used, in correlation with the equations developed earlier, to quickly design any new mechanism. The width and thickness ratios are not applicable for these configurations and are emitted from the table.

7.3 Class 1B

This class of CFMs consists of the *psp* and *plp* configurations.

7.3.1 Optimization Details

The optimization of these configurations was similar to the Class 1A configurations. These configurations also only contain one flexible pivot, the second pivot, indicating that this pivot is the primary pivot and all configurations are suitable for both in-plane and out-of-plane orientations.

For the optimization, K_1 must be set equal to 1, while K_2 is set equal to 0. Again, this leaves only R to be used as a design variable. The optimization is not complicated and new mechanisms for the three new sub-classes are easily defined.

Table 7.2 Parameter summary for new mechanisms in Class 1A.

Configuration	Sub-Class	Primary Pivot	Ξ'_{ex}	R	K_1	K_2	κ_1	κ_2	κ_3	Φ	β	Ψ	λ	M	n	d_{Nmax}
lpp	a	1	99.7	0.8274	0		3.50	-		0.4537	2.901	1.000	1.097	0.4501	0.5004	26.96
	a99		99.0	0.8018			3.45			0.4439	2.759	1.046	1.098	0.4373	0.4994	26.90
	a95		95.0	0.7106			3.28			0.4067	2.279	1.239	1.103	0.3923	0.4952	26.57
	a90		90.0	0.6185			3.10			0.3653	1.832	1.492	1.109	0.3479	0.4898	26.04
lpp	b	1	97.6	0.8853	0		3.61	-		0.4773	3.248	1.002	1.094	0.4788	0.5033	39.79
	b99															
	b95		95.0	0.8595			3.56			0.4630	3.065	1.052	1.095	0.4683	0.5000	39.68
	b90		90.0	0.8226			3.49			0.4421	2.812	1.129	1.097	0.4535	0.4949	39.47
spp	a	1	99.7	0.8274	0		18.27	-		0.4537	15.152	0.039	1.027	2.3511	0.5004	26.96
	a99		99.0	0.8018			18.02			0.4439	14.412	0.041	1.028	2.2841	0.4994	26.90
	a95		95.0	0.7104			17.10			0.4066	11.895	0.049	1.029	2.0482	0.4951	26.57
	a90		90.0	0.6187			16.19			0.3654	9.576	0.059	1.031	1.8177	0.4898	26.04
spp	b	1	97.6	0.8853	0		18.85	-		0.4773	16.964	0.039	1.027	2.5006	0.5033	39.79
	b99															
	b95		95.0	0.8595			18.60			0.4630	16.010	0.041	1.027	2.4460	0.5000	39.68
	b90		90.0	0.8226			18.23			0.4421	14.686	0.044	1.027	2.3687	0.4949	39.47

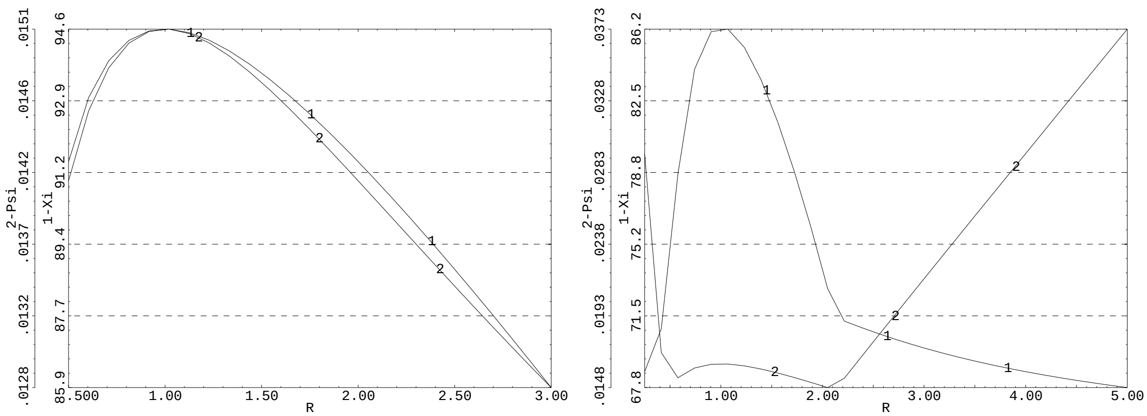

(a) (b)

Figure 7.3 Explore plots for (a) Class 1B-*psp*-a (b) Class 1B-*psp*-b

7.3.2 Optimization Observations

Four explore plots were generated, one each for every combination of configuration and displacement percentage. Figure 7.3 shows the explore plots for the *psp* configuration. The peaks in the parameter Ξ'_{ex} are clearly visible and correspond to the values found in the original works. Additionally, according to Figure 7.3a, Ψ peaks at the same point as Ξ'_{ex} for the Class 1B-*psp*-a mechanism, thus indicating that no improvements are possible. Examination of Ψ in Figure 7.3b shows that increases in Ψ occur only once Ξ'_{ex} has decreased below 75. This indicates that stiffer mechanisms for the three new subclasses cannot be determined for Class 1B-*psp*-b.

The explore plots for the *plp* configurations in Figure 7.4 appear similar to the explore plots in Figure 7.3. In fact, within the same percent deflection and between the two configurations, the curves for Ξ'_{ex} are identical. The differences are in the Ψ curves.

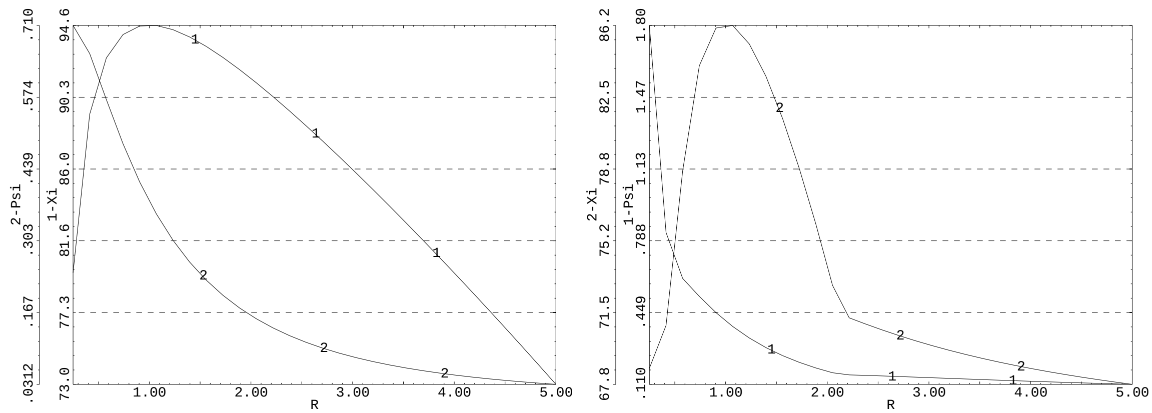

(a) (b)

Figure 7.4 Explore plots for (a) Class 1B-*plp*-a (b) Class 1B-*plp*-b

This is consistent with expectations as Ξ'_{ex} is based on the PRBM which does not change between configurations within a certain class, while Ψ is based on the actual configuration of flexible segments.

Once again the peaks in Ξ'_{ex} correspond with the original work, indicating no improvement in Ξ'_{ex}. However, the peaks in the Ψ curves do not correspond to the peaks in the Ξ'_{ex} curve as they did with the *psp* configurations. This offset between the Ξ'_{ex} and Ψ curves provides an opportunity for trade-offs between stiffness and percent constant-force.

7.3.3 Optimization Results

The results of the optimization are summarized in Table 7.3. As expected, no feasible mechanisms for the *psp* with either percent deflection were found that offered a higher stiffness while keeping percent constant-force above 90.

For the Class 1B-*plp*-a mechanisms, feasible mechanisms for percent constant-force values of 95 and 99 could not be found. Therefore, stiffer mechanisms were searched for at percent constant-force levels of 80, 85, and 90. The Class 1B-*plp*-a90 mechanism showed an increase of 70% while the Class 1B-*plp*-a80 mechanism increased in stiffness by 88%.

Improved mechanisms for Class 1B-*plp*-b were found for 80 and 85 percent constant-force values. These mechanisms showed an increase of 22% and 45% in stiffness from the original mechanism. The summary of the parameters for the Class 1B mechanisms is found in Table 7.4

Table 7.3 Optimization results for Class 1B configurations

Configuration	Sub-class	Ξ'_{ex}	Ψ	R	$\%\Delta\Psi$	$\%\Delta\Xi'_{ex}$
psp	a	94.6	0.015	1.0000	-	-
	a99	N/A				
	a95	N/A				
	a90	N/A				
psp	b	86.3	0.016	1.0000	-	-
	b99	N/A	N/A	N/A		
	b95	N/A	N/A	N/A		
	b90	N/A	N/A	N/A		
plp	a	94.6	0.378	1.0000	-	-
	a99	N/A	N/A	N/A		
	a95	N/A	N/A	N/A		
	a90	90	0.644	0.4388	70.4%	-4.9%
	a85	85	0.698	0.3170	84.7%	-10.2%
	a80	80	0.710	0.2530	87.8%	-15.5%
plp	b	86.3	0.409	1.0000	-	-
	b99	N/A				
	b95	N/A				
	b90	N/A				
	b85	85	0.500	0.7919	22.1%	-1.5%
	b80	80	0.596	0.6043	45.5%	-7.3%

7.4 Class 2A

The Class 2A mechanisms consist of the *slp* and *ssp* configurations. These mechanisms are combinations of the Class 1A-*spp* and Class 1B-*psp* and pl_3p configurations.

7.4.1 Optimization Details

These configurations presented more difficulty to the optimization and in determining which mechanisms to include in this work. This difficulty comes from the introduction of a second design variable because of the use of two flexible segments. Additionally, the ratios between the thickness and width of these two flexible segments are important and must be considered during optimization.

The parameters R and K_1 are the two design variables for the optimization, while the thickness and width ratios for the first two pivots are added as design functions. Multiple starting points were used to find different local minimums.

Table 7.4 Parameter summary for new mechanisms of Class 1B

Configuration	Sub-Class	Primary Pivot	Ξ'_{ex}	R	K_1	K_2	κ_1	κ_2	κ_3	Φ	β	Ψ	λ	M	n	d_{Nmax}
psp	a	2	94.6	1	1	0	-	20.00	-	2.0560	82.242	0.015	1.000	5.6291	0.5062	27.13
psp	b	2	86.3	1	1	0	-	20.00	-	2.1500	86.000	0.016	1.000	5.4974	0.5164	40.00
plp	a		94.6	1				3.83		2.0561	15.747	0.378	1.088	1.0777	0.5062	27.13
	a90	2	90.0	0.4387	1	0	-	2.75	-	3.4511	13.677	0.644	1.123	0.8380	0.5115	24.03
	a85		85.0	0.3170				2.52		4.4878	14.904	0.698	1.134	0.8214	0.5176	21.34
	a80		80.0	0.2529				2.40		5.4987	16.527	0.710	1.141	0.8272	0.5239	19.11
plp	b		86.3	1				3.83		2.1501	16.466	0.409	1.088	1.0525	0.5164	40.00
	b85	2	85.0	0.7919	1	0	-	3.43	-	2.4473	15.046	0.500	1.098	0.9468	0.5178	39.24
	b80		80.0	0.6043				3.07		2.9399	14.487	0.596	1.110	0.8593	0.5233	36.46

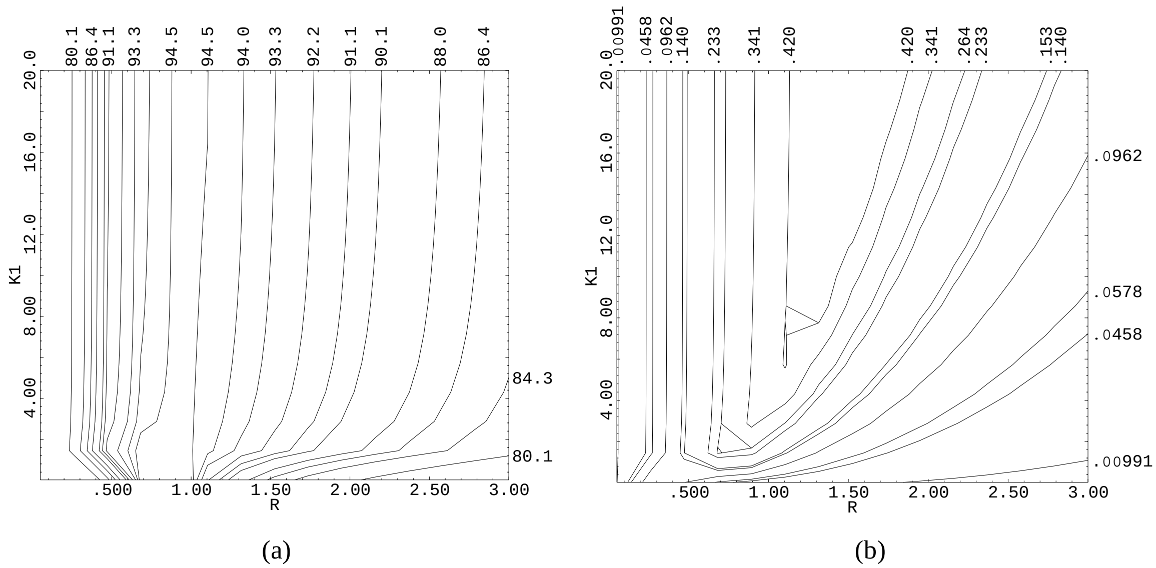

Figure 7.5 2-D explore plots for *slp*-a of R and K_1 with contours of (a) Ξ'_{ex} and (b) Ψ

7.4.2 Optimization Observations

The *slp*-a configuration was considered first. Two 2-D explore plots were generated for this mechanism and are shown in Figure 7.5 with R and K_1 on the horizontal and vertical axes. These plots show contours of Ξ'_{ex} in Figure 7.5a and Ψ in Figure 7.5b. Examination of these plots show that Ξ'_{ex} is fairly independent of K_1 but highly dependent on R. Additionally, K_1 has very little effect on Ψ for values of R below 1, but a large effect on Ψ for larger values of R. The parameter R also affects Ψ.

These observations are valuable and give insight into the mechanism. The value for K_1, since it has little effect on Ξ'_{ex}, should be made as large as possible. However, by increasing K_1, the ratio of the spring constants is increased, affecting the width and thick-

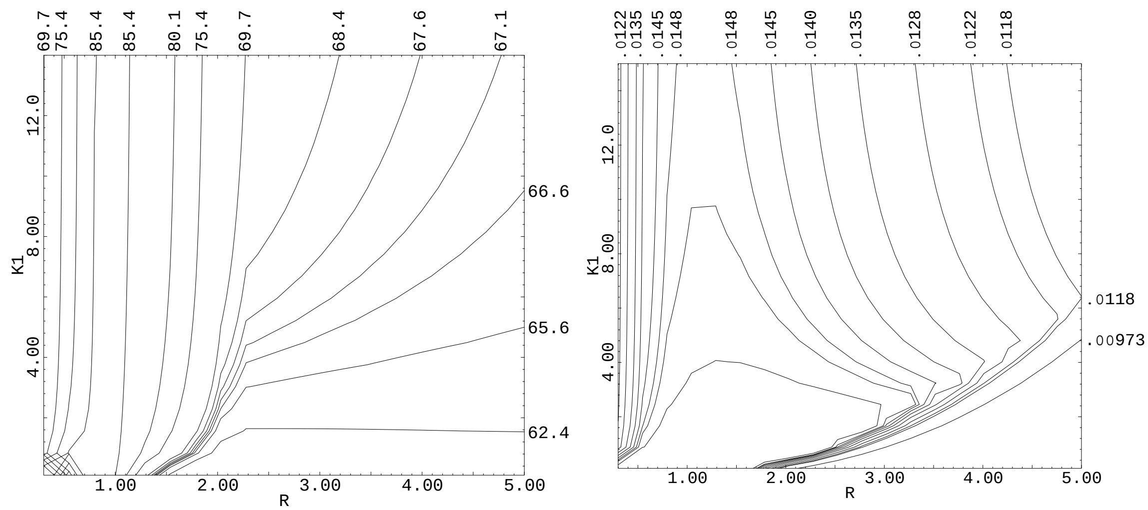

(a) (b)

Figure 7.6 2-D explore plots for *ssp*-a with R vs. K_1 and contours of (a) Ξ'_{ex} and (b) Ψ

ness ratios. Ultimately, K_1 can only be increased so much before fabricating the mechanism becomes infeasible.

The 2-D explore plots for *slp*-b showed similar relationships among the parameters. These plots can be found in Appendix C under Figure C.1.

The *ssp*-a and *ssp*-b configurations were examined in the same way as the *slp* configurations. The 2-D explore plots for the *ssp*-a configurations can be found in Figure 7.6. These plots show that the contours of Ξ'_{ex} are similar to those found in Figure 7.5a. However, the contours for Ψ are different. In this mechanism, the area in which Ψ is the highest corresponds to the area with the highest Ξ'_{ex}. Additionally, in this area, as K_1 decreases, Ψ increases, indicating that K_1 should be minimized.

The *ssp*-b explore plots, shown in Figure C.2 in Appendix C, display the same trends as those found in the *ssp*-a configuration.

7.4.3 Optimization Results

The optimization of the Class 2A mechanisms resulted in the identification of stiffer mechanisms and the definition of mechanisms suitable for in-plane and out-of-plane fabrication orientations. These improvements are summarized in Table 7.5.

The original *slp*-a sub-class was suitable for in-plane orientations, and possibly suitable for out-of-plane orientations. A new sub-class was found that had the same level of constant-force, was suitable for both in-plane and out-of-plane orientations, and had a 50% increase in stiffness. Another sub-class was found for this configuration that allowed the level of constant-force to decrease to 90, but increased the stiffness by 268%. This rep-

Table 7.5 Optimization results for Class 2A

Configuration	Sub-Class	Ξ'_{ex}	Ψ	R	K_1	$\%\Delta\Psi$	$\%\Delta\Xi'_{ex}$
slp	asI	99.8	0.145	0.3950	0.1906	-	-
	a99IO	99	0.219	0.5057	0.2640	51.4%	-0.8%
	a95Io	95	0.338	0.8237	1.6370	133.6%	-4.8%
	a90I	93	0.534	1.5278	15.0000	268.7%	-6.8%
	a90IO	97.7	0.233	0.5437	0.3521	61.0%	-2.1%
slp	bIO	99.8	0.181	0.4323	0.2237	-	-
	b99	N/A	N/A	N/A	N/A		
	b95IO	96	0.294	0.6248	0.3924	62.9%	-3.8%
	b90Io	90	0.331	0.7267	0.8283	83.4%	-9.8%
ssp	asI	99.8	0.017	0.3950	0.1906	-	-
	a99I	99	0.042	0.7864	0.1000	141.4%	-0.8%
	a95I	96.2	0.048	0.9182	0.1000	176.9%	-3.6%
	a95IO	95	0.022	0.9563	0.5113	24.3%	-4.8%
	a90IO	90	0.028	1.4688	0.4050	59.5%	-9.8%
ssp	bsI	99.4	0.019	0.4323	0.2237	-	-
	b99	N/A	N/A	N/A	N/A		
	b94I	94	0.030	0.3000	0.1000	54.5%	-5.4%
	b90IO	90	0.022	0.8714	0.5343	14.7%	-9.5%
	b90o	91.2	0.052	0.9325	0.1000	170.8%	-8.2%

resents a fairly large increase in stiffness, with only a marginal decrease in percent constant-force. The other new sub-classes for *slp*-a are shown in Table 7.5.

In the *slp*-b configuration, the original sub-class was the best mechanism that could be found for the given value of Ξ'_{ex}. However, a decrease of 10 in Ξ'_{ex} provided an increase of 83% in stiffness.

The original *ssp*-a configuration was improved by 141% without changing Ξ'_{ex}. However, the original sub-class was possibly suitable for out-of-plane orientation, while the new sub-class was not suitable for out-of-plane orientation. When the out-of-plane orientation constraints were removed from the optimization, the stiffest mechanism that could be found with Ξ'_{ex} values between 90 and 100 was the a95M sub-class. This sub-class has a Ξ'_{ex} value of 96.2 and a 176.9% increase in stiffness over the original sub-class. However, forcing the optimization to look for sub-classes suitable for in-plane and out-of-plane orientations resulted in improvements of 24% for 95 percent constant-force and 60% increase for 90 percent constant-force.

The final configuration in this class of CFMs is the *ssp*-b. As with the *slp*-b, the original sub-class was the stiffest mechanism that could be found for 99 percent constant-force. However, a sub-class, not suitable for in-plane orientation and only possibly suitable for out-of-plane fabrication orientation, was found for 90 percent constant-force with a 170% increase in stiffness.

In all, the results of the optimization are promising. Many new sub-classes are presented in Table 7.5. The important design parameters for these new sub-classes are summarized in Table 7.6 while the thickness and width ratios determined from the optimization are summarized in Table 7.7.

Table 7.6 Summary of Class 2A parameters

Configuration	Sub-Class	Primary Pivot	Ξ'_{ex}	R	K_1	K_2	κ_1	κ_2	κ_3	Φ	β	Ψ	λ	M	n	d_{Nmax}
slp	aIo	2	99.8	0.3950	0.1906	0	13.95	6.76	-	0.9573	18.628	0.145	1.086	2.0988	0.5132	23.23
	a99IO	2	99.0	0.5057	0.2640	0	15.06	5.70	-	1.1290	25.595	0.219	1.092	1.6933	0.5097	24.97
	a95Io	1	95.0	0.8237	1.6370	0	18.24	4.24	-	4.1829	139.117	0.338	1.107	2.3414	0.5002	26.95
	a90I	1	93.3	1.5278	15.0000	0	25.28	3.17	-	26.3159	1681.489	0.534	1.126	4.3532	0.5175	26.28
	a90IO	2	97.7	0.5437	0.3521	0	15.44	5.44	-	1.3688	32.622	0.233	1.095	1.5975	0.5090	25.39
slp	bIO	2	99.4	0.4323	0.2237	0	14.32	6.34	-	1.0467	21.473	0.181	1.088	1.8373	0.5341	30.18
	b99															
	b95IO	1	96.2	0.6248	0.3924	0	16.25	4.98	-	1.4438	38.116	0.294	1.099	1.9768	0.4578	36.92
	b90Io	1	90.0	0.7267	0.8283	0	17.27	4.55	-	2.5248	75.281	0.331	1.103	2.1734	0.4794	38.58
ssp	aIo	2	99.8	0.3950	0.1906	0	13.95	20.00	-	0.9573	18.628	0.017	1.036	6.2080	0.5132	23.23
	a99I	2	99.0	0.7864	0.1000	0	17.86	20.00	-	0.6718	21.440	0.042	1.028	5.6676	0.5066	26.85
	a95I	2	96.2	0.9182	0.1000	0	19.18	20.00	-	0.7015	25.810	0.048	1.026	5.6339	0.5062	27.09
	a95IO	2	95.0	0.9563	0.5113	0	19.56	20.00	-	1.5750	60.277	0.022	1.026	5.6304	0.5062	27.12
	a90IO	2	90.0	1.4688	0.4050	0	24.69	20.00	-	1.3429	81.851	0.028	1.020	5.7279	0.5073	26.43
ssp	bIo	2	99.4	0.4323	0.2237	0	14.32	20.00	-	1.0467	21.473	0.019	1.035	5.7929	0.5341	30.18
	b99															
	b94I	2	94.1	0.3000	0.1000	0	13.00	20.00	-	0.6423	10.854	0.030	1.038	6.3534	0.5372	23.08
	b90IO	2	90.0	0.8714	0.5343	0	18.71	20.00	-	1.7057	59.736	0.022	1.027	5.5051	0.5168	39.74
	b90o	2	91.2	0.9323	0.1000	0	19.32	20.00	-	0.7255	27.087	0.052	1.026	5.4994	0.5165	39.93

Table 7.7 Summary of Class 2A thickness and width ratios

Configuration	Sub-Class	Primary Pivot	C_1	C_2	C_3	D_{1equal}	D_{2equal}	D_{3equal}	D_{1min}	D_{2min}	D_{3min}
slp	aIo	2	1.71	1.00	-	2.54	1.00	-	0.51	1.00	-
	a99IO	2	1.13	1.00	-	1.43	1.00	-	1.00	1.00	-
	a95Io	1	1.00	1.92	-	1.00	7.04	-	1.00	1.00	-
	a90I	1	1.00	4.82	-	1.00	119.69	-	1.00	1.07	-
	a90IO	2	1.00	1.00	-	1.00	1.00	-	1.00	1.00	-
slp	bIO	2	1.47	1.00	-	1.98	1.00	-	0.63	1.00	-
	b99										
	b95IO	1	1.00	1.09	-	1.00	1.28	-	1.00	1.00	-
	b90Io	1	1.00	1.47	-	1.00	3.14	-	1.00	1.00	-
ssp	aIo	2	5.07	1.00	-	7.52	1.00	-	0.06	1.00	-
	a99I	2	2.54	1.00	-	11.20	1.00	-	0.68	1.00	-
	a95I	2	2.18	1.00	-	10.43	1.00	-	1.01	1.00	-
	a95IO	2	2.09	1.00	-	2.00	1.00	-	0.22	1.00	-
	a90IO	2	1.33	1.00	-	2.00	1.00	-	0.84	1.00	-
ssp	bIo	2	4.63	1.00	-	6.24	1.00	-	0.06	1.00	-
	b99										
	b94I	2	6.67	1.00	-	15.38	1.00	-	0.05	1.00	-
	b90IO	2	2.30	1.00	-	2.00	1.00	-	0.17	1.00	-
	b90o	2	2.15	1.00	-	10.35	1.00	-	1.05	1.00	-

7.5 Class 2B

The *lps* and *sps* configuration make up the 2B class of CFMs. The original configurations in this class of CFMs exhibit the lowest values for percent constant-force of all the original mechanisms.

7.5.1 Optimization Details

The optimization of the Class 2B configurations was done similar to the Class 2A configurations with the only difference being a broadening of focus from increasing stiffness to increasing stiffness and increasing the percent constant-force.

7.5.2 Optimization Observations

The optimization of the *lps* found many different sub-classes that looked promising, making the task of selecting sub-classes to be presented in this work challenging. An optimum plot was generated to help view the design area, and is shown in Figure 7.7. The plot shows the values for Ξ'_{ex} and Ψ, as well as the optimal value for K_2, for any given R value. Two peaks in Ξ'_{ex} are present in the graph. The peak centered at an R value of 2.50 corresponds with higher values of Ξ'_{ex} than the peak centered at 0.75. Therefore, mechanisms within this area were considered. The optimum plot for the lps-b mechanism can be found in Figure C.2 in Appendix C.

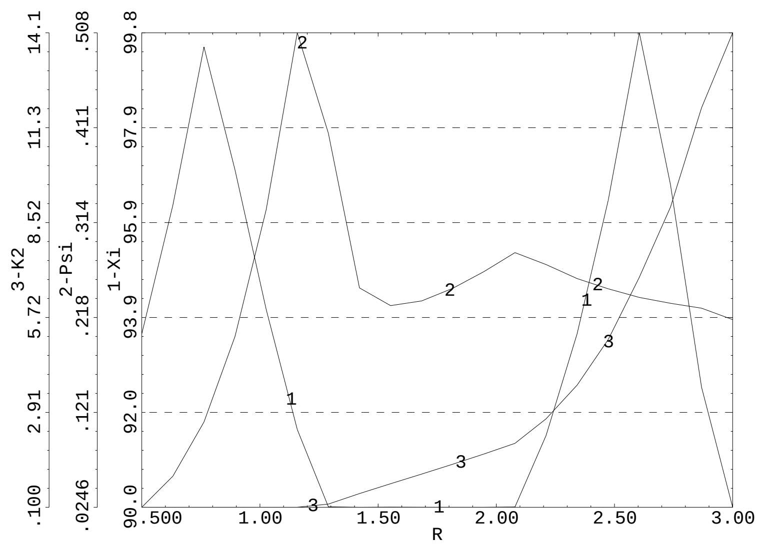

Figure 7.7 Optimum plot for *lps*-a which shows Ξ'_{ex}, Ψ and optimal K_2 for given R values

The change in the type of flexible segments from the *lps* to the *sps* greatly affects the optimization problem and the associated results. Explore plots, similar to those generated for the Class 2A configurations were generated for the *sps*-a configuration. The highest Ξ'_{ex} and Ψ values are located around an R value of 1 and a K_2 value of 1, as seen in Figure 7.8. It is in this area that the search was focused and new sub-classes were found. Similar plots and results were found for the *sps*-b configuration and can be seen in Figure C.4 in Appendix C.

7.5.3 Optimization Results

Large improvements in the Class 2B configurations were found. These improvements are summarized in Figure 7.8. For the *lps*-a configuration, improvements ranged from increases in stiffness of 565% to 1000%, depending on the level of constant-force

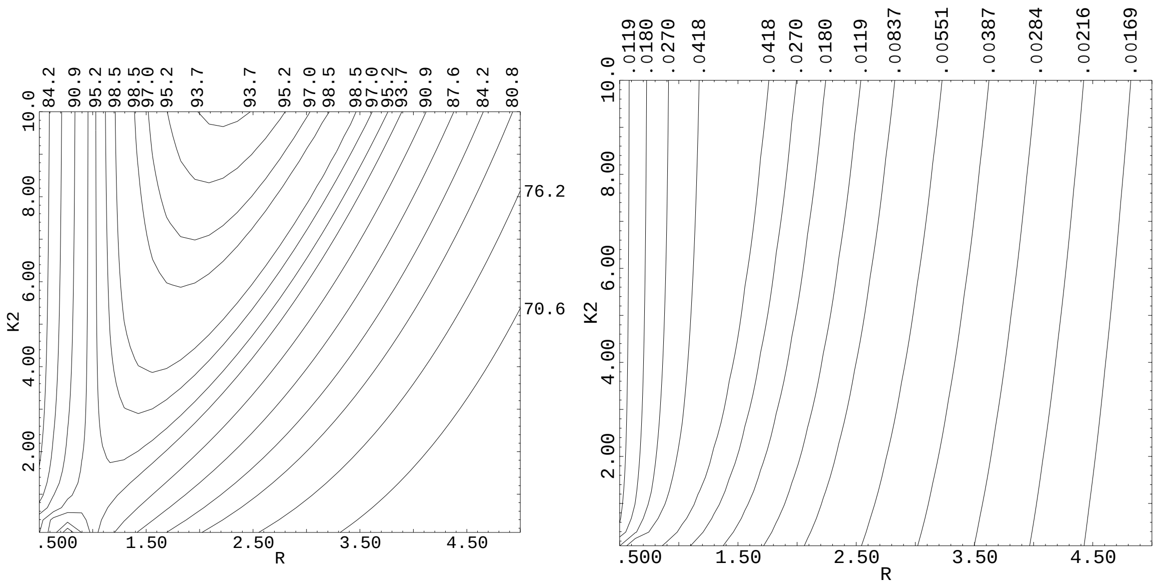

(a) (b)

Figure 7.8 2-D explore plots for *sps*-a with *R* vs. K_2 and contours of (a) Ξ'_{ex} and (b) Ψ

Table 7.8 Optimization results for Class 2B

Configuration	Sub-Class	Ξ'_{ex}	Ψ	R	K_2	$\%\Delta\Psi$	$\%\Delta\Xi'_{ex}$
lps	aIo	93.2	0.026	0.7591	1.0029		
	a99I	99	0.241	2.5750	6.4256	826.5%	6.2%
	a95I	95	0.253	2.4050	4.3690	873.1%	1.9%
	a90	90	0.286	2.0960	2.0313	1000.0%	-3.4%
	a99IO	99	0.173	2.1623	5.1740	565.4%	6.2%
	a95IO	95	0.211	2.1623	3.6510	711.5%	1.9%
	a90IO	90	0.278	2.1623	2.4156	968.5%	-3.4%
lps	bsI	83.7	0.035	0.8441	1.0230		
	b99IO	99	0.222	1.9335	4.9463	539.8%	18.3%
	b95IO	95	0.235	1.9339	4.5230	576.4%	13.5%
	b90IO	90	0.252	1.9290	3.9830	626.2%	7.5%
	b95I	95	1.053	0.8561	0.0100	2934.2%	13.5%
	b90I	90	1.137	0.8177	0.0100	3177.2%	7.5%
sps	aIO	93.1	0.028	0.7591	1.0029		
	a99I	99	0.063	0.7328	0.1845	123.8%	6.7%
	a90IO	95	0.057	1.0000	1.0022	104.6%	1.7%
sps	bsI	84	0.037	0.8441	1.0235		
	b98Io	98	0.031	0.6528	0.2549	-17.2%	17.6%
	b86IO	86	0.062	1.0000	1.0000	68.6%	3.2%

and manufacturing process constraints. In all, six new sub-classes were added for 16% deflection, three suitable for both in-plane and out-of-plane orientations, and three unconstrained by manufacturing orientations.

The *lps*-b configurations had increases in stiffness from 539% to 3177%. This represents a significant improvement. In fact, the b95I and b90I sub-classes have higher stiffness parameters than any of the original configurations and sub-classes. Additionally, the level of constant-force was increased from the original value of 84 to a high of 99. In all, five new sub-classes were added to this configuration.

The *sps*-a configuration showed moderate increases in stiffness of about 100%. The level of constant-force was increased from 93 to 99 while stiffness for the same sub-class was increased 123%. The a90IO sub-class was constrained to greater than or equal to 90 percent constant-force. However, the result was a sub-class suitable for out-of-plane and in-plane orientation, 95 percent constant-force, and an increase of 104% in stiffness.

Very little increase in stiffness was found for the *sps*-b configuration. For the b86IO sub-class, stiffness was increased by only 68%. However, a large increase from the original value of 84 to a high of 98 percent constant-force was achieved with sub-class b98Io . This is a substantial increase in the level of constant-force.

All of the important design parameters for the CFM Class 2B are summarized in Figure 7.9, with the thickness and width ratios summarized in Figure 7.10.

7.6 Class 3A

The last class of CFMs is Class 3A, consisting of only the *sss* configuration.

7.6.1 Optimization Details

The optimization of the *sss* configuration requires that R, K_1, and K_2 be design variables. Additionally, all of the width and thickness ratios must be added as design func-

Table 7.9 Summary of Class 2B parameters

Configuration	Sub-Class	Primary Pivot	Ξ'_{ex}	R	K_1	K_2	κ_1	κ_2	κ_3	Φ	β	Ψ	λ	M	n	d_{Nmax}
lps	alo	3	93.1	0.7591	0	1.0029	3.37	-	23.17	1.2248	7.257	0.026	1.122	3.7184	0.5137	26.77
	a99I	3	99.0	2.5750	0	6.4256	6.84	-	13.88	1.4238	34.840	0.241	1.085	1.2616	0.4656	23.10
	a95I	3	95.0	2.4052	0	4.3688	6.52	-	14.16	1.2692	28.177	0.253	1.087	1.3261	0.4699	23.63
	a90	1	90.0	2.0960	0	2.0313	5.93	-	14.77	1.0408	19.101	0.287	1.091	1.1869	0.5256	24.60
	a99IO	3	99.0	2.1623	0	5.1740	6.05	-	14.62	1.4476	27.717	0.173	1.090	1.4370	0.4761	24.39
	a95IO	3	95.0	2.1623	0	3.6510	6.05	-	14.62	1.2475	23.885	0.211	1.090	1.4370	0.4761	24.39
	a90IO	3	90.8	2.1623	0	2.4156	6.05	-	14.62	1.0851	20.776	0.278	1.090	1.4370	0.4761	24.39
lps	blo	3	83.7	0.8441	0	1.0230	3.53	-	21.85	1.2126	7.895	0.035	1.119	3.1623	0.5331	39.60
	b99IO	3	99.0	1.9336	0	4.9463	5.62	-	15.17	1.5344	25.282	0.222	1.093	1.7882	0.4250	33.91
	b95IO	3	95.0	1.9339	0	4.5230	5.62	-	15.17	1.4816	24.419	0.235	1.093	1.7881	0.4249	33.91
	b90IO	3	90.0	1.9292	0	3.9830	5.61	-	15.18	1.4161	23.263	0.252	1.093	1.7902	0.4254	33.95
	b95I	1	95.0	0.8561	0	0.0100	3.55	-	21.68	0.4683	3.089	1.053	1.118	0.4670	0.4995	39.66
	b90I	1	90.0	0.8178	0	0.0100	3.48	-	22.23	0.4472	2.829	1.137	1.120	0.4516	0.4942	39.44
sps	alO	3	93.1	0.7591	0	1.0029	17.59	-	23.17	1.2248	37.901	0.028	1.050	3.7183	0.5137	26.77
	a99I	1	99.3	0.7328	0	0.1845	17.33	-	23.65	0.5711	17.147	0.063	1.050	2.1056	0.4963	26.67
	a90IO	3	94.6	1.0000	0	1.0022	20.00	-	20.00	1.0292	41.166	0.057	1.050	2.8145	0.5062	27.13
sps	blo	3	83.7	0.8441	0	1.0235	18.44	-	21.85	1.2129	41.247	0.037	1.050	3.1623	0.5331	39.60
	b98lo	3	98.4	0.6528	0	0.2549	16.53	-	25.32	0.6380	17.429	0.031	1.050	3.9715	0.5572	37.47
	b86IO	3	86.3	1.0000	0	1.0000	20.00	-	20.00	1.0750	43.001	0.062	1.050	2.7487	0.5164	40.00

Table 7.10 Summary of Class 2B thickness and width ratios

Configuration	Sub-Class	Primary Pivot	C_1	C_2	C_3	D_{1equal}	D_{2equal}	D_{3equal}	D_{1min}	D_{2min}	D_{3min}
lps	alo	3	9.07	-	1.00	6.86	-	1.00	0.01	-	1.00
	a99I	3	0.68	-	1.00	0.32	-	1.00	1.00	-	1.00
	a95I	3	0.79	-	1.00	0.50	-	1.00	1.00	-	1.00
	a90	1	1.00	-	0.84	1.00	-	0.82	1.00	-	1.37
	a99IO	3	1.00	-	1.00	0.47	-	1.00	0.47	-	1.00
	a95IO	3	1.00	-	1.00	0.66	-	1.00	0.66	-	1.00
	a90IO	3	1.00	-	1.00	1.00	-	1.00	1.00	-	1.00
lps	blo	3	7.33	-	1.00	6.05	-	1.00	0.02	-	1.00
	b99IO	3	0.99	-	1.00	0.55	-	1.00	0.56	-	1.00
	b95IO	3	0.99	-	1.00	0.60	-	1.00	0.61	-	1.00
	b90IO	3	1.00	-	1.00	0.68	-	1.00	0.68	-	1.00
	b95I	1	1.00	-	0.13	1.00	-	0.00	1.00	-	0.73
	b90I	1	1.00	-	0.12	1.00	-	0.00	1.00	-	0.98
sps	alO	3	1.74	-	1.00	1.31	-	1.00	0.25	-	1.00
	a99I	1	1.00	-	0.52	1.00	-	0.14	1.00	-	0.98
	a90IO	3	1.00	-	1.00	1.00	-	1.00	1.00	-	1.00
sps	blo	3	1.40	-	1.00	1.16	-	1.00	0.42	-	1.00
	b98lo	3	2.35	-	1.00	6.01	-	1.00	0.46	-	1.00
	b86IO	3	1.00	-	1.00	1.00	-	1.00	1.00	-	1.00

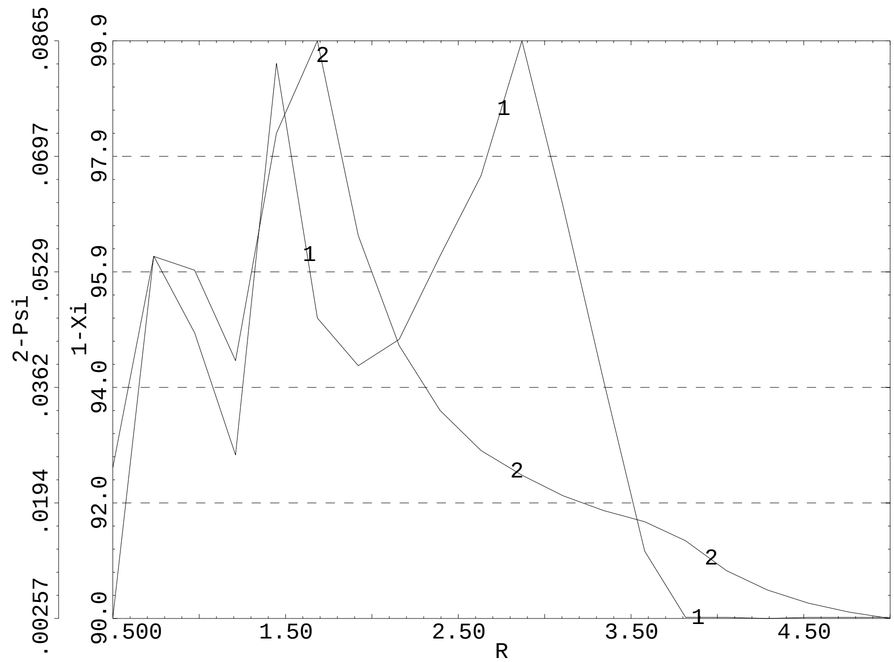

Figure 7.9 Optimum plot of design variables K_1 and K_2 versus R for *sss*-b with curves of Ξ'_{ex} and Ψ

tions. The increase in the number of design variables and design functions complicates the optimization.

7.6.2 Optimization Observations

The addition of a third design variable limits the usefulness of 2-D explore plots. Therefore, an optimum plot, shown in Figure 7.9, was generated with R as the independent variable and K_1 and K_2 as design variables. This plot clearly shows the local optima, the peaks of both Ξ'_{ex} and Ψ, and their correlation. Both curves have peaks around an R value of 1.5. It is in this area that the optimization was concentrated. The explore plot for *sss*-b is similar to Figure 7.9 and can be found in Figure C.5 in Appendix C.

7.6.3 Optimization Results

Four new sub-classes are added for the *sss*-a configuration. The a99 sub-class has the same level of constant-force, but shows an increase of 291% in stiffness. The a95IO and the a90IO sub-classes are both suitable for in-plane and out-of-plane orientations. The a95I sub-class is not suitable for out-of-plane orientation, but shows a 317% increase in stiffness over the original sub-class. The results, plus the results for *sss*-b, are summarized in Table 7.11.

For the *sss*-b configuration, three sub-classes are added. The b99 and b90I sub-classes showed a 14% and 158% increase in stiffness respectively with the b90I sub-class finding the stiffest mechanism to be 96 percent constant-force. The final sub-class, b88IO, is the highest percent constant-force mechanism found suitable for in-plane and out-of-plane fabrication orientations.

Once again, the important parameters have been summarized and can be found in Table 7.12, with width and thickness ratios found in Table 7.13.

Table 7.11 Optimization results for Class 3A

Configuration	Sub-Class	Ξ'_{ex}	Ψ	R	K_1	K_2	$\%\Delta\Psi$	$\%\Delta\Xi'_{ex}$
sss	a	99.97	0.020	0.3950	1.0000	12.6700		
	a99	99	0.079	1.4903	0.3497	8.3820	291.7%	-1.0%
	a95IO	95	0.021	1.3464	1.7047	2.9708	5.4%	-5.0%
	a95I	96	0.084	1.6573	0.4140	15.3420	317.8%	-4.4%
	a90IO	91	0.031	1.5518	0.3969	0.6459	52.5%	-9.0%
sss	b	99.5	0.029	2.0821	1.0000	9.3816		
	b99	99	0.033	1.8709	0.6930	7.1497	13.7%	-0.5%
	b90I	96	0.076	1.2420	0.3329	5.4511	157.8%	-3.2%
	b88IO	88	0.024	1.1990	1.8187	3.3349	-19.8%	-11.3%

7.7 Optimization Results Summary

Many improvements in stiffness were made within each class of CFMs. In some classes, increases in stiffness of as much as 3000% were made. However, the maximum stiffness of CFMs did not see much increase. Originally, the Class 1A-*lps*-a mechanism had the largest stiffness parameter with a value of 1.

Table 7.12 Summary of Class 3A parameters

Configuration	Sub-Class	Primary Pivot	Ξ'_{ex}	R	K_1	K_2	κ_1	κ_2	κ_3	Φ	β	Ψ	λ	M	n	d_{Nmax}
sss	a	1	100.0	2.6633	1.0000	12.6700	36.63	20.00	13.75	3.4016	456.482	0.020	1.050	8.2162	0.5324	22.82
	a99	1	99.4	1.4903	0.3497	8.3820	24.90	20.00	16.71	3.4388	213.264	0.079	1.050	4.2382	0.5168	26.37
	a95IO	2	95.0	1.3464	1.7047	2.9708	23.46	20.00	17.43	4.6011	253.313	0.021	1.050	5.6882	0.5068	26.71
	a95I	3	95.6	1.6573	0.4140	15.3423	26.57	20.00	16.03	4.6831	330.679	0.084	1.050	1.7796	0.4888	25.93
	a90IO	2	91.1	1.5518	0.3970	0.6459	25.52	20.00	16.44	1.4903	97.043	0.031	1.050	5.7582	0.5076	26.21
sss	b	1	99.5	2.0821	1.0000	9.3816	30.82	20.00	14.80	3.6285	344.684	0.029	1.050	5.2859	0.5883	32.44
	b99	1	99.0	1.8709	0.6930	7.1497	28.71	20.00	15.34	3.0645	252.583	0.033	1.050	4.7814	0.5768	34.51
	b90I	3	96.3	1.2420	0.3330	5.4510	22.42	20.00	18.05	3.1967	160.686	0.076	1.050	2.3326	0.4923	39.35
	b88IO	2	88.4	1.1990	1.8187	3.3349	21.99	20.00	18.34	5.4789	264.926	0.024	1.050	5.5108	0.5172	39.54

Table 7.13 Summary of Class 3A thickness and width ratios

Configuration	Sub-Class	Primary Pivot	C_1	C_2	C_3	D_{1equal}	D_{2equal}	D_{3equal}	D_{1min}	D_{2min}	D_{3min}
sss	a	1	1.000	1.332	7.099	1.000	1.832	33.744	1.000	0.775	0.094
	a99	1	1.000	0.745	2.222	1.000	0.435	12.492	1.000	1.052	1.139
	a95IO	2	1.462	1.000	2.693	0.500	1.000	2.000	0.160	1.000	0.102
	a95I	3	0.340	0.289	1.000	0.039	0.022	1.000	0.997	0.895	1.000
	a90IO	2	1.260	1.000	3.104	1.974	1.000	1.979	0.986	1.000	0.066
sss	b	1	1.000	1.041	4.338	1.000	1.541	19.533	1.000	1.365	0.239
	b99	1	1.000	0.936	3.502	1.000	0.995	13.377	1.000	1.215	0.311
	b90I	3	0.589	0.381	1.000	0.148	0.055	1.000	0.724	0.996	1.000
	b88IO	2	1.610	1.000	2.398	0.500	1.000	2.000	0.120	1.000	0.145

Table 7.14 Largest stiffness parameters and percent increase

Configuration	Sub-Class	Ξ'_{ex}	Ψ	R	K_2	$\%\Delta\Psi$
lpp	a	99.7	1.000	0.8274	-	-
	a99	99	1.046	0.8018	-	4.6%
	a95	95	1.239	0.7106	-	23.9%
	a90	90	1.490	0.6185	-	49.0%
lpp	b	97.6	1.000	0.8853	-	-
	b95	95	1.052	0.8595	-	5.2%
	b90	90	1.129	0.8226	-	12.9%
lps	b95M	95	1.053	0.8561	0.0100	5.3%
	b90M	90	1.137	0.8177	0.0100	13.7%

Review of the optimization results indicates that three 16% deflection mechanisms and four 40% deflection mechanisms have a stiffness parameter greater than 1. These mechanisms are defined in Table 7.14, along with the percent increase in the stiffness parameter. The largest increase of 49% occurred in Class 1A-*lpp*-a90. All three of the sub-classes with 16% deflection belong to Class 1A-*lpp*. Two of the 40% deflection mechanisms belong to Class 1A-*lpp*, while the other two belong to Class 2B-*lps*.

These increases in stiffness will provide designers with greater flexibility and additional options for design. The design space for the existing configurations has been explored and the best mechanisms for a variety of circumstances have been defined.

CHAPTER 8

DESIGN APPROACH AND METHODS

CFMs have the potential of being used in a wide variety of applications. To be used in these applications, the CFMs must first be designed to meet all of the application's requirements. An understanding of a suitable approach to design is desired to simplify the process used by designers. This chapter looks at the design aspect of CFMs including general design procedures, infeasible mechanism elimination methods, secondary issues, and trends between variables. The chapter ends by presenting different design example problems and solutions.

8.1 General Design Approach

Every CFM design problem can be approached with the same general method. This allows designers to quickly become familiar with the process. The length of the process varies depending upon the constraints and requirements of the problem. In some cases, an immediate and direct solution can be found while in others, iteration must be used until a satisfactory design is determined.

8.1.1 Background, Assumption, and Limitations

The design method outlined in this chapter utilizes the stress and force parameters, along with other parameters, developed in earlier chapters. Since these parameters attempt to remove PRBM details such as individual link lengths, knowledge of the PRBM is not necessary to use the design method outlined in this chapter.

This design method builds upon the assumptions used throughout this work. Although the general steps outline in this chapter can always be used, the tabulated parameters must be used in connection with the assumptions made earlier.

Additionally, since the parameters for each mechanism use estimated values for the PRBM and other parameters, the accuracy of the designs that come from this design method cannot be guaranteed. For the most accurate design, a complete CFM model must be constructed and more accurate approximations based on the given design problem must be utilized. Wittwer (2001) addressed some of these accuracy issues and methods to determine variability in the PRBM.

8.1.2 Principal Equations

There are three principal equations that are necessary in designing a CFM. These equations are combinations and modifications of equations presented earlier in this work. The first equation is a modified force feasibility equation. In Chapter 4, the force feasibility equation was introduced in Equation (4.44) as

$$F = \frac{\beta E I_1}{r_{tot}^2} \tag{8.1}$$

Substitution of Equation (4.52) (moment of inertia ratios), Equation (5.1) (length parameter equation), and the equation for the moment of inertia for a rectangular cross-section into Equation (8.1) results in

$$F = \frac{\lambda^2 \kappa_p b_p h_p^3 \beta E}{12 l_{tot}^2 \kappa_1 K_{p-1}} \tag{8.2}$$

This equation will be referred to as the force design equation.

The only exception to Equation (8.2) is for Class 1B mechanisms. The force design equation for this class of mechanisms is

$$F = \frac{\beta \lambda^2 E I_2}{l_{tot}^2} \tag{8.3}$$

The second principal design equation is a modified form of the stress feasibility equation introduced in Equation (4.19) in Chapter 4 as

$$\alpha A = \frac{\Omega}{SF} \tag{8.4}$$

Substitution of $\alpha = M d^n$ and $A = \frac{\lambda h}{2 l_{tot}}$ into Equation (8.4) results in

$$\frac{\Omega}{SF} = \lambda M d^n \frac{h}{2 l_{tot}} \tag{8.5}$$

This equation will be referred to as the stress design equation.

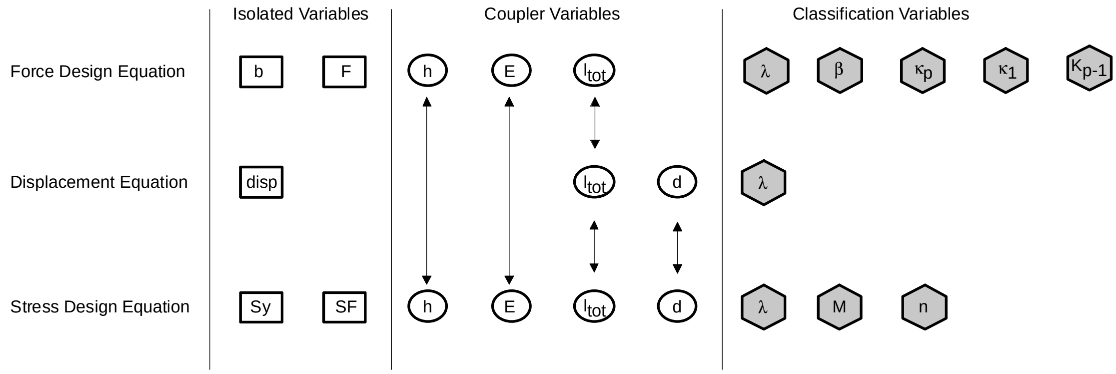

Figure 8.1 Interdependencies of coupled primary equations

The final principal equation is a combination of the percent deflection equation found in Equation (2.16) and Equation (5.1), the length parameter equation. The third equation is

$$disp = \frac{dl_{tot}}{100\lambda} \tag{8.6}$$

This equation is an intermediate equation which helps to provide needed values for variables in both the force and stress design equations. It is referred to as the displacement equation.

These three equations are coupled through different variables and must be solved to determine a design. A graphical representation of the interdependencies of these equations are given in Figure 8.1.

8.1.3 Variable Types

The boxed variables in Figure 8.1 are isolated variables, or those variables that occur only in one of the three equations. There are a total of five isolated variables in the three equations, two in each of the force design equation and stress design equation, and one in the deflection equation. For the system to be solvable, at least one of the two isolated variables must be known in both the force design and stress design equations.

The circled variables in Figure 8.1 are shared between two or more of the principal equations and are termed coupler variables. The number of coupler variables that must be known to solve the system depends on which coupler variables are known and how many isolated variables are known. No easy method, other than examining the missing variables in Figure 8.1, has been determined for deciding how many coupler variables are needed.

The final type of variable in the principal equations are the classification variables. These variables, outlined by a hexagon in Figure 8.1, can only be determined by choosing a specific classification of mechanism and substituting the values for the variables into the equations. If the classification is not known, then efforts must be made to reduce the number of possible classifications, and an iterative process may be required. Methods for eliminating infeasible mechanisms will be discussed later.

8.1.4 Variable Value Types

The three types of variables in the principal equations can have three types of values: known, constraint, or unknown. A known variable value is one that the designer must specify to a certain value due to design requirements.

A constraint variable value is one that has no exact value given by the design requirements, but is limited by constraints in the design requirements. Constraint values can be used in the principal equations to help determine design feasibilities and an initial design.

An unknown variable value is one that has no set value and is not constrained by upper and lower bounds. These values can be solved for or chosen as free variables if additional values are needed to solve the principal equations.

8.1.5 Basic Design Steps

As with any system of equations, enough variable values must be determined before the equations can be solved. The following steps outline the order in which types of variables and methods should be used.

1. *Identify a suitable mechanism*. If the design does not specify a specific mechanism, then one must be chosen. It is ideal to choose the classification that is best suited for the design problem. The following points should be considered when choosing a mechanism.
    - Stress and Force Feasibility (Section 8.2)
    - Percent constant-force (Section 8.3.1)
    - Flexible segment configuration (Section 8.3.2)
    - Manufacturing orientations such as in-plane and out-of-plane (Section 8.3.3)
    - Normal Displacement (Section 8.3.4)

These points can be used to reduce the number of mechanisms by eliminating any mechanism that is not feasible, greatly simplifying the selection process.

2. *Fill in all the known values*. Start by identifying all of the known values and their location in the principal design equations. Figure 8.1 is useful for this purpose.

3. *Add constraint values, starting with the most important ones, until the equations can be solved*. From Figure 8.1, determine how many more variables are required to solve the equations. Use the constraint values of the design problem to fill in the needed number of variables. The constraint value chosen depends on the needs of the design objectives. Section 8.4 can be used to identify the direction in which the constraint value should be adjusted to achieve the desired performance. At this point, the process will become iterative until a suitable design is chosen.

4. *Use unknown variables as free variables if needed*. If, after adding all constraint variables, there are still not enough variable values to solve the equations, use reasonable assumptions for unknown values until there are enough to solve the system.

5. *Remove variables if system is over-constrained*. If, at any point, the system is over-constrained, remove the least important values first.

These steps, along with the steps in the following sections, are summarized in the flow chart in Figure 8.2. This flow chart, along with the diagram in Figure 8.1, will help solve the system of equations for basic design cases. Examples of how to use these tools will be given in Section 8.5.

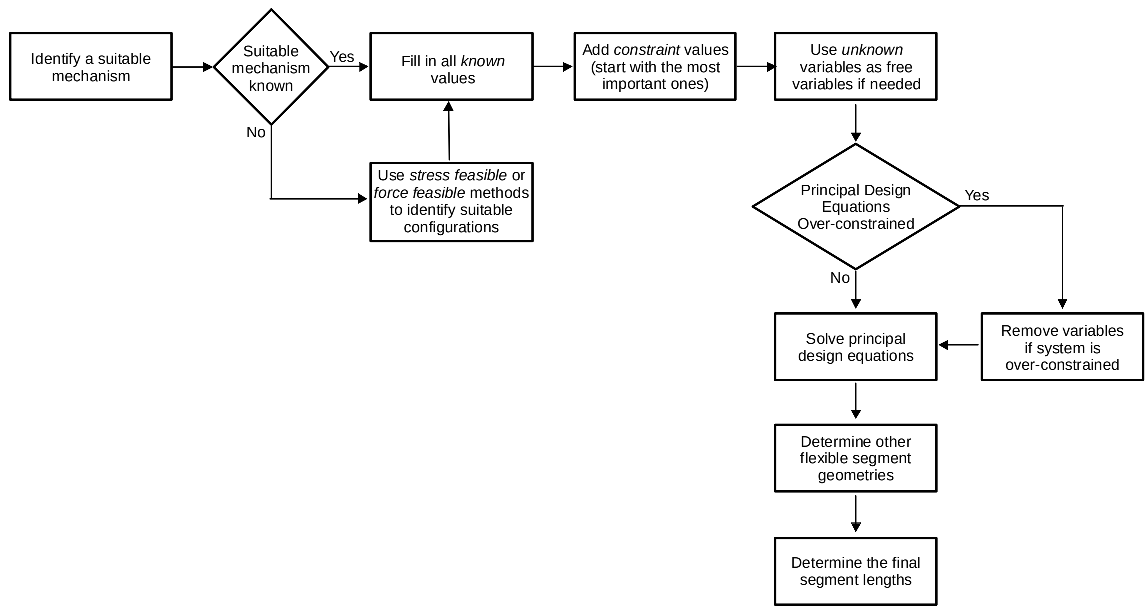

Figure 8.2 Flow chart of CFM design steps

8.1.6 Other Flexible Segments

The principal equations listed above identify only the geometry of the primary pivot. The following equations can be used after the basic design of the mechanism is complete to determine, and if needed, verify the feasibility of the other flexible segments' geometries. Of course, for the Class 1A and 1B mechanisms, this is not necessary.

The important equation for the design of the other flexible segments is

$$I_i = \frac{K_{i-1}\kappa_p I_p}{K_{p-1}\kappa_i} \tag{8.7}$$

This equation relates the moment of inertia of the primary pivot with the moment of inertia of any other flexible segment.

The limits on the other flexible segments can be determined quickly by using the width and thickness ratios. The equation for determining the thickness limitation is

$$c_i \leq C c_p \tag{8.8}$$

The minimum thickness of any of the other flexible segments is found by using

$$b_i \geq D_{min} b_p \tag{8.9}$$

If an out-of-plane orientation is used, then the width of the other flexible segments is found to be

$$b_i = D_{equal} b_p \tag{8.10}$$

Equation (8.7) can be used to quickly calculate the geometry of the other flexible segments in the mechanism. The ratio values and Equations (8.8) and (8.9) can be used to verify the geometries of the other flexible segments if neither an out-of-plane (equal thicknesses) or in-plane (equal widths) orientation is used. However, if either one of these orientations, including the perhaps out-of-plane orientation are used, then the geometries of the flexible segments do not need to be verified. They are guaranteed to have acceptable stress levels and satisfy Equations (8.8) and (8.9).

8.1.7 Final Segment Lengths

The final step in the design is to determine the length of the flexible and rigid segments of each link. The following steps, along with the definitions in Figure 8.3, can be used to lengths of the individual segments:

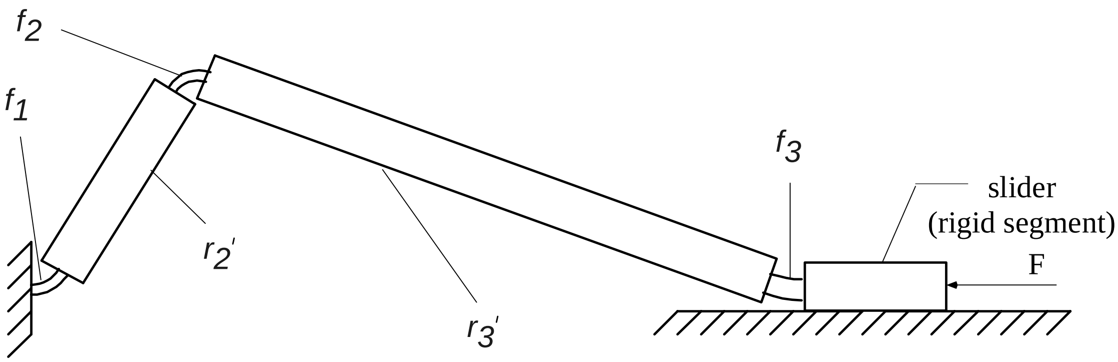

Figure 8.3 Definition of flexible and rigid segment lengths

1. Calculate r_{tot} using the length parameter

2. Calculate r_2, r_3, and r_{ave} where (from Equations (4.8) to (4.12))

$$r_i = \frac{r_{tot}}{\zeta} \tag{8.11}$$

and for

$$r_2 \ldots \quad \zeta = R + 1 \tag{8.12}$$

$$\mathrm{r}_3 \ldots \quad \zeta = \frac{1}{R} + 1 \tag{8.13}$$

$$r_{ave} \ldots \zeta = 2 \tag{8.14}$$

3. Use Table 8.1 to calculate the flexible segment lengths

4. Use the relations in Table 8.1 to calculate the lengths of the rigid sections

5. Replace flexible segments of length zero with pin-joints

8.2 Feasible Configurations

In some cases the configuration to be used is not specified, requiring a suitable mechanism to be chosen. The following two methods can be used to identify mechanisms that are suitable for a given design problem based on either stress or force feasibility. These methods utilize the classification variables and design constraints to eliminate mechanisms that are infeasible, leaving only those mechanisms that can provide the needed deflection or force without violating the constraints.

Table 8.1 Needed values to calculate flexible and rigid segment lengths

To get:	f_1	f_2	f_3	r_2'	r_3'
Do	Multiply r_2 by	Multiply r_{ave} by (except where noted)	Multiply r_3 by	Subtract from r_2	Subtract from r_3
spp	0.1	0	0	$f_1/2$	0
lpp	$\frac{1}{0.85}$	0	0	r_2	0
psp	0	0.1	0	$f_2/2$	$f_2/2$
plp	0	$\frac{1}{0.85}$ (times r_2)	0	r_2	$0.15*f_2$
ssp	0.1	0.1	0	$f_1/2+f_2/2$	$f_2/2$
slp	0.1	$\frac{1}{0.85}$ (times r_3)	0	$f_1/2+0.15*f_2$	r_3
sps	0.1	0	0.1	$f_1/2$	$f_3/2$
lps	$\frac{1}{0.85}$	0	0.1	r_2	$f_3/2$
sss	0.1	0.1	0.1	$f_1/2+f_2/2$	$f_2/2+f_3/2$

Since all 3 principal equations contain classification variables, some approximations must be made. For this reason, the results of these methods are only as accurate as the approximations and must be verified.

8.2.1 Method 1 - Stress Feasibility

This method uses the α curve fit parameter M and the stress design equation to identify stress feasible mechanisms. The mechanisms identified are capable of producing the desired deflection without violating any of the stress and geometry constraints. Although these mechanisms are stress feasibly, they are not guaranteed to be able to produce the desired force.

There are two types of stress feasible mechanisms. The first type, guaranteed stress feasible mechanisms, are those mechanisms with an M value less than M_{min}, the minimum M value calculated for the worst of the design constraints. These mechanisms are guaranteed to be stress feasible anywhere within the constrained design space.

The second set of mechanisms are simply referred to as the stress feasible mechanisms and can be identified using the maximum value of M, M_{max}, calculated using the conservative constraints. These mechanisms with M values less than M_{max}, but greater than M_{min}, are stress feasible for only part of the constrained design space. At certain points in the constrained design space, these mechanisms will not be able to achieve the desired deflection without violating the given constraints.

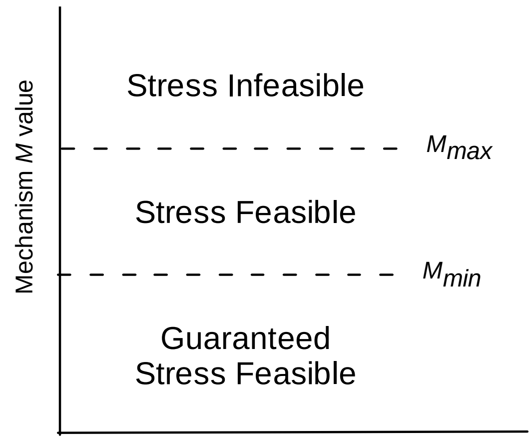

Figure 8.4 Summary of *M* value requirements for different types of identified mechanisms

Any mechanisms that have an *M* value greater than M_{max} can not obtain the desired deflection without violating the design constraints. A graphical summary of the required values for *M* for each type of mechanism is shown in Figure 8.6.

In most cases, it is most beneficial to identify and use the guaranteed stress feasible mechanisms. However, at times, guaranteed stress feasible mechanisms may not exist or it may only be necessary to identify stress feasible mechanisms.

To use this method, the following must be satisfied:

- In the deflection equation, 2 out of the 3 isolated and coupler variables must have known or constraint values.
- All of the isolated and coupler variables in the stress design equation must have known or constraint values.

This method consists of the following :

1. *Solve the displacement equation.* If a specific type of configuration is desired, use the highest λ value for M_{min} and lowest value for M_{max}. Otherwise, use $\lambda = 1.12$ for M_{min} and $\lambda = 1$ for M_{max}.

2. *Calculate the desired M value.* Calculate the *M* value that corresponds with the type of mechanism to be identified. Table 8.2 defines which constraint values to use to calculate the different *M* values.

3. *Eliminate mechanisms.* Any sub-classes with a value for *M* larger than the *M* value calculated can be eliminated from the group of mechanisms being identified. Table D.3 in Appendix D contains all of the mechanisms and their parameters sorted by *M*.

Table 8.2 Summary of stress and force feasibility methods

Variable Values	Stress Feasiblity - Method 1		Force Feasibility - Method 2
	M_{min}	M_{max}	Ψ_{min} (*lpp*-a/*lpp*-b)
F	-	-	Calculated
Sy	minimum	maximum	minimum
E	maximum	minimum	maximum
I_{tot}	minimum	maximum	minimum
disp	maximum	minimum	maximum
b	-	-	maximum
h	maximum	minimum	Maximum for *lpp* configuration
SF	minimum	minimum	minimum
β	-	-	2.901/3.248
M	Calculated	Calculated	0.4501/0.4788
n	maximum for desired type of configurtaion or 0.5256	minimum for desired type of configuration or .4699	0.5004/0.5033
λ	maximum for desired type of configuration or 1.12	minimum for desired type of configuration or 1.00	1.09
Identifies	Mechanisms that can undergo deflection without violating design constraints		Mechanisms that can produce the desired force and deflection without violating design constraints
Domain	Full Constrained Design Space	Partial Constrained Design Space	Full Constrained Design Space
Unkown	If Force is feasible		If thickness satisfies constraints

4. *Choose mechanism and verify.* It should be noted that those mechanisms that have an M value close to M_{min} and M_{max} may or may not be suitable due to the approximations made during the calculations. After choosing a mechanism, the actual n, M, and λ values should, together with the stress design equation, be used to verify that the constraints have not been violated.

5. *Finish the design.* Once mechanisms have been eliminated, a mechanism must be chosen and the design process continued.

8.2.2 Method 2 - Force Feasibility

This method uses the corresponding percent deflection *lpp* configuration and the parameter Ψ to identify mechanisms that are force feasible, those mechanisms capable of delivering the required force without violating the stress, width, and length design constraints. Even though these mechanisms can produce the desired force, due to the nature of the method, it can not be guaranteed that the thicknesses of the flexible segments will fall within the design constraints.

This method requires that the following be satisfied:

- In the deflection equation, 2 out of the 3 isolated and coupler variables must have known or constraint values.
- All of the isolated and coupler variables in the stress and force design equations must have known or constraint values, except for h.

Method 2 consists of the following steps.

1. *Calculate maximum h*. The stress design equation can be used to calculate the maximum *h* value for the *lpp*-a or *lpp*-b mechanisms. Use the classification variable values that correspond to the *lpp* configuration.

2. *Calculate maximum force*. Calculate the maximum force possible for the *lpp*-a or *lpp*-b sub-classes using the maximum *h* value and the other variables in the force design equation. Use the classification variable values that correspond to the *lpp* configuration.

3. *Divide forces*. Divide the needed force by the maximum force found in step 2. This gives Ψ_{min}, the minimum Ψ value that can be used to achieve this force.

4. *Eliminate mechanisms.* Any sub-class with the same deflection percentage used in step 1 and a Ψ value greater than Ψ_{min} is capable of producing the required force without violating design constraints given the same length, stress, and flexible segment widths used in step 1. All other mechanisms can be eliminated from consideration. Table D.5 in Appendix D contains all of the mechanisms and their parameters sorted by Ψ.

5. *Determine thickness.* The actual thickness, which will be different than the thickness in step 1, must be determine. This can be accomplished by using the classification variable values that correspond to the chosen mechanism in the force design equation.

Once a mechanism is chosen, there is no need to re-solve the stress design equation as long as all parameters, except the thickness, remain the same. However, if any con-

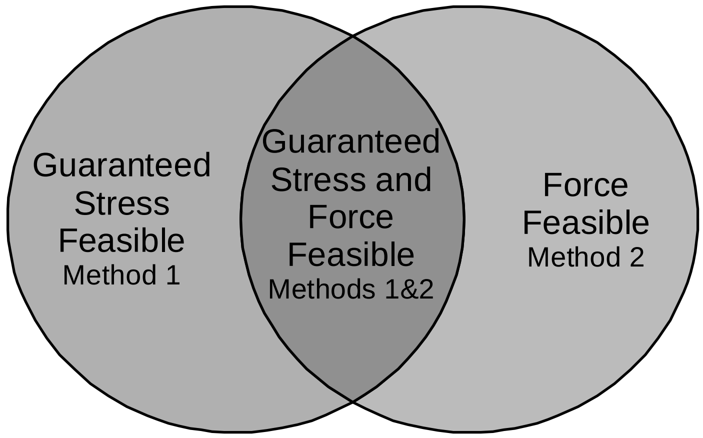

Figure 8.5 Overlap of guaranteed stress and force feasible mechanisms

straint values are modified, it becomes necessary to re-check all of the principal equations. Table 8.2 contains a summary of force feasible method, including the variable values required to calculate Ψ_{min}.

8.2.3 Combined Stress and Force Feasibilities

Either of the two methods can be used to identify feasible mechanisms for a given problem depending upon the objective and needs of the design problem. In some cases, it is advantageous to use both methods on the same problem. This, in a sense, overlaps the two types of feasible regions to generate a region in which both types of feasibilities exist, as graphically demonstrated in Figure 8.5. The mechanisms within this region are those mechanisms that have been identified as guaranteed stress and force feasible. All of these mechanisms will satisfy all of the constraints in all circumstances (assuming approximations are close). This makes the selection process very simple, allowing the designer to pick any one of the mechanisms for the design problem.

8.3 Other Mechanism Considerations

The methods discussed in Section 8.2 identify those mechanisms that are stress and force feasible. This section discusses other aspects of CFMs that must be considered when choosing and designing a CFM.

8.3.1 Percent Constant-Force

The percent constant-force must be considered when defining the design problem and choosing a mechanism. When selecting a mechanism, it is generally best to choose the lowest percent constant-force value possible. These mechanisms tend to have a higher stiffness than the mechanisms with a higher percent constant-force allowing them to achieve higher forces for the same relative stress. If a minimum percent constant-force value is specified, it can be used to eliminate infeasible mechanisms.

8.3.2 Flexible Segment Configuration

The requirements for the flexible segment configuration can also be used to eliminate infeasible mechanisms. If the design problem consists of constraints that limit the use of certain types of flexible pivots or pin-joints, then those configurations that are not suitable can be eliminated.

8.3.3 Manufacturing

The types of manufacturing processes that can be used to make a given mechanism are summarized in the sub-class name. If a certain process is to be used, a configuration suitable for this process must be identified and used.

8.3.4 Normal Displacement

The normal displacement of the mechanism can be used to eliminate mechanisms or verify a design if the design problem contains normal displacement constraints. The normal displacement can be calculated quickly using the equations developed in Chapter 5. Solving Equation (5.37) for Δy and using d_{Nmax} and the length parameter equation results in

$$\Delta y_{max} = \frac{d_{Nmax} l_{tot}}{100\lambda} \tag{8.15}$$

Equation (8.15) can be used to calculate the maximum normal deflection when the mechanism is deflected the maximum deflection percentage for the sub-class (16 for sub-class a, 40 for sub-class b). For deflection percentages below the maximum value, Equation (5.45) can be used.

For design purposes, the normal displacement information can be used to determine the upper limits on the length and/or deflection percentage when a maximum normal displacement is specified. The normal displacement equation can be used at any time during the basic design. The location of their use in the basic design steps depends on the type of variable values that result from Equation (8.15).

8.4 Variable Manipulation

During the iterative process found at times in CFM design, it is valuable to have an understanding of the relations between variables so that beneficial manipulations can be made.

Variable Increased	E	S_y	SF	b	h	I_{tot}	$disp$	d	M	Ψ	β	λ
Effect on Force	$\uparrow$	$\uparrow$ L	$\downarrow$ L	$\uparrow$	$\uparrow^3$	$\downarrow^2$	-	$\downarrow$ L	-	$\uparrow$	$\uparrow$	$\uparrow^2$
Effect on Stress	$\uparrow$	$\uparrow$ L	$\downarrow$ L	-	$\uparrow$	$\downarrow$	$\uparrow$	$\uparrow$	$\uparrow$	-	-	$\uparrow$

Key

$\downarrow^n$ $\uparrow^n$ Decrease, Increase in Magnitude by power n (default is 1)

$\downarrow$ L $\uparrow$ L Decrease, Increase in Magnitude Limit

Figure 8.6 Summary of variable effects on force and stress magnitudes for an increase in variable magnitudes

8.4.1 Variable Relationships

The variables in Equations (8.2), (8.5), and (8.6) affect the force and/or stress magnitudes of a CFM. Some of these variables have a direct effect on the magnitude of the force or stress, while others affect the limits of the force or stress magnitude. The effect of an increase in magnitude of these variables on force and stress are summarized in Figure 8.6.

This figure can be used to determine which directions the variables should move to affect the stress, force, or other variables. Figure 8.6 can also be used to decide whether the lower or upper limit of a constraint value should be used in the principal equations.

8.4.2 General Guidelines

Several general guidelines can be established from the trends illustrated in Figure 8.6. These guidelines provide insights into the response of CFMs to changes in the variables.

1. *Adjust width to change force*. For deflection loads, the width increases the force by a 1:1 ratio, but has no affect on the stress.

2. *Length verses thickness.* Length and thickness both have a 1:1 ratio with the stress design equation. However, any changes in thickness are cubed and any changes in length are squared in the force design equation. Therefore, the following can be concluded:

    - Adjust thickness to change the force while minimizing the change in stress
    - Adjust length to change stress while minimizing the change in force

3. *Maximize the length of the mechanism.* Most design problems tend to have have more difficulty satisfying the stress design equation rather than the force design equation. Therefore, generally, it is best to maximize the length of the mechanism for the reasons stated directly above

4. *Minimize safety factor.* Use the smallest possible value rather for the safety factor. This allows for the largest design space.

5. *Increase the yield strength.* Increasing the yield strength is not always an option, but it is very useful. Changes in yield strength affect only the limit on the stress, and not the stress or force itself.

6. *Change the type of mechanism to affect force.* By moving to a mechanism with a higher Ψ, a larger force can be achieved for the same given stress level. However, the flexible segments thicknesses will adjust and the usefulness of this method depends upon the constraints of the system. Generally, increases in Ψ can be achieved without switching flexible segment configurations. However, a decrease in Ξ' may be necessary.

In some design cases, the force may be too high, and manufacturing limits on the widths or thicknesses may be preventing the force from being lowered. In this case, most of the rules listed above can be reversed to help decrease the magnitude of the force.

8.5 Design Examples

8.5.1 Example 1 - Basic Design Case

A steel Class 1A-*lpp* mechanism is needed that produces 25 lbs of force and displaces 4 inches. The mechanism should also be as high of level of constant-force possible. The length must be between 12 and 15 inches and the width must be between 3 and 5 inches. The material comes in sizes ranging from 0.04 to 0.07 inches thick with a range of 50 to 200 Kpsi yield strength, with the material becoming more expensive as yield strength increases. Even though cost needs to be minimized, a safety factor of at least 1.2 is required. Design a mechanism that satisfies the criteria summarized in Table 8.3.

1. Choose a mechanism

The configuration of the mechanism has been specified, but the sub-class has not. However, Table D.1 indicates that sub-classes a and b have the highest percent constant-force for the *lpp* configuration. Additionally, solving the deflection equation for the maximum and minimum mechanism lengths gives the high and low values of d as 36.6 and 29.3. This leads to the conclusion that the *lpp*-b mechanism must be used.

2. Fill in known values

This example has four known values for the three principal equations. Examination of Figure 8.1 indicates that more variable values are needed.

3. Fill in constraint values

The constraint values are chosen based on the objective of the problem. In this example, the cost (yield strength) needs to be minimized. According to Figure 8.6, the required yield strength can be decreased by decreasing the stress. Figure 8.6 also indicates that increasing the length and decreasing the thickness will decrease the stress. Therefore, the maximum length, and the minimum thickness should be used in the principal equa-

Table 8.3 Example 1 design requirements

Variable	Units	Required	Low	High
F	lbs	25	-	-
S_y	Kpsi	-	50	200
E	Kpsi	30000	-	-
l_{tot}	in	-	12	15
disp	in	7.5	-	-
b	in	-	3.0	5.0
h	in	-	0.04	0.07
SF	-	1.2	-	-
Ξ'_{ex}	-	Highest		
Orientation	-	NA	-	-

tions. Using the maximum length results in a value for *d* of 29.3. This value can also be added to the design equations.

Examination of the force design equation shows that it can now be solved for b without adding additional constraint values. To achieve the desired force, *b* must be 8.99 inches, which exceeds the upper constraint. This now indicates that *b* must be a constraint value and that one of the previous constraint values must be removed from the system. According to the Figure 8.6 and the general guidelines, *h* should be used rather than l_{tot} to change the force while minimizing the affect on stress (yield strength).

By removing the constraint value for *h* and adding the maximum *b* value, the force design equation can now be solved for the need *h* to achieve the desired force. This results in a value for *h* of 0.049 inches. The final step is to resolve the stress design equation for the needed value of S_y for the given geometries. This results in a final value for S_y of 167 Kpsi. This is the smallest yield strength that can be used to achieve the desired force using the geometry and mechanism constraints.

In this example, a suitable design, summarized in Table 8.4, was defined. By using Figures 8.1 and 8.6, as well as the general design steps and guidelines presented in this chapter, a suitable design was quickly discovered without the need for large numbers of iterations or optimization methods.

8.5.2 Example 2 - Mechanism Elimination - Method 1

A mechanism is to be stamped in an in-plane orientation from a sheet of Phosphor Bronze. A force of 3 mN is required from a mechanism that has a length of 150 mm and a displacement of 7.5 mm. The thicknesses of the flexible segments must be between 1.5 and 2.0 mm thick. It is also necessary that the mechanism is at least 90 percent constant and has a safety factor of 1.1 or greater. A summary of all of the requirements can be found in Table 8.5.

Question: Is it possible to use a fully compliant configuration for the above design problem?

1. Start with the basic design steps

Table 8.4 Final design values

Variable	Units	Value
F	lbs	25
S_y	Kpsi	167
E	Kpsi	30000
l_{tot}	in	15
disp	in	7.5
b	in	5
h	in	0.049
SF	-	1.2
Ξ'_{ex}	-	97.6
Orientation	-	NA

The first basic design step is to choose a configuration. In this particular problem, a specific mechanism can not be chosen. Therefore, it is necessary to eliminate as many mechanisms as possible using one of the two methods described in Section 8.2.

2. Determine which elimination method can and should be used

The deflection equation is missing one of the coupler variables and the classification variable, which satisfies the first requirement for both methods. Examination of the stress design equation shows that all of the isolated and coupler variables have either known or constraint values, while the force design equation is missing values for the variable *b*. This indicates that only method 1 can be used for this problem.

3. Calculate the percent displacement

In this case, we are looking for a fully compliant mechanism. All of these mechanisms have a λ value of 1.05. Using this value and Equation (8.6) results in

$$d = 100\frac{disp(\lambda)}{l_{tot}} = 100\frac{0.0075(1.05)}{0.15} = 5.25 \quad \textbf{(8.16)}$$

4. Calculate M_{max} to identify feasible mechanisms

Table 8.5 Summary of example 2 design requirements

Variable	Units	Required	Low	High
Force	mN	3	-	-
S_y	Pa	5.52E+08	-	-
E	Pa	1.10E+11	-	-
r_{tot}	mm	150	-	-
disp	mm	7.5	-	-
b	mm	-	-	-
h	mm	-	1.5	2.0
SF	-	1.1	-	-
Ξ'_{ex}	-	-	90	
Orientation	-	In-plane	-	-

Since the only objective is to determine if a fully compliant CFM can be used, only the stress feasible mechanisms need to be identified using method 1 and M_{max}. This value can be found by using a form of Equation (8.5) and the appropriate values given above.

$$M_{max} = \frac{2\Omega l_{totmax}}{SF_{min}\lambda h_{min} d^{n_{approx}}} = \frac{(2)5.02 \times 10^{-3}(0.15)}{1.1(1.05)(0.0015)(5.25^{0.5})} = 0.3792 \tag{8.17}$$

5. Use Table D.3 to eliminate configurations

Examination of Table D.3 shows that the smallest *M* value for any *sss* configuration that is suitable for an in-plane orientation is the *sss*-a95I mechanism with an *M* value of 1.7796, well above the maximum *M* value calculated above. This leads to the conclusion that the fully compliant mechanism can not be used for these design constraints.

Question: What length of mechanism is needed to be able to use the fully compliant mechanism without changing any of the other design constraints?

1. Choose a mechanism

The *sss* configuration with he lowest *M* value was identified above. This mechanism also has the highest Ψ value of all of the *sss*-a mechanisms. Therefore, this mechanism, the *sss*-a95I, will be used.

2. Calculate the needed length

A non-linear method must be used to calculate the needed length due to the interdependencies between the stress design equation and displacement equation. Performing the calculation with the appropriate values for *M* (1.7796) and *n* (.4888) for the *sss*-a95I mechanism, as well as the other known values results in a length of 418.4 mm. This is more than double the initial length value.

Question: What thickness would be required to be able to use a fully compliant mechanism and all of the original design constraints?

1. Choose a mechanism

The *sss*-a95I mechanism will be used for the same reasons listed above.

2. Calculate the maximum thickness for the primary pivot

Using the appropriate values for *M* (1.7796) and *n* (.4888) and Equation (8.5), the maximum thickness can be calculated as

$$h_{max} = \frac{2\Omega l_{tot}}{\lambda M d^n SF} = 2\frac{5.02 \times 10^{-3}(0.15)}{(1.05)1.7796(5.25^{0.4888})1.1} = 0.326 \text{ mm} \tag{8.18}$$

This leads to the conclusion that the *sss*-a95I mechanism can be used for the given length and deflection if the primary pivots thickness is no larger than 0.326 mm.

Question: Assuming that the thickness above is suitable, what width of material would be required to achieve the desired force?

1. Calculate the required width to achieve the force using the force design equation, Equation (8.2)

The equation is

$$b_p = \frac{12 F l_{tot}^2 \kappa_1 K_{p-1}}{\lambda^2 \kappa_p h_p^3 \beta E} = \frac{12(0.003)0.15^2(26.57)15.3423}{1.05^2(16.03)(0.000326^3)2.279(1.1 \times 10^{11})} = 2.15 \text{ mm} \tag{8.19}$$

Equation (8.19) indicates that the width of the flexible segments must be 2.15 mm wide.

Question: What are the required thicknesses for the other flexible segments?

Equation (8.7), together with the equation for the moment of inertia for a rectangular cross section can be used to calculate the thicknesses of the other beams. These thickness are 0.111 mm and 0.091 mm for the first and second flexible segments respectively.

Question: Is the above design feasible?

The only thing that has not been verified are the stresses in the other flexible segments. However, this is not necessary. The highest stress in the mechanism is found in the primary pivot assuming that the other flexible segments satisfy the inequality in Equation (8.8), and because all of the flexible segments have the same width and this mechanism is suitable for in-plane orientation, this inequality must be satisfied.

8.5.3 Example 3 - Feasible Mechanisms Only

A CFM is needed that produces 100 lbs of force over 6 inches of deflection and with 10% or less variation in the force magnitude. The mechanism must be exactly 2 feet long and 5 inches wide. The mechanism is to be made out of spring steel with a yield strength of 200 Kpsi and a thickness between 0.01 and 0.035 inches. Identify all of the configurations that satisfy all of the design requirements as summarized in Table 8.6.

1. Choose a mechanism.

The mechanism was not identified in the problem. However, the value for *d*, using a λ value of 1, is found to be 25. This indicates that a 40% mechanism (b sub-classes) must be used. To identify all of the possible mechanisms, both the stress and force feasibilities must be used.

2. Use force feasibility method to elimination mechanisms

Using the design constraints and the stress design equation, a maximum value for the thickness of the *lpp*-b sub-class can be calculated. This turns out to be 0.116 inches. This value can now be used in the force design equation to determine the maximum force the *lpp*-b configuration can generate given the design constraints. The maximum force is 130.3 lbs.

Dividing the needed force of 100 lbs by the maximum force of 130.3 results in a Ψ_{min} of 0.767. Any mechanism with a value of Ψ greater than Ψ_{min} will be able to generate the needed force without violating the design constraints (assuming the same width and lengths are used).

Table 8.6 Design problem summary for example 3

Variable	Units	Required	Low	High
F	lbs	100	-	-
S_y	Kpsi	2.00E+02	-	-
E	Kpsi	30000	-	-
l_{tot}	in	24	-	-
disp	in	6	-	-
b	in	5	-	-
h	in	-	0.01	0.035
SF	-	1	-	-
Ξ'_{ex}	-	NA		
Orientation	-	NA	-	-

The application of this method reduces the number of sub-class b mechanisms down to 5 mechanisms, 3 *lpp* configurations and 2 *lps* configurations.

3. Use method 1 to identify guaranteed mechanisms

Using Equation (8.5), and the maximum thickness constraint together with the other constraints results in a M_{min} value of 1.83. Using this value and Table D.3 in Appendix D, 11 guaranteed mechanisms can be identified.

4. Determine overlap of two methods

Method 1 resulted in 11 guaranteed mechanisms being identified, 5 of which were identified also using method 2. Therefore, any one of these 5 mechanisms (*lps*-b90I, *lpp*-b90, *lps*-b95I, *lpp*-b95, and *lpp*-b) can be used to satisfy the design requirements of this example.

CHAPTER 9

CONSTANT-FORCE ELECTRICAL CONTACT

The objective of this chapter is to demonstrate the potential benefits and viability of applying constant-force mechanism technology to electrical contact design. The successful development of a CFEC that meets all of the requirements of an electrical contact will lay a ground work for further exploration and introduction of CFEC's into industry applications.

The chapter begins by discussing current electrical contact industry practices and standards. It then presents a discussion of constant-force mechanism technology. Different configurations are explored to discover one suitable for application as a CFEC in a presented case study. (The CFEC case study presented in this chapter is focused on limitations and common industry practices associated with Personal Digital Assistants (PDA) docks, but the principles are applicable to a wide range of connector applications.) The chapter finishes by describing the modeling, optimization, and verification of a CFEC that meets the requirements of the case study.

9.1 Introduction

The reliability of high-cycle electrical connectors is of great concern to designers, and methods to improve this reliability are always being evaluated. According to Deshpande and Subbarayan (2000), the reliability of high-cycle electrical connectors is related to electrical signal propagation, and mechanical performance and stability. To achieve this reliability in practice, the connector contacts must transmit the electrical signal with minimal contact resistance under all types of use conditions and accommodate expected geometric variations in manufacture and assembly.

The factor that contributes most significantly to the reliability of electrical contacts is the contact-surface mating conditions. Two physical parameters that greatly affect mating conditions are contact surface finish, and contact normal force at mating. When contact surface finish remains corrosion free, either by being corrosion resistant or by being self-cleaning, greater reliability is achieved. When contact normal force is maintained above a certain level, greater reliability is also achieved (Harper, 1997). Contact normal forces must be small enough to minimize plating damage over the life of the contact, yet large enough to overcome co-planarity differences from adjacent contacts and other geometric variations. Thus a desirable contact system would maintain an optimal contact force regardless of variations in assembly or use.

In addition to achieving high levels of reliability, the electrical contact industry is being driven to produce innovative products that have faster speeds, smaller packages, and higher contact density. To remain competitive, performance gains must be achieved with designs that can be produced at low cost (Brush Wellman, 1999).

The recent introduction and advancements in design of simple constant-force mechanisms, have created the potential for small-scale, low-cost, constant-force electrical contacts (CFECs). CFECs differ from traditional contacts and springs by the separation or disassociation of contact normal force and contact deflection. Traditional mechanics describe force (F) and deflection (d) of springs as $= kd$ where k is the spring constant that represents the stiffness of the connector.

A CFEC uses constant-force technology to separate the contact normal force and the contact deflection, resulting in a relationship where force is relatively independent of deflection. By removing the traditional constraints imposed by forces and deflections that are dependent on each other, the addition of new types of electrical connectors previously dismissed or undiscovered can be explored.

The disassociation of contact normal force and contact deflection could lead to three advantages. First, current electrical contacts require tight manufacturing and assembly tolerances to ensure that the contact deflection is within acceptable limits. The decoupling of the force and deflection may allow the tolerances to be loosened, while still having acceptable performance. This can help to reduce the cost and difficulty of manufacturing and assembly.

The second advantage may be in applications were the user interacts with the electrical contacts, such as docking stations. In this case, the decoupling of the force and

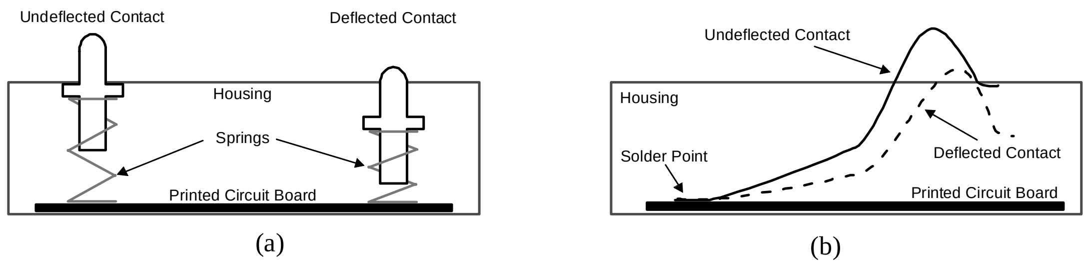

Figure 9.1 (a) Pogo type connector and (b) cantilever type connector

deflection helps prevent any variation introduced by the user, such as different docking methods, from affecting the performance of the electrical contacts.

The third advantage that may be seen from decoupling is in applications where the output force needs to remain relatively constant to ensure performance, but the deflection does not remain constant due to movement and/or vibrations of the contacts due to the system environment. Examples of this include connectors in aircraft, vehicles, and machinery.

9.2 Electrical Contacts

Traditionally, electrical contacts for use in PDA docks have consisted of linear spring assemblies or an arrangement of cantilever beams (See Figure 9.1). These configurations usually require large deflections to obtain the desired force and must be long to keep stresses to an acceptable level.

9.2.1 Electrical Contact Industry Practice and Standards

The electrical contact industry has several practices and standards that constitute essential performance characteristics for electrical contacts. The most basic and important of these are divided into subgroups for presentation here, but it is not intended to be an exhaustive list of all design issues.

The first standard is that electrical continuity must be continuous. The electrical path created by an electrical contact can not be interrupted or contain high resistive areas. Additionally, this path should consist of few parts (preferably one piece) which are easily assembled.

Electrical contacts can be fabricated from any conductive material, but current industry practice is to use alloys that contain copper. Phosphor bronze is a common alloy that is easy to use and readily available. Beryllium copper and titanium copper are commonly used to achieve higher yield strengths. Unfortunately, they are more difficult to use and more expensive than phosphor bronze.

Manufacturability is an important aspect of electrical contact design. Electrical contacts are being produced in ever increasing volumes at lower costs. Current industry practice is to use progressive stamping techniques to shape the metallic beams. Generally, the contacts are stamped at the desired pitch distance and are left attached to the flashing. This allows for easier material handling and assembly, but limits the shape and design of the contact. Some of the limitations imposed on designs due to this manufacturing process are:

- Minimum Material Thickness - There is a minimum material thickness that is suitable for stamping.
- Minimum Bend Radius - There is a minimum bend radius allowed during stamping operations. A general rule used is 4 times the thickness of the material.

Many industry practices are associated with assembly of the electrical contacts. In this case, assembly deals with packaging the electrical contacts into a housing that is suitable for use. Design for assembly is vital to achieve a low cost and reliable part. Some of the practices associated with assembly are:

- Mount type - Through-hole mounts are generally easier to use and most commonly used. Surface mounts usually are more difficult to do, but take up less room on the board (one side only).
- Single Assembly - Assembly of all of the contacts into the housing at one time is the standard method. This greatly simplifies the process.
- Housing - The plastic housing that holds the contacts generally is one or two pieces. This part holds the contacts into place.

The design of electrical contacts is well defined and understood. However, examination of traditional contacts shows that they are not suitable for use as constant-force mechanisms, requiring that a new configuration be developed for the CFEC.

9.3 Constant-Force Mechanisms as Electrical Contacts

Traditional CFM configurations such as the one shown in Figure 9.2 are not suitable for use as electrical contacts for several different reasons which include:

- Manufacturability - The stamping of the necessary geometry would be difficult.
- Material - The deflections and size constraints would cause extremely high stresses compared to the strengths of common electrical contact materials.
- Assembly - The assembly of pin-joints makes the use of traditional slider-crank configurations in electrical contacts unlikely.

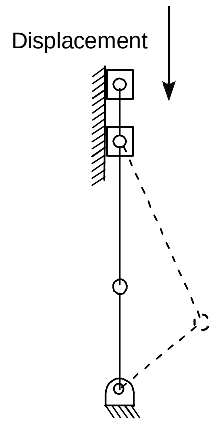

Figure 9.2 Typical compression slider-crank constant-force configuration

- Electrical Continuity - Pin joints would introduce gaps and areas of high resistance in the electrical path making the contact inefficient and unreliable.

Evaluation of the latest configurations shows that pin-joints and small-length flexural pivot can not be used in electrical contacts, indicating that different configurations that combine the benefits of both electrical contacts and CFMs must be developed for use as a CFEC.

9.4 CFEC Configurations

The development of configurations for use as a CFEC is required. Although traditional electrical contacts and current constant-force mechanisms are not acceptable for use as electrical contacts, they provide a starting point in the search for new configurations suitable for CFECs.

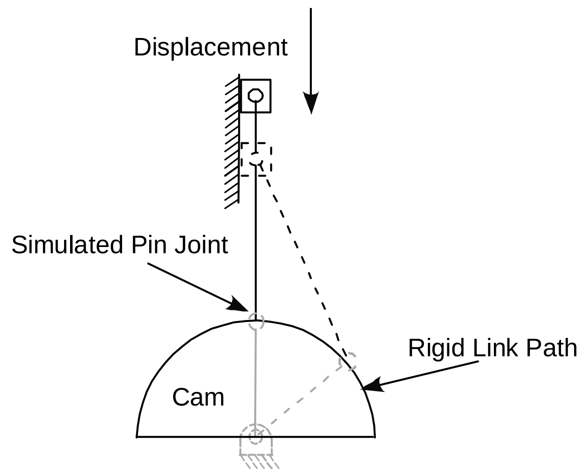

Figure 9.3 Simulation of pin joints with a circular cam

9.4.1 Simulated Pin Joints.

The slider-crank constraints can be greatly simplified by using a method that simulates the function and motion of a fixed-pinned flexible segment and a rigid link joined by a pin joint. In this method a circular cam is used to represent the rigid-link. If the simulated joint remains in compression, then the flexible link will follow the cam profile - the exact path of the replaced rigid body link - as shown in Figure 9.3.

However, there are limitations to the simulated pin joint method. It must be in compression to ensure that the tip of the beam remains in contact with the cam (See Figure 9.4c). It is also important to ensure that the simulated pin joint has minimal friction so that there is smooth motion around the cam. This can be partially accomplished by rounding over the tip of the beam and providing smooth surface finishes on the cam as shown in Figure 9.4d.

If the flexible beam is loaded, but doesn't slide around the cam, then the beam could buckle. Slider crank change points should be avoided. At these points, it may be difficult to get the beam to begin to slide around the cam. This can be done by changing the initial angle of the beam or changing the eccentricity of the slider-crank as illustrated in Figure 9.4a and Figure 9.4b.

There is also a limit to how far around the circular cam the flexible link can travel. If the mechanism is deflected beyond the point at which the flexible beam is tangent to the cam, the tip of the flexible beam will no longer be in contact with the cam (See Fig. 9.4e).

Figure 9.4 shows a graphical summary of the limitations, along with the methods to overcome these limitations, associated with the simulated pin joint method. Despite these exceptions, the simulation of pin joints with the use of a circular cam is an important tool.

To combine the strengths of constant-force mechanisms and bent beam electrical contacts, many different possible configurations were evaluated. Using the industry practice and standards criteria and a screening process, the configuration determined most viable for use in a CFEC is one in which a slider-crank mechanism is attached directly to the end of a bent cantilever beam as illustrated in Figure 9.5. A concept drawing of the CFEC inside of a PDA dock is shown in Figure 9.6.

This configuration is easy to manufacture and assemble, and has electrical continuity. Additionally, the beam and cam combination provide the necessary increases in

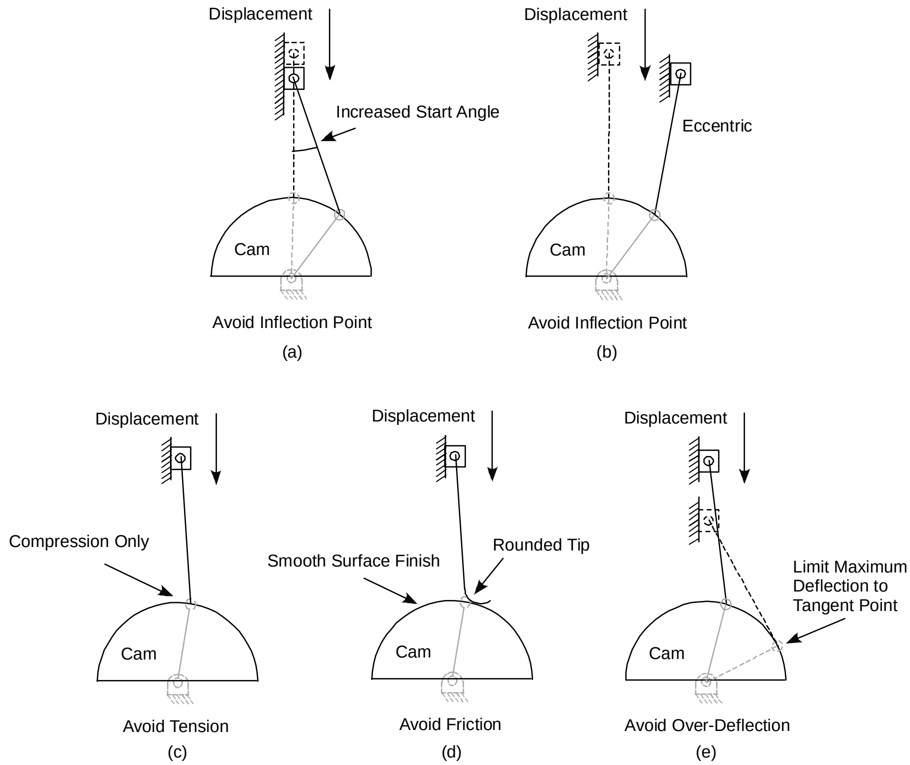

Figure 9.4 Limitations and solutions to limitations of simulated pin joint method

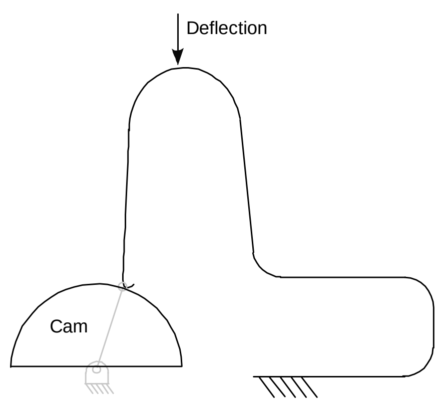

Figure 9.5 Selected constant-force electrical connector configuration

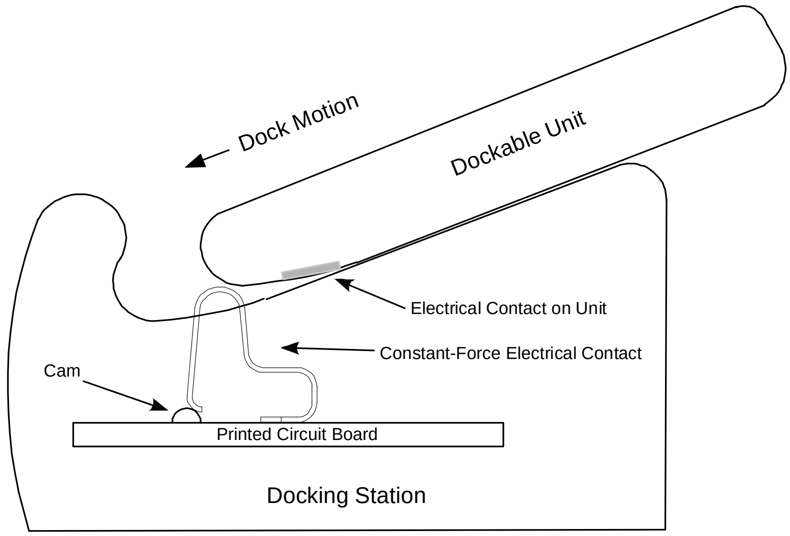

Figure 9.6 Selected CFEC configuration in PDA dock.

mechanical advantage and the strain energy storage device necessary for constant-force behavior.

9.4.2 Parameter Definitions

Parameters establish the shape and size of the mechanism and are used as inputs in the model and optimization. Among these parameters are link lengths, angles, and cross sectional geometries. Some of the parameters are also used to assess performance relative to design requirements associated with the industry practice and standards. A graphical summary of each of the important parameters for the selected configuration is shown in Figure 9.7.

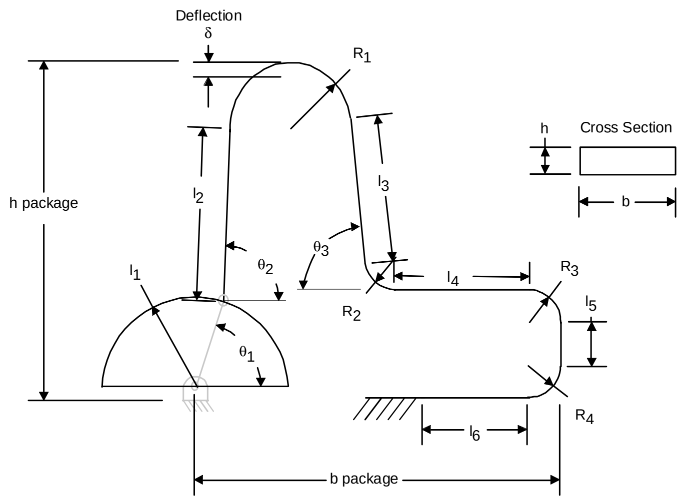

Figure 9.7 Important parameters for general CFEC.

9.5 Case Study Details

The process of moving from the chosen configuration to a commercially-viable CFEC is demonstrated by using a specific case study of electrical contacts for Personal Digital Assistants (PDAs) docking stations. Specific requirements for the case study were gathered based on existing dock designs and by working closely with the engineers of a leading manufacturer of these devices.

Phosphor Bronze, a common bronze alloy used in electrical contacts, is selected for this contact because it is relatively common, cheap, and easy to work with during production when compared to other alternatives. The force range for the design is 294 - 588 mN (30 - 60 gf), and the maximum stress in the contact should not exceed the yield strength. The CFEC is required to have a cross sectional height, h, of 0.2 mm and a width, b, of 1 mm. The case study also requires that the contact fit inside of a 12 mm wide by 6 mm tall rectangle. The final design constraint is that the output force of the mechanism should be at least 60% constant. This means that there is only a 40% variation between the minimum force and the maximum force within the possible displacement range. Table 9.1 summarizes the design constraints for the case study. The symbols for the model functions for each constraint are listed in the first column. The second column contains the general constraint symbol which represents the fixed design constraints for any problems, while column 3 lists the actual constraint values for the case-study.

9.6 Model Development

An accurate model in which the governing parameters can be modified and accurate resulting forces and displacements can be calculated is needed. During the optimiza-

Table 9.1 Summary of case-study constraints

Model Function Symbol	General Constraint Symbol	Constraint Value for Case-Study
$h_{package}$	h_{pc}	≤ 6 mm
$b_{package}$	b_{pc}	≤ 12 mm
h	h_c	0.2 mm
b	b_c	1.0 mm
Bend Radius	R_c	≥ 0.7 mm
E	E_c	110e9 Pa
S_y	Sy_c	552e6 Pa
SF	SF_c	≥ 1.0
F_{ave}	$F_{ave,\ c}$	≈ 441 mN (45 gf)
F_{min}	$F_{min,c}$	≥ 294 mN (30 gf)
F_{max}	$F_{max,\ c}$	≤ 588 mN (60 gf)
Percent Constant (Ξ')	Ξ'_c	60

tion phase, the model is called many times to calculate function values and derivatives. Therefore a simple model is preferred, but it must also be accurate.

Originally, a combination of a numerical CFM model based on the PRBM and a numerical bent beam model based on Euler’s Method were combined to model the CFEC configuration. However, the model was not accurate enough due to violations of assumptions in the CFM model. The CFM portion of the CFEC does not act as a pure slider. The motion is not straight line and the moment assumed not to pass through the slider, is actually passed to the bent beam. These differences proved too much for the joint numerical model.

To overcome the model problem, a finite element analysis (FEA) program capable of nonlinear analysis (ANSYS) was used to model the deflections, contact forces, and stresses in the CFEC. A parametric model was used so that values could be passed between the FEA and optimization programs.

The FEA model was generated using the input parameters to calculate the location of the key points shown in Figure 9.8. Once all the key points have been defined, a total of 175 beam elements are used to model the CFEC.

The cam is replaced with the rigid link (segment A) that it is simulating. This requires that segment A be pinned to ground at key point 1, and that key points 2 and 3 be constrained to have the same x and y displacement, thus forming a pin-joint. Segment A is given a large width and height to ensure that it is rigid.

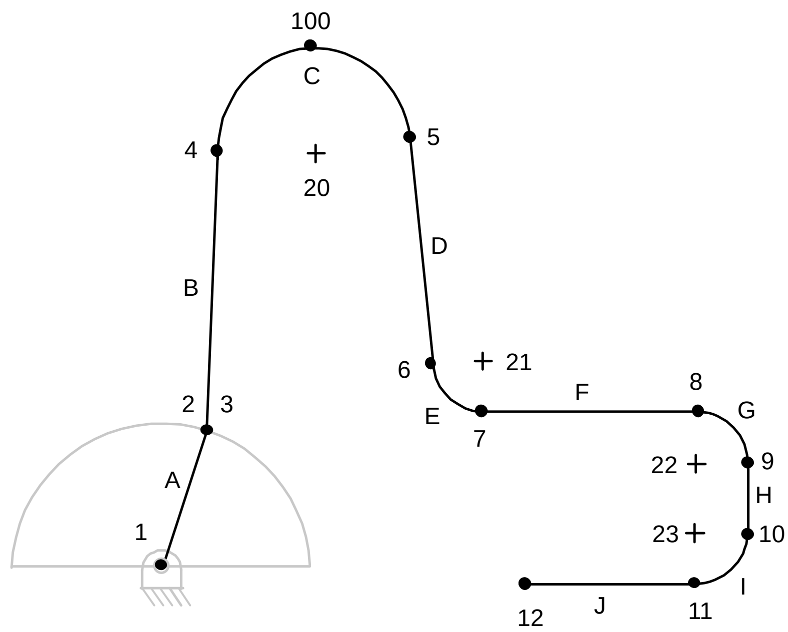

Figure 9.8 Key Points for the finite element model

It is also necessary to constrain segment J at key point 12 in the x and y directions, as well as rotation about the z -axis. This represents the way the bent beam attaches to ground as a cantilever, simulating its attachment when soldered to a printed circuit board (PCB). Finally, 5 vertical displacement load steps in the downward direction are applied to the top of the mechanism at key point 100.

Once the model has run for the 5 different load steps, the contact force for each load step and the highest stresses over the total deflection are written to a data file for use by the optimization software (Optdes-X).

9.7 Model optimization

As with the CFM, it is necessary to establish an objective function, design variables, design functions, and constraints that facilitates the development of a constant-force mechanism from the layout presented in Figure 9.5 that satisfies all of the design constraints.

As with any CFM, the principle objective function is the parameter Ξ'. The lengths, angles, and radii described in Figure 9.7 are established as design variables in the optimization problem with reasonably assumed bounds. The beam height (*h)*, width (*b*), modulus of elasticity (*E*), and safety factor (*SF)* are set up as analytical variables. The values for the analytical variables are established by the requirements of the case study as described in Table 9.1. The remaining constraints of the case study show up in the design functions calculated from variables and other model results.

9.7.1 Optimization

Using the design constraints of the case study, the optimization problem can be formally stated in as:

$$\text{Maximize } \Xi' \tag{9.1}$$

Subject to the constraints:

$$\Xi' > \Xi'_c \tag{9.2}$$

$$F_{ave} > F_{min_c} \tag{9.3}$$

$$F_{ave} < F_{max_c} \tag{9.4}$$

$$SF \geq SF_c \tag{9.5}$$

$$b_{package} < b_{pc} \tag{9.6}$$

$$h_{package} < h_{pc} \tag{9.7}$$

With the following constraints on the design variables:

$$R_1 > R_c \tag{9.8}$$

$$R_2 > R_c \tag{9.9}$$

$$R_3 > R_c \tag{9.10}$$

$$R_4 > R_c \tag{9.11}$$

Where the variables with a subscript *c* denote the constraint values found in Table 9.1.

The optimization and FEA model were linked together in a similar manner as the CFM model. At first, a feasible starting point was difficult to find so the constraints were loosened by 10%-15%. Once a starting point was found, the optimization was allowed to run and the constraints were tightened. This was repeated until a suitable design was found.

The final design chosen satisfied the design constraints and requirements of the case study. A detailed drawing of the final design chosen for the case study is shown in Figure 9.9. The model values for the design and constraint parameters are listed in Table 9.2.

9.8 Model Validation

To confirm the behavior of the CFEC and the accuracy of the model, 9 prototypes of the final design were produced for testing. The photo in Figure 9.10 illustrates the comparative size of the prototypes.

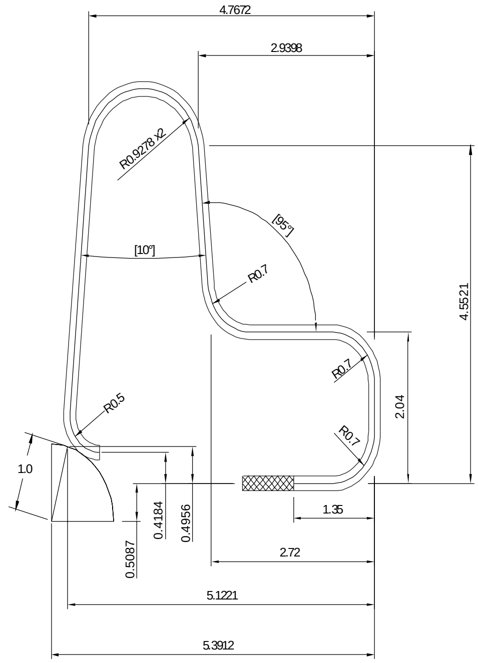

Figure 9.9 CFEC final design

Table 9.2 Parameter summary of final design

Model Function Symbol	Final Design	Constraint Value for Case-Study
$h_{package}$	5.9 mm	≤ 6 mm
$b_{package}$	5.4 mm	≤ 12 mm
h	0.2 mm	0.2 mm
b	1.0 mm	1.0 mm
Bend Radius	0.7 mm	≥ 0.7 mm
E	110e9 Pa	110e9 Pa
S_y	552e6 Pa	552e6 Pa
SF	1.29	≥ 1.0
F_{ave}	478 mN (48.8 gf)	≈ 441 mN (45 gf)
F_{min}	423 mN (43.2 gf)	≥ 294 mN (30 gf)
F_{max}	577 mN (58.9 gf)	≤ 588 mN (60 gf)
Percent Constant (Ξ')	73.2	60

Figure 9.10 CFEC prototype as compared to a dime

9.8.1 Dimensional Analysis

A dimensional analysis was performed to determine how close the prototypes' dimensions were to the specified dimensions. An optical comparator was used to take 16 dimensional measurements from each of the 9 prototypes to determine the variation between the measured values and the design values.

A weighted sum of the variation in each prototype was calculated to determine which of the prototypes were closest to the final design. The three prototypes closest to the final design were chosen for testing. The results of the dimensional analysis for the three contacts chosen are found in Table 9.3.

9.8.2 Testing

A rigid test fixture was designed to allow for easy and accurate placement of the prototype. The cam was fabricated as a separate piece to help ensure tight tolerances and allow for different materials for the cam to be used, including polypropylene and teflon.

The purpose of the different materials was to investigate how different material types affected the performance of the prototype.

A force transducer was attached to a computer-controlled actuator. The computer controlled the actuator and collected position and force data. During testing, the contacts were deflected to 0.75 mm and back. Figure 9.11a shows a photo of the general test setup and Figure 9.11b shows a close-up photo of the contact in the test fixture.

9.9 Results

The prototypes were each tested using two different cams. Figure 9.12 shows a graph of testing results for prototype 3 with a polypropylene cam. The mechanism maintained a near constant-force throughout the deflection and behaved as predicted.

Table 9.3 Dimensional analysis of CFEC prototypes

Dim	Design	Weight	Contacts 3 Value	Contacts 3 Variation	Contacts 4 Value	Contacts 4 Variation	Contacts 5 Value	Contacts 5 Variation	All Contacts STDEV	All Contacts Average	All Contacts Median
A	5.2809	3	5.401	0.068	5.335	0.031	5.443	0.092	0.200	5.393	5.401
B	2.9116	1	2.925	0.005	2.946	0.012	2.992	0.028	1.496	1.561	2.790
C	1.45	1	1.490	0.028	1.511	0.042	1.446	0.003	0.746	0.807	1.394
D	0.2	2	0.183	0.170	0.176	0.240	0.186	0.140	0.071	0.191	0.178
d2	0.2	2	0.199	0.010	0.217	0.170	0.196	0.040	0.081	0.132	0.186
E	0.8	1	0.700	0.125	0.915	0.144	0.919	0.149	0.364	0.505	0.449
F	0.8	1	0.738	0.078	0.836	0.045	0.813	0.016	0.416	0.498	0.738
G ang	90	2	90.000	0.000	88.850	0.026	90.000	0.000	46.788	48.154	87.700
G	2.24	1	2.287	0.021	2.256	0.007	2.245	0.002	1.155	1.197	2.220
H	5.5188	3	5.334	0.100	5.453	0.036	5.602	0.045	2.796	2.955	5.200
I	0.4184	3	0.394	0.175	0.457	0.277	0.503	0.607	0.859	0.818	0.503
J	0.6	1	0.475	0.208	0.547	0.088	0.569	0.052	0.241	0.328	0.475
K	0.8	1	0.537	0.329	0.480	0.400	0.565	0.294	0.109	0.443	0.470
L	95	2	96.100	0.023	96.500	0.032	93.200	0.038	50.066	51.540	93.200
M	10	2	10.300	0.060	11.400	0.280	9.400	0.120	5.873	6.158	8.200
N	1.0278	1	0.952	0.074	1.294	0.259	0.999	0.028	0.470	0.597	0.758
Total Weighted Variation				1.473		2.088		1.653			
Rank			1		3		2				

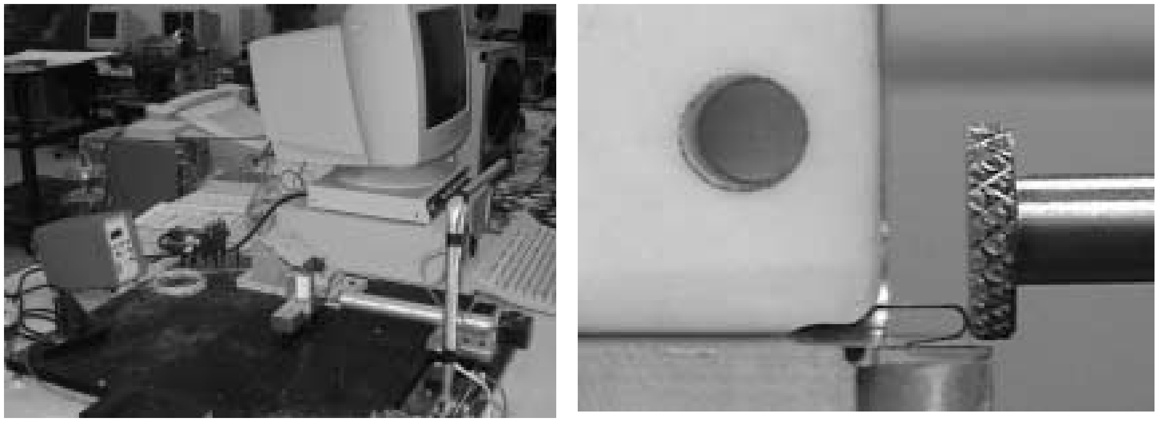

(a) (b)

Figure 9.11 (a) General testing setup and (b) close-up of contact with fixture and probe

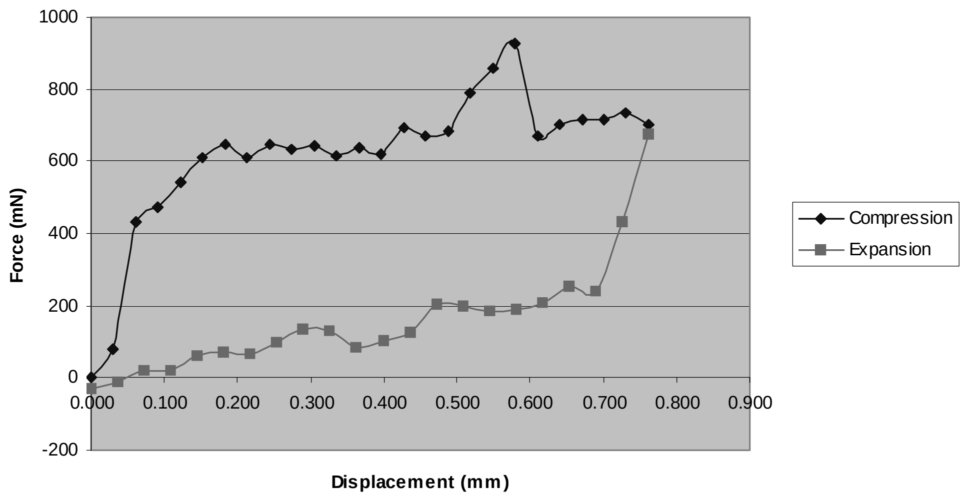

Figure 9.12 Graph of force versus displacement from test data

There are two interesting phenomenon that were observed in every test. First, since there is no pre-load on the mechanism, the initial force must be zero. However, as the mechanism goes through the initial displacement (about 0.05 mm), there is a sharp rise from zero force to the intended constant-force. The phenomenon was observed in every test and in fact was observed by Millar et al. (1996) during initial testing of constant-force mechanisms. This is easily addressed by applying a deflection preload of 0.05 mm.

The second phenomenon observed is a difference in force between the compression and expansion strokes of the testing. During the compression stroke, the mechanism experienced a higher force than predicted. As the mechanism reverses direction, there is a sharp decrease in the force to a point below the predicted force which persists throughout the expansion stroke.

This phenomenon was consistent throughout testing and is found in all types of electrical contacts and mechanisms. In fact, this same phenomenon was also observed by Boyle (2001) while studying the dynamics of constant-force mechanisms. In all cases, this behavior is consistent with the effects of friction, which acts in the direction to oppose motion. Boyle (2001) was successful at modeling this phenomenon as friction found within the mechanism and testing system.

The accuracy of the model can be verified by comparing the testing results with the predicted results. However, the model used for the case study does not account for the friction, requiring that the effects of the friction be removed from the test data. Assuming that the difference in force between the compression and expansion strokes and the force of the mechanism without friction is the magnitude of the friction force, the effects of friction can be removed by averaging the compression and expansion strokes .

Additionally, to make the comparison between test results and model predictions, new predictions were made based on the actual shape and size of prototype 3. These predictions are listed in Table 9.4 while Figure 9.13 shows the predicted and adjusted-measured forces for prototype 3.

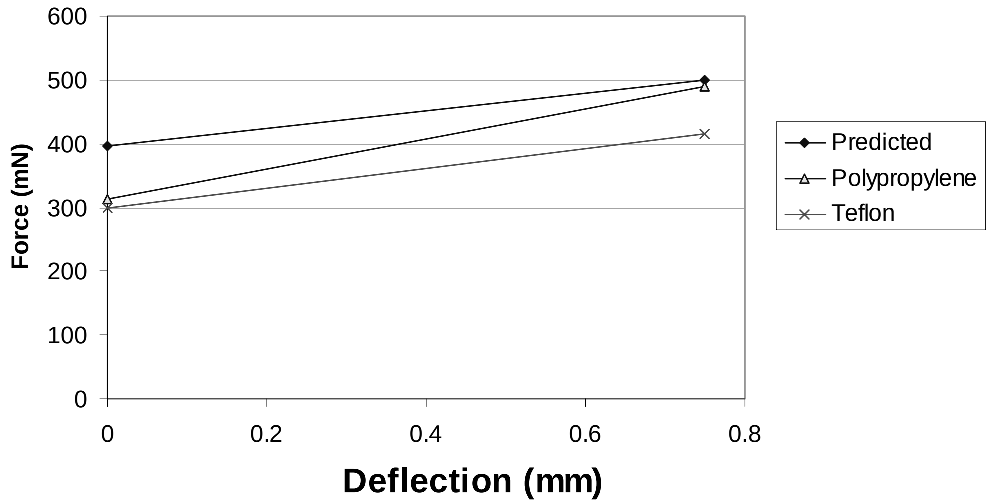

Figure 9.13 Average and predicted force comparison

Table 9.4 Parameter summary of prototype 3

Function Symbol	Prototype 3	Constraint Value for Case-Study
$h_{package}$	5.6 mm	≤ 6 mm
$b_{package}$	5.5 mm	≤ 12 mm
h	0.2 mm	0.2 mm
b	1.0 mm	1.0 mm
Minimum Bend Radius	0.7 mm	≥ 0.7 mm
E	110e9 Pa	110e9 Pa
S_y	552e6 Pa	552e6 Pa
SF	1.29	≥ 1.0
F_{ave}	448 mN (45.7 gf)	≈ 441 mN (45 gf)
F_{min}	418 mN (42.6 gf)	≥ 294 mN (30 gf)
F_{max}	500 mN (51.0 gf)	≤ 588 mN (60 gf)
Percent Constant (Ξ')	79.4	60

The percent constant-force for prototype 3 can be calculated by using Equation (9.1). However, since the model does not include the region of quickly rising forces in the initial deflections, the method introduced in Section 5.3 must be used to calculate the extrapolated percent constant-force, Ξ'_{ex}. This value is found by using Equation (5.27) with the lowest average force on the flat part of the curve as F_{min} and the highest force as F_{max}. This results in a value for Ξ'_{ex} that is within 12% of the predicted extrapolated percent-constant force. Table 9.5 contains a summary of the comparison between the testing and predicted values.

9.10 Case Study Conclusions and Recommendations

This chapter has presented work done to develop near-constant-force mechanisms for use in electrical connectors. Viable configurations were developed, and one configuration was chosen for use in a case study. A design for the chosen configuration was generated, prototyped, and tested. The testing results indicated that the model predicted the performance of the prototype.

The application of constant-force mechanism technology to electrical contacts could provide a number of benefits in terms of performance, robustness, and package size.

Table 9.5 Summary of testing and prediction comparisons

	Level of Constant Force		Average Force		
	Ξ'_{ex}	% Error	Force (mN)	Force (gf)	% Error
Predicted	79.42	-	447.97	45.68	
Measured-Teflon Cam	71.89	9.49	402.62	41.06	10.12
Measured - Polypropylene Cam	63.86	11.17	357.59	36.46	20.17

The successful demonstration of the uncoupling of the force and deflection in an electrical contact promises to create new possibilities in electrical contact designs, possibilities in lowering required manufacturing tolerances, reduction of system sensitivity to variations introduced by the user, and increased system robustness in applications where movement and/or vibrations exist.

Further work to explore the contribution of CFECs to these areas must be done. The size and force limitations and the affects of tolerances on CFECs should be better understood as well as a better understanding of the phenomenon observed.

CHAPTER 10 SUMMARY, CONCLUSIONS, AND RECOMMENDATIONS

10.1 Review of Research Purposes

The five purposes for this research were:

- Seek to understand compliant constant-force mechanism behavior from both a stress and force viewpoint.
- Develop different ways of comparing constant-force mechanisms.
- Define new mechanisms with improved performance.
- Outline a design method that can be used independent of the pseudo-rigid-body model.
- Incorporate constant-force behavior into electrical contacts.

10.2 Summary

The purposes listed above were attained through the main contributions of this research including:

- Non-dimensionalized parameters were developed. These parameters can be used to assess stress and force feasibilities.

- The classification system for CFMs was refined and expanded to include naming methods for groups of mechanisms, families of mechanisms, and individual mechanisms.

- Methods for comparing constant-force mechanisms were established and defined.

- A detailed optimization model was developed that incorporated the new non-dimensionalized parameters.

- The model was used, together with the comparison methods, to seek out and identify new and improved mechanisms. This effort resulted in the discovery of mechanisms with major improvements in stiffness and feasible manufacturing orientations.

- A design methodology, including detailed examples, was outlined and set forth to assist designers in the design of CFMs. Included were the primary design equations, methods to identify stress and force feasible mechanisms, and description of variable interactions and trends.

- A constant-force electrical contact was developed and tested. The CFEC performed as intended and the details and results were presented.

10.3 Conclusions

Before this research was performed, the CFM knowledge base was limited. This work has resulted in new understanding and insights into CFMs. Important new comparison methods were developed that can be used to identify new mechanisms and aid in the design process.

While it was not known whether or not improvements over the original CFMs could be made, this work showed that improvements were possible. In most cases, the level of constant-force could not be improved. However, for the Class 2B mechanisms, the level of constant-force was improved from 93 percent constant to 99 percent constant for the sub-class a mechanisms. For the sub-class b mechanisms in this class, the percent constant-force increased from 84 to 99, an 18% increase.

For every class of mechanism, an increase in the stiffness was made without increasing the relative stress in the mechanism. Each class of mechanisms had some kind of increase (ranging from 5% to 3000%) with the largest improvements in Class 2B.

Four 16% deflection mechanisms and five 40% deflection mechanisms were defined with a stiffness parameter greater than or equal to 1 (see Table 10.1). These mechanisms were in the *lpp* and *lps* configurations and are the stiffest known CFMs.

It was also observed that the configurations with at least one long flexible segment had higher stiffness parameters than their counterparts with only small-length flexural pivots. The use of long flexible beams is important in gaining stiffness without increasing stress.

This work also showed that a reasonable design approach is possible. This design approach was defined and works for many different design scenarios. The design method-

Table 10.1 Mechanisms with highest stiffness

Configuration	Sub-Class	Ξ'	Ψ	R	K_2	$\%\Delta\Psi$
lpp	a	99.7	1.000	0.8274	-	-
	a99	99	1.046	0.8018	-	4.6%
	a95	95	1.239	0.7106	-	23.9%
	a90	90	1.490	0.6185	-	49.0%
lpp	b	97.6	1.000	0.8853	-	-
	b95	95	1.052	0.8595	-	5.2%
	b90	90	1.129	0.8226	-	12.9%
lps	b95M	95	1.053	0.8561	0.0100	5.3%
	b90M	90	1.137	0.8177	0.0100	13.7%

ology allows the designer to make educated decisions and choices based on the information summarized in the tables. Additionally, two methods were outlined that identify mechanisms that are either feasible from a stress or force standpoint. It was also shown that when these methods are used together, it is possible to identify all of the mechanisms that will satisfy all of the design constraints.

It can be concluded from this work that the methods and techniques used to design CFMs can be used to develop models for mechanisms other than the traditional slider crank. The CFEC developed in this work is such a mechanism. A number of viable configurations were developed, and one configuration was chosen. From this configuration, a design was generated, prototyped, and tested. Testing results showed that the CFEC displayed constant-force behavior and characteristics similar to the models predictions.

Additionally, the successful demonstration of the uncoupling of the force and deflection in an electrical contact promises to create new possibilities in electrical contact designs, possibilities in lowering required manufacturing tolerances, reduction of system sensitivity to variations introduced by the user, and increased system robustness in applications where movement and/or vibrations exist. This could lead to benefits in terms of performance, robustness, and package size.

10.4 Recommendations for Further Research

This section recommends and outlines some of the areas in which future work should be undertaken.

10.4.1 New Configurations

Much work was done to understand the limitations of the original configurations. However, much work is needed to understand the following types or variations of configurations.

- *Cam*- Replacement of link with circular cam
- *Offset* - Mechanisms that utilize the eccentricity of the mechanism
- *Orthoplaner* - Configurations that start in an orthoplaner (in plane) position
- *Linear Spring* - Configurations that include a linear spring
- *Perpendicular Force* - The movement of the force from a horizontal position to a vertical position
- *Inverted Mechanisms* - These are mechanisms that work under tension
- *Series/Parallel configurations* - Different arrangements of CFM in series and parallel to achieve desired displacement/force
- *Pre-loads* - Different pre-loads on the torsional and linear springs
- *lpl*- Configuration with two long flexible segments attached with a pin

The model developed for this work had the ability to add pre-loads, linear springs, and offsets to the traditional mechanisms, as well as consider orthoplaner type CFMs. It is recommended that further work be done to fully understand the effects and possibilities presented by these types of mechanisms.

10.4.2 Physical Implementation

Going from theory to physical implementation presents many challenges. During the development of the CFEC, several different phenomenon where observed that affected the performance of the CFEC. These phenomenon included:

- Sharp rise as the mechanism is initially displaced
- Difference in force between compression and expansion strokes
- Sensitivity to tolerances

The effects of physical implementation of CFMs should be studied more fully. These phenomenon and others should be studied, allowing CFMs to be used in future applications.

10.4.3 Other Mechanisms

The requirements for constant-force mechanisms were partially outlined in this work. With the development of the CFEC, a different type of mechanism was developed that exhibited constant-force behavior. It is recommended that further work be undertaken to examine other types of mechanisms for the properties required for constant-force behavior. Some of these mechanisms include: centrifugal clutches and four-bar mechanisms.

10.4.4 Other Flexible Segment Configurations

The *lpp* configuration exhibited the highest stiffness of the configurations examined. Other configurations were constrained by stress due to small-length flexural pivots. It can then be reasoned that the *lpl* configuration, which adds a second long flexible segment without affecting stress, should exhibit an even greater stiffness than the *lpp* configuration. It is recommended that further work should be done to understand the behavior of the *lpl* configuration, its stiffness, and its susceptibility to stress.

10.4.5 Applications

The improved mechanisms and the design methodology developed can be used to develop CFMs for applications. It is recommended that work be done to implement CFMs in viable commercial applications. This can be in conjunction with the work of Boyle (2001) on the dynamics of CFMs to develop CFMs for dynamic applications.

10.4.6 Constant-Force Electrical Contacts

Further work to explore the contribution of CFECs to reduction in required manufacturing tolerances, reduction in system sensitivities to variation, and increased design robustness must be done. The size and force limitations and the affects of tolerances on CFECs should be better understood, as well as a better understanding of the effects of the observed phenomenon on electrical contact performance.

References

Bossert, D., Ly, U. L., and Vagners, J., 1996, “Experimental Evaluation of a Hybrid Position and Force Surface Following Algorithm for Unknown Surfaces,” *Proceedings - IEEE International Conference on Robotics asnd Automation,* Vol. 3, pp. 2252-2257.

Boyle, C. L. , 2001, “A Closed-Form Dynamic Model of the Compliant Constant-Force Mechanism using the Pseudo-Rigid-Body Model,” M.S. Thesis, Brigham Young University, Provo, Utah.

Brush Wellman Inc., 1999, *Connector Engineering Design Guide: Material Selection in the Design of Spring Contacts and Interconnections*, Brush Wellman Inc.

Chang, L. H., and Fu, L. C., 1997, “Nonlinear adaptive control of a flexible manipulator for automated deburring,” *Proceedings - IEEE International Conference on Robotics asnd Automation,* Vol. 4, pp. 2844-2849.

Deshpande, A. and Subbarayan, G., 2000, “LGA Connectors: An Automated Design Technique for Shrinking Design Space,” *Journal of Electronic Packaging*, Vol. 122, pp. 247-254.

Evans, M. S., and Howell, L. L., 1999, “Constant-Force End-Effector Mechanism,” *Proceedings of the IASTED International Conference, Robotics & Applications,* Santa Barbara, CA, USA, pp. 250-256.

Harper, C. A. 1996, *Electronic Packaging & Interconnection Handbook -Second Edition,* McGraw-Hill, New York.

Herder, J.L., Tuijthof, G.J.M., “Two Spatial Gravity Equilibrators,” *Proceedings of the 2000 Design Engineering Technical Conferences and Computer in Engineering Conference,* DETC2000/MECH-14120.

Herder, J. L., van den Berg, F. P. A., “Statically Balanced Compliant Mechanisms (SBCM’s), An Example and Prospects,” *Proceedings of the 2000 Design Engineering Technical Conferences and Computer in Engineering Conference*, DETC2000/MECH-14144.

Howell, L. L., 2001, *Compliant Mechanisms*, John Wiley and Sons, New York.

Howell, L. L., Midha, A., and Murphy, M. D., 1994, “Dimensional Synthesis of Compliant Constant-Force Slider Mechanisms,” *Proceedings of DETC’94, ASME Design Engineering Technical Conferences*, DETC98/MEMD-71.

Howell, L. L. and Midha, A., 1994, “The Development of Force-Deflection Relationships for Compliant Mechanisms,” *Proceedings of the 1994 ASME Mechanisms Conference*, DE-Vol. 71, pp. 501-508.

Howell, L. L., and Midha, A., 1995, “Determination of the Degrees of Freedom of Compliant Mechanisms Using the Pseudo-Rigid-Body Model Concept,” *Proceedings of the Ninth World Congress on the Theory of Machines and Mechanisms*, Milano, Italy, Vol. 2, p. 1537-1541.

Howell, L. L., and Midha, A., 1996, “A Loop-Closure Theory for the Analysis and Synthesis of Compliant Mechanisms,” *ASME Journal of Mechanical Design*, Vol. 118, No. 1, pp. 121-125.

Jenuwine, J. G., and Midha, A., 1994, “Synthesis of Single-Input and Multiple-Output Port Mechanisms with Springs for Specified Energy Absorption,” *Journal of Mechanical Design,* Trans. ASME, Vol. 116, No. 3, September, pp. 937-943.

Midha, A., Murphy, M. D., and Howell, L. L., 1995, “Compliant Constant-Force Mechanism and Devices Formed Therein”, U.S. Patent 5649454, Issued July 22, 1997.

Millar, A. J., Howell, L. L, and Leonard, J. N., 1996, “Design and Evaluation of Compliant Constant-Force Mechanisms,” *Proceedings of the 1996 ASME Design Engineering Technical Conferences and Computers in Engineering Conference*, 96-DETC/MECH-1209.

Murphy, M. D., Midha, A., and Howell, L. L., 1994, “Methodology for the Design of Compliant Mechanisms Employing Type Synthesis Techniques with Example,” *Proceedings of the 1994 ASME Mechanisms Conference,* DE-Vol. 70, pp. 61-66.

Nathan, R. H., 1985, “A Constant Force Generation Mechanism,” *Journal of Mechanisms, Transmissions, and Automation in Design*, Trans. ASME, Vol. 107, December, pp. 508-512.

Parkinson, M. B., Howell, L. L., and Cox, J. J., 1997, “A Parametric Approach to the Optimization-Based Design of Compliant Mechanisms,” *Proceedings of the 23rd Design Automation Conference*, DETC97/DAC-3763.

Paul, B. 1979, *Kinematics and Dynamics of Planar Machinery*, Prentice-Hall, Englewood Cliffs, New Jersey.

Wahl, A., 1963, *Mechanical Springs*, 2nd. Ed. McGrawHill, New York.

Wittwer, J. W., 2001, "Predicting the Effects of Dimensional and Material Property Variations in Compliant Mechanisms," M.S. Thesis, Brigham Young University, Provo, Utah.

Williman, J., 1995, "Small Torque," *Engineering (London)*, Gillard Welch Associates, pp. 27-28.

APPENDIX A PSEUDO-RIGID-BODY MODEL

The Pseudo-Rigid-Body Model (PRBM) plays an important part in the design and analysis of compliant mechanisms. This appendix offers a closer look at the PRBM. It gives a brief overview and then discusses the nomenclature and equations for several different types of flexible segments. However, no attempt is made to show evidence of the validity of the PRBM or its limitations. For further information and details, the reader is referred to the work from which this appendix was summarized (Howell, 2000).

A.1 PRBM Overview

The design and analysis of compliant mechanisms can be complicated. Traditionally, the large non-linear deflections have caused significant difficulties in the design of compliant mechanisms. Techniques such as finite element analysis (FEA) and elliptic integrals provide accurate information, but make design very drawn out and complicated.

Fortunately, the development of the PRBM has greatly increased the speed and ease in which compliant mechanisms can be designed. The PRBM allows for the approximation of the force-deflection characteristics of flexible segments. Thus, the PRBM is intended to be an intermediate design tool, allowing for the rapid design and analysis of first generation compliant mechanisms. Afterwards, techniques such as FEA and other numerical methods can be used to refine the designs. The PRBM becomes a tool to take beginning ideas to refined designs.

The power of the PRBM comes from its ability to model compliant members using rigid members that have the same force-deflection characteristics as the original member. Continuous work in developing the PRBM has shown it to accurately model the behavior of compliant mechanism in displacement, force, velocity, and acceleration. Thus, designers can draw from the vast number of traditional mechanism design and analysis tools.

For each type of flexible segment, several parameters are defined. The first of these is the *characteristic pivot*. The characteristic pivot is the center of the arc created by the path of the end of the beam. This pivot lies on the flexible beam and is represented as a pin joint in the PRBM. Equations for the position of this characteristic pivot is given for each type of flexible segment and is easily determined. Additionally, the variable Θ is the *pseudo-rigid-body angle* and equations relating it to the end angle of the beam are presented.

The strain energy stored in each flexible member is represented by a torsional spring with a spring constant of K. This spring constant is determined by geometric and material properties and is also dependent upon the type of flexible member. Formulas for each of these spring constants will be given.

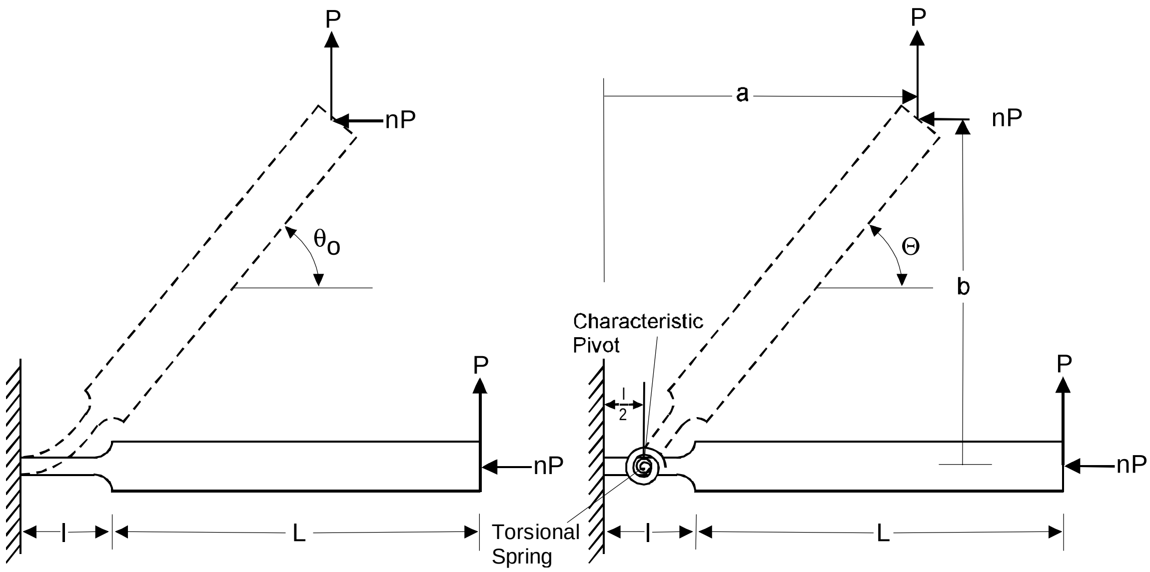

Figure A.1 (a) A small-length flexural pivot and (b) its PRBM

These are the main parameters that will be described below. Each section gives a diagram for the flexible segment and its corresponding PRBM diagram, the characteristic pivot, and the torsional spring constant. Additionally, the formula for the maximum stress in each flexible element will be given.

A.2 Small-Length Flexural Pivots

A small-length flexural pivot is one in which a large beam is grounded or pinned through a smaller beam, as illustrated in Figure A.1a. Typically, a small-length flexural pivots satisfies the following conditions:

$$L \gg l \tag{A.1}$$

$$(EI)_L \gg (EI)_l \tag{A.2}$$

The characteristic pivot is located at the center of the small-length flexural pivot as shown in Figure A.1b. For small-length flexural pivots, the basic equations are

$$\Theta = \theta_o \quad \text{(A.3)}$$

$$K = \frac{(EI)_l}{l} \quad \text{(A.4)}$$

$$T = K\Theta \quad \text{(A.5)}$$

The *x* and *y* coordinates of the end of the beam can be found through

$$a = \frac{l}{2} + \left(L + \frac{l}{2}\right)\cos\Theta \quad \text{(A.6)}$$

and

$$b = \left(L + \frac{l}{2}\right)\sin\Theta \quad \text{(A.7)}$$

The stress equations for this flexible segment are

$$\sigma_{top} = \frac{-(Pa + nPb)c}{I} - \frac{nP}{A} \quad \text{(A.8)}$$

$$\sigma_{bot} = \frac{(Pa + nPb)c}{I} - \frac{nP}{A} \quad \text{(A.9)}$$

The equations presented here are sufficient in most cases. At times, the size of the small-length flexural pivot is small enough that the spring constant can be ignored if other larger torques are present. This special case small-length flexural pivots are called living hinges.

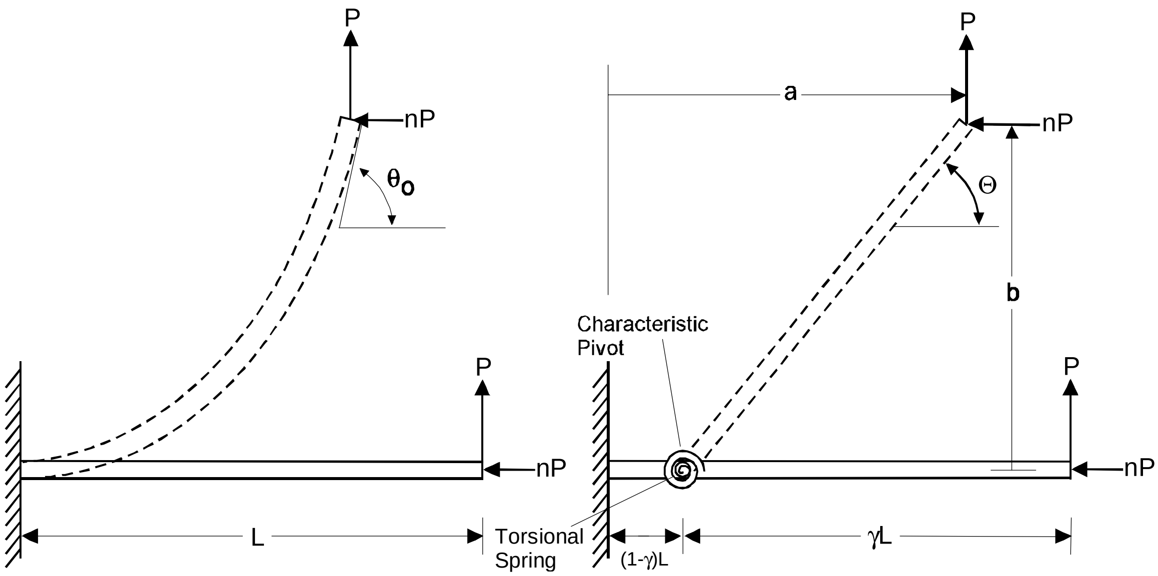

Figure A.2 (a) Cantilever beam with force at end and (b) its PRBM

A.3 Cantilever Beam with Force at End

A second type of flexible segment is a cantilever beam with a force at the end. Figure A.2a show the cantilever beam with its PRBM and corresponding parameters (Figure A.2b).

The characteristic pivot is located a distance γL from the free end where γ is the *characteristic radius factor*. The value of the characteristic radius factor is a function of the direction of the applied force and can be expressed in terms of n as follows:

$$\gamma = 0.841655 - 0.0067807n + 0.000438n^2; \qquad (0.5 < n < 10.0) \tag{A.10}$$

$$\gamma = 0.852144 - 0.0182867n; \qquad (-1.8316 < n < 0.5) \tag{A.11}$$

$$\gamma = 0.912364 + 0.0145928n; \qquad (-5 < n < -1.8216) \tag{A.12}$$

For values of n between -0.5 and 1.0,

$$\gamma_{ave} = 0.85 \quad \text{(A.13)}$$

There is some slight deviation between the pseudo rigid body angle and the actual angle of the beam. This variation is almost linear and is compensated through

$$\theta_o = c_\theta \Theta \quad \text{(A.14)}$$

where

$$c_\theta \approx 1.24 \quad \text{(A.15)}$$

The value of c_θ, the *parametric angle coefficient*, varies between 1.256 and 1.179. Values for different values of *n* are tabulated in Howell (2000).

The torsional spring constant for a cantilever beam with a force on the end can be found from

$$K = \gamma K_\theta \frac{EI}{l} \quad \text{(A.16)}$$

$$K_\theta \approx 2.65 \quad \text{(A.17)}$$

The value K_θ is called the *stiffness coefficient*. The approximation given in Equation (A.17) is accurate in most cases. However, more accurate values are given in Howell (2000). With the spring constant, force and torque calculations can be made according to Equation (A.5).

The *x* and *y* coordinates of the end of the beam can be found through

$$a = L - \gamma L(1 - \cos\Theta) \quad \text{(A.18)}$$

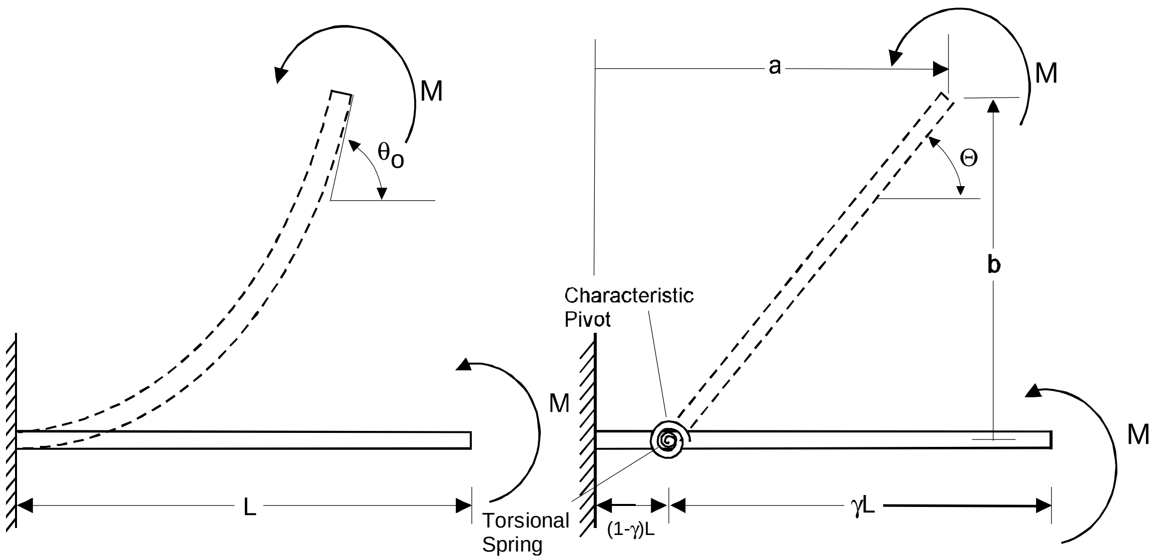

Figure A.3 (a) Cantilever beam with force at end and (b) its PRBM

and

$$b = \gamma L \sin\Theta \tag{A.19}$$

The stress in the beam can be calculated from Equation (A.8) and Equation (A.9), which are the same equations used for the small-length flexible segment.

A.4 Cantilever Beam with End Moment Loading

A cantilever beam is often loaded with an end moment. Figure A.3 show this loading configuration along with its PRBM. The equations for this configuration are identical to the previous configuration. However, there are some differences in the values of the parameters. The characteristic radius factor is

$$\gamma = 0.7346 \tag{A.20}$$

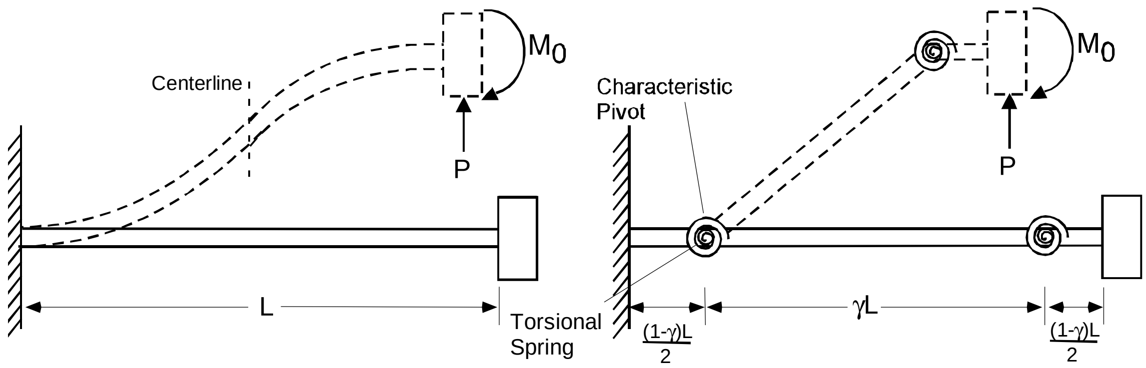

Figure A.4 (a) Fixed-guided beam and (b) its PRBM

The parametric angle coefficient is

$$c_\theta = 1.5164 \tag{A.21}$$

and the stiffness coefficient is

$$K_\Theta = 2.0643 \tag{A.22}$$

A.5 Fixed-Guided Beam

A common type of flexible segment is the fixed-guided beam. This beam consists of a beam fixed on one end, while the other end is kept perpendicular to ground during displacement. This is commonly see in mechanisms such as parallel and folded beam mechanisms and is illustrated in Figure A.4.

Close observation of the fixed-guided beam shows that the curvature is zero at the middle due to symmetry. It is also known that the curvature at the end of a cantilever beam with an end load is also zero. Therefore, the fixed-guided beam can be modeled as two cantilever beams each half the length of the original beam. Thus, the PRBM is easily found.

The parameters for this beam are similar to previous parameters. The characteristic radius factor is

$$\gamma = 0.8517 \qquad \text{(A.23)}$$

Since the beam has a constant end angle, the parametric angle coefficient is trivial and

$$c_\theta = 0 \qquad \text{(A.24)}$$

The spring constant is found to be

$$K = 2\gamma K_\theta \frac{EI}{l} \qquad \text{(A.25)}$$

From observation, it can be seen that the spring constant for the fixed-guided beam is twice that for cantilever beams. This indicates that the overall stiffness of the fixed-guided is four times that of the cantilever beam.

Since the end of the beam is constrained, a reactionary moment, M_o is created. The formula for this moment is

$$M_o = \frac{Pa}{2} \qquad \text{(A.26)}$$

or

$$M_o = \frac{Pl}{2}[1 - \gamma(1 - \cos\Theta)] \qquad \text{(A.27)}$$

The maximum stress occurs at the ends of the beam where the moment is largest. It has a value of

$$\sigma_{max} = \frac{Pac}{2I} \quad \text{(A.28)}$$

APPENDIX B MODEL AND OPTIMIZATION CODE

B.1 MatLab Code

The CFM model is written in Matlab. Matlab has the ability to manipulate files, store matrices, and use functions. However, a significant advantage is that no compiling is required as in C. Changes can be made and the program can be execute immediately. This allows for quick and easy changes. Unfortunately, this software requires that Matlab is installed and running on the computer to run the code.

B.1.1 File Run Order

The 4 separate Matlab files make up the CFM model. These files each serve a different purpose allowing the model to be either independently or linked to the optimization code. The different operating paths of the model and the run order of the files are summarized in Figure B.1. The primary file, *CFMModel*, is the model core. This file contains all of the relationships and functions used by the model.

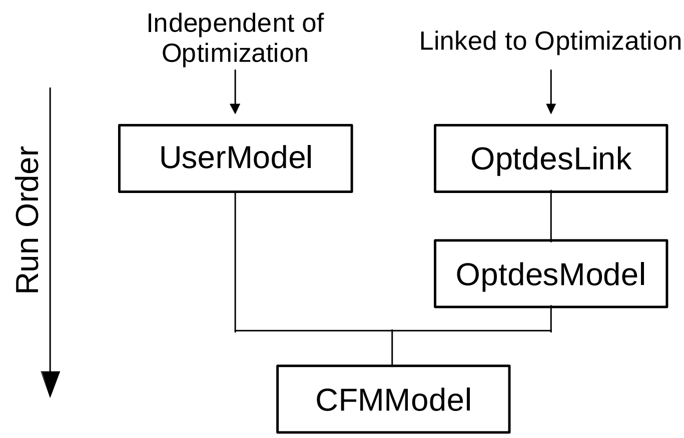

Figure B.1 Summary of Matlab file paths and run order

The *UserModel* file is used by the user to run the model independent of the optimization software. The user can change the input values within this file. This file then calls and passes all important parameters to *CFMModel. UserModel* then receives all the output values from *CFMModel*.

The file *OptdesModel* is similar in purpose to *UserModel*. However, this file receives all the needed information from data files created by the optimization code. It then calls *CFMModel* and passes and receives all important values. Its final duty is to create an output file that is read by the optimization code.

The final file is OptdesLink. This file handles the handshaking that goes on between Matlab and OptdesX. It triggers OptdesModel, telling it when the optimization code is finished creating data files. It then tells the optimization code when Matlab is finished and the output file has been generated.

B.1.2 Variable Name Mapping

Due to the number of variables required, there relationship to one another, and requirements for input and output of data, the variable names in the Matlab and OptdesX code are not necessarily intuitive. In some cases, to simplify the writing of the code, two names were used. Table B.1 outlines the variable names, any second names that may exist, and the parameter or item that the variable represents. This table can be used to help understand more fully the code.

B.1.3 *CFMModel* Code

```
%[cfparam,deltax,phi]=cfmmodel(r2,r3,k1,k2,k3,percentage)
%percentage in
%r2,r3
```

Table B.1 Mapping of parameter names to names in Matlab and OptdesX code

Variable Name	Alternate Name	Parameter	Variable Name	Alternate Name	Parameter
Matprop(1)		E	di		Initial displacement (manufactured position)
Matprop(2)		S_y	d		d
Matprop(3)		Sy/E	ds		Linear Spring Preload
SF		Safety Factor			
stress(x)		stress	rtot		r_{tot}
			ltot		l_{tot}
lengths(1)	ri	r_i	L		λ
lengths(2)	r2	r_2			
lengths(3)	r3	r_3	roe(x)		ρ
lengths(4)	r4	r_4	zeta(x)		ζ
			ka(x)		κ_x
geoparam(x,1)		b_x	deltax		deflection vector
geoparam(x,2)		h_x			
geoparam(x,3)		I_{flex}	alpha		α at each displacment
			fparam		Ψ at each displacement
pivotparam(x,1)		Pivot Type	F		Force at each displacement
pivotparam(x,2)		Reference (1B)	Fave		Average Force
pivotparam(x,3)	thetaxo	Preload angle			
pivotparam(x,4)	kx	k_x	r4		length of r_4 -eccentricity portion
pivotparam(x,5)	thetaxi	Initial angle	r4type		0 - Regular 1- Forces orthoplaner
pivotparam(x,5)	thetaxfinal	Final angle	A(x)		A
			I(x)		moment of inertia
cfparam(1)	R	R	maxstresspivot		primary pivot
cfparam(2)	K1	K_1	changepivot		# of changes in primary pivot
cfparam(3)	K2	K_2			
cfparam(4)	K3	K_3	DesignParameter(x,1)	hpx	max h_x given same b
cfparam(5)	averagephi	Average Φ	DesignParameter(x,2)	bpx	max b_x given same h
cfparam(6)	averagephis	average Φ_s	DesignParameter(x,3)	Dx	D
cfparam(7)	Xi	Ξ'	DesignParameter(x,4)	Areax	Design Area
configparam(1)		alphamax	fit		Turn Curve Fit On (1) or Off (0)
configparam(2)		primary pivot	pc(1)		M
configparam(3)		changepivot	pc(2)		n
configparam(4)		average_Beta	C		C
configparam(5)	fp	Ψ			
configparam(6)	dN	d_N			

* note: in AnasubC, array values are all shifted down by 1due to C code requirments.

```
function[lengths,cfparam,configparam,pivotparam,geoparam,deltax,F,di,d,SF,pc,alpha,Beta,fparam,phi,ka,C,Des
        ignParam]=cfmmodel(ltot,r4type,r4,di,d,ds,geoparam,pivotparam,cfparam,matprop,fit)
gamma=[0,1,0.85];
roedata=[1,0.1,1/0.85];        %One in first place is to avoid dividing by zero.
Ktheta=[0,1,2.65];
fgoal=.4518;
%10.2483;
Ldata=[1,1.05,gamma(3)];
%Spot at which f parameter is compared.
%if d==16
 % famount=15.9/100;
%elseif d==40
%  famount=0.05;
%end

R=cfparam(1);
geoparam(2,1)=geoparam(1,1);
geoparam(3,1)=geoparam(1,1);

K1=cfparam(2);
K2=cfparam(3);
K3=cfparam(4);
K(1)=1;
K(2)=K1;
K(3)=K2;
K(4)=K3;
k1=pivotparam(1,4);
k2=K1*k1;
k3=K2*k1;
pivotparam(1,4)=k1;
pivotparam(2,4)=k2;
pivotparam(3,4)=k3;

Lvalues(1)=R;
Lvalues(2)=1;
Lvalues(3)=1;

if pivotparam(1,1)==2
  Lvalues(2)=Lvalues(2)*Ldata(2);
elseif pivotparam(1,1)==3
  Lvalues(1)=Lvalues(1)*Ldata(3);
  Lvalues(3)=Lvalues(3)+1;
end
if pivotparam(2,1)==3
  if pivotparam(1,1)==2
    Lvalues(2)=Lvalues(2)*Ldata(3);
    Lvalues(3)=Lvalues(3)+1;
  elseif (pivotparam(2,2)==3)
    Lvalues(2)=Lvalues(2)*Ldata(3);
    Lvalues(3)=Lvalues(3)+1;
  else
    Lvalues(1)=Lvalues(1)*Ldata(3);
    Lvalues(3)=Lvalues(3)+1;
   end
 end
 if pivotparam(3,1)==2
   Lvalues(1)=Lvalues(1)*Ldata(2);
 elseif pivotparam(3,1)==3
   Lvalues(2)=Lvalues(2)*Ldata(3);
   Lvalues(3)=Lvalues(3)+1;
 end

 if Lvalues(3)==1
```

```
  Lvalues(3)=R+1;
 else
  Lvalues(3)=Ldata(3)*(R+1);
 end
L=(Lvalues(1)+Lvalues(2))/Lvalues(3);

rtot=ltot/L;
r3=rtot/((1+1/R));                    %Calculate r3 value
r2=rtot/(1+R);                    %Calculate r2 value



d=d/100;
class1B=0;                    %Boolean for class 1B config.
for i=1:3
  roe(i)=roedata(pivotparam(i,1));
  zeta(1)=R+1;
  zeta(3)=1+1/R;
  if (pivotparam(2,1)==2)%Small length in center
    zeta(2)=2;
  elseif (pivotparam(2,1)==3)       %Long flexible in center
    if pivotparam(1,1)==1
      if (pivotparam(2,2)==2)         %Associated with r2
        zeta(2)=zeta(1);
      else
        zeta(2)=zeta(3);            %Associated with r3
      end
    else
      zeta(2)=zeta(3);
    end
   else
    zeta(2)=1;                    %Sets to arbitary 1 (not zero so can divide w/o error
  end
  geoparam(i,3)=rtot*roe(i)/zeta(i);   %Calculate flexible segment lengths

  if pivotparam(i,1)==1
    I(i)=0;
    geoparam(i,2)=0;
  else
    I(i)=pivotparam(i,4)*geoparam(i,3)/(gamma(pivotparam(i,1))*Ktheta(pivotparam(i,1))*matprop(1));    %Calcu-
      late spring constants
    geoparam(i,2)=(12*I(i)/geoparam(i,1))^(1/3);
  end
  A(i)=geoparam(i,2)/(2*rtot);  %Calculate A value
  ka(i)=gamma(pivotparam(i,1))*zeta(i)*Ktheta(pivotparam(i,1))/roe(i);
end

if (pivotparam(1,1)==1)
  class1B=1;
  geoparam(1,3)=geoparam(1,2);
  pivotparam(1,4)=pivotparam(2,4);
  A(1)=A(2);
  ka(1)=ka(2);
end



type=0;
if (r4type==1)                  %Forces Orthoplaner position by changing r4 from user defined to ideal for orthoplaner
  r4=(1-R)*r2;
end
ks=K3*k1/(r2*r2);
```

```
pivotparam(4,4)=ks;
rimin=0;
if (r3+r4>r2) %& ~(r4==0)     %Limits ri so that mechanisms doesn't go back on itself
   theta3max=asin((r4-r2)/r3);    %Limits to where r2 is vertical.  Finds theta3max
   rimin=r3*cos(theta3max);       %Sets start point and limits for non-linear solver
   thetaT = pi/4;
   limit = pi/2;
elseif (r3+r4<r2) %& ~(r4==0)     %Limits to where r3 and r4 are vertical. Finds theta2max
   theta2max=asin((r4+r3)/r2);
   rimin=r2*cos(theta2max);
   thetaT = theta2max/2;
   limit = theta2max;
elseif (r3+r4==r2)                %OrthoPlaner position
   thetaT=pi/4;
   limit=2*pi;
end

ri=sqrt((r2+r3)^2-r4^2)*(1-di);    %Calculate initial displacement (rest)
if (ri<rimin) %& (d<0)        %Force ri to be no longer than maximum allowable displacement with given geometery
   ri=rimin;
   di=1-ri/(r2+r3);
   if d>0                    %Don't allow any compression because ri=rimin
      d=0;
   end
elseif (d>0) & (ri*(1-d)<rimin)     %checks to see if compression mechanism is going too far
   d=1-rimin/ri;                        %Resets percd to maximum allowable
end

%Solve for theta i's
if (di==0) & (r4==0)%if initially flat
   theta2i=0;
   theta3i=2*pi;
   theta4i=pi;
elseif (di==1)                        %if orthoplaner
   theta2i=pi/2;
   theta3i=3*pi/2;
elseif (r4==0)
  theta2i=acos((ri*ri+r2*r2-r3*r3)/(2*ri*r2));   %Solves for initial angles (not pre-load)
  theta3i=2*pi+asin(-r2*sin(theta2i)/r3);         %Solves for initial angle 3 (not pre-load)
else
   del = 1e-6;
   tol = 1e-3;
   theta2i = Newton(type,'theta2',thetaT,[ri,r2,r3,r4],limit,del,tol);
   theta3i = asin((r4-r2*sin(theta2i))/r3)+2*pi;
end


theta2o=theta2i+pivotparam(1,3);   %Initial angle + Pre-load-->Pre-load is Counter Clock-wise resulting in nega-
        tive torque (radians)
theta3o=theta3i+pivotparam(2,3);   %Initial angle + Pre-load-->Pre-load is Counter Clock-wise resulting in nega-
        tive torque (radians)
theta4o=2*pi-theta3i+pivotparam(3,3);

%d is the percent deflection of mechanism.
if (d>0)   %If d is >0, then is percent of rest length.
   deltax=0.001:0.001*ri*d:(ri)*d;  %Set up percentage vector
   [r1]=ri-deltax;
else  % if d <0, then is percent of total allowable(total length - rest length)
   deltax=0.001:0.001*(sqrt((r2+r3)^2-ri^2)):(sqrt((r2+r3)^2-r4^2)-ri)*d*-1;
   [r1]=ri+deltax;                      %Set up r1 vector
end

[trash,sz]=size(deltax);                    %Find value of lengths
```

```
for i=1:sz
  darray(i)=deltax(i)/ri*100;
end


%bo=0;
%for i=1:sz
% if (deltax(i)>ri*famount) & (bo==0)
%   bo=1;
%   fspot=i
% end
%end

fspot=sz;      %calculate f at d
deltax(fspot)=ri*d;
if (d>0)
  r1(fspot)=ri-deltax(fspot);
else
  r1(fspot)=ri+deltax(fspot);
end


changepivot=-1;
maxstresspivot=0;

dd=d*100;
dN=100*(1/(R+1))*sin(acos((-1/200)*((dd^2*R-200*dd*R-200*dd+20000+dd^2)/(dd-100))));

%%%%%%%%%%%%%%%%%%%%%%%%%%%%%%%%%%%%%%%%%%%%%%%%%%%%%%%
       %%%%%%%%%%%%%%%%%%%%%%%%%%%%%%%%%%%%%%%%%%%%%%%%
%Basic slider crank model
for i=1:sz

  if r4==0
     theta2(i)=acos((r1(i)^2+r2^2-r3^2)/(2*r1(i)*r2));
     tempangle=asin((-r2*sin(theta2(i)))/r3);
  else  %solves equations using Newton Raphson if r4!=0
     del = 1e-6;
     tol = 1e-3;
     limit=2*pi;
     if i==1
        theta2temp = Newton(type,'theta2',theta2i,[r1(i),r2,r3,r4],limit,del,tol);
     else
        theta2temp = Newton(type,'theta2',theta2(i-1),[r1(i),r2,r3,r4],limit,del,tol);
     end
     theta2(i) = theta2temp;

     tempangle = asin((r4-r2*sin(theta2(i)))/r3)+2*pi;
  end
  if tempangle<0
    theta3(i)=2*pi+tempangle;
  else
     theta3(i)=tempangle;
  end
  if i==sz
     theta2final=theta2(i);
     theta3final=theta3(i);
  end


  %Equation to solve for non-dimensionalized parameter phi
  % Note: Equation for 1B mechanism is not the same as for others.
  if class1B==0
```

```
  phi(i)=(R*cos(theta3(i))*((theta2(i)-theta2o)+K1*(theta3o+theta2(i)-theta3(i)-theta2o))...
   +cos(theta2(i))*(K1*(theta3o+theta2(i)-theta3(i)-theta2o)+K2*(theta3o-theta3(i))))/(R*sin(theta2(i)-theta3(i)));

else

  phi(i)=(R*cos(theta3(i))*(K1*(theta3o+theta2(i)-theta3(i)-theta2o))...
   +cos(theta2(i))*(K1*(theta3o+theta2(i)-theta3(i)-theta2o)))/(R*sin(theta2(i)-theta3(i)));

end

phis(i)=K3*((cos(theta2(i))-(1-ds)*cos(theta2i))+R*(cos(theta3(i))-(1-ds)*cos(theta3i)));
F(i)=k1*(phi(i)-phis(i))/r2;   %Force equation



%Calculate Beta
if class1B==1
   Beta(i)=gamma(pivotparam(2,1))*Ktheta(pivotparam(2,1))*(R+1)*zeta(2)*phi(i)/roe(2);
else
   Beta(i)=gamma(pivotparam(1,1))*Ktheta(pivotparam(1,1))*(R^2+2*R+1)*phi(i)/roe(1);
end


%Equations to calculate alpha
alpha(1,i)=gamma(pivotparam(1,1))*zeta(1)*Ktheta(pivotparam(1,1))*(theta2(i)-theta2o)/roe(1);
       alpha(2,i)=gamma(pivotparam(2,1))*zeta(2)*Ktheta(pivotparam(2,1))*(theta3o+theta2(i)-theta3(i)-theta2o)/
     roe(2);
alpha(3,i)=gamma(pivotparam(3,1))*zeta(3)*Ktheta(pivotparam(3,1))*(theta3o-theta3(i)-theta4o)/roe(3);

%Equations to calculate stress
stress(1,i)=alpha(1,i)*A(1)*matprop(1);
stress(2,i)=alpha(2,i)*A(2)*matprop(1);
stress(3,i)=alpha(3,i)*A(3)*matprop(1);

%Equations to calculate which pivot has the highest stress
if (stress(1,i)>=stress(2,i)) & (stress(1,i)>=stress(3,i))
   if (maxstresspivot==1)
      maxstresspivot=1;
   else
      maxstresspivot=1;
      changepivot=changepivot+1;
   end
elseif (stress(2,i)>stress(1,i)) & (stress(2,i)>stress(3,i))
   if (maxstresspivot==2)
      maxstresspivot=2;
   else
      maxstresspivot=2;
      changepivot=changepivot+1;
   end
elseif (stress(3,i)>stress(2,i)) & (stress(3,i)>stress(2,i))
   if (maxstresspivot==3)
      maxstresspivot=3;
   else
      maxstresspivot=3;
      changepivot=changepivot+1;
   end
end

%Calculate f parameter by normalizing highest stress parameter  (Offset for K already applied)


fparam(i)=ka(maxstresspivot)*(1/alpha(maxstresspivot,i))^3/(ka(1)*L*K(maxstresspivot));
```

```
  %Equations for calculating force on sliding Cam
  Fx(i)=((theta2(i)-theta2o)*k1)/((cos(theta3o-theta3(i))*sin(theta2(i)-theta2o)*r2)/sin(theta3o-theta3(i))...
     +cos(theta2(i)-theta2o)*r2);
  Fy(i)=(-Fx(i)/tan(theta3o-theta3(i)));
  Fcam(i)=sqrt(Fx(i)^2+Fy(i)^2);
end

for i=1:3
if alpha(i,sz)==0
    C(i)=-1;
  else
    C(i)=alpha(maxstresspivot,sz)/alpha(i,sz);
  end
  end


%%%%%%%%%%%%%%%%%%%%%%%%%%%%%%%%%%%%%%%%%%%%%%%%%%%%%%%%%%%%%%%%%%%%%%%%%%%%%%%%%%%%%%%%%%%%%%%%%%%
        %%%%%%%%%%%%%%%%%%%%%%%%%%%%%%%%%%%%%%%%%%%%%%%%%%%%%%%%%%%%%%%%%%%%%%%%%%%%%%


% Return important parameters back to the interace function.
pivot=maxstresspivot;
kapivot=ka(pivot)
ka1=ka(1)
Kpivot=K(pivot)

for i=1:3
 if(pivotparam(i,1)==1)
    DesignParam(i,1)=-1
    DesignParam(i,2)=-1
    DesignParam(i,3)=-1
    DesignParam(i,4)=-1
  else
    DesignParam(i,1)=(K(i)*kapivot/(ka(i)*Kpivot))^(1/3)        %maximum h given same stress and b values
    DesignParam(i,2)=(K(i)*kapivot/(ka(i)*Kpivot))              %maximum b given same stress and h values
     DesignParam(i,3)=(K(i)*kapivot/(ka(i)*Kpivot)*C(i)^3)         %D  ratio of maximum b to primary stress pivot b
        given max h on x
    DesignParam(i,4)=(11-DesignParam(i,3))*(C(i))               %A
  end
 end



[alphamax,temp]=max(alpha(maxstresspivot,:));
alphamax;
Amax=A(pivot);

maxstress=max(stress(maxstresspivot,:));
SF=matprop(3)/alphamax/Amax;

lengths(1)=ri;
lengths(2)=r2;
lengths(3)=r3;
lengths(4)=r4;
lengths(5)=L;

pivotparam(1,5)=theta2i;
pivotparam(2,5)=theta3i;
pivotparam(1,6)=theta2final;
pivotparam(2,6)=theta3final;

%Average array values
```

```
average_phi=average(phi);
average_phis=average(phis);
average_Beta=average(Beta);
average_alpha=average(alpha(maxstresspivot,:));



%Multiply in the average Beta value
for i=1:sz
  fparam(i)=fparam(i)*average_Beta;     %Must use end average
end

Fmin=min(F);
Fmax=max(F);

if d>0
   xi=((Fmin/Fmax))*100;
else
   xi=abs(Fmin/Fmax);
end

fp=fparam(fspot);
fp=fparam(fspot)/fgoal;
pc=[-1,-1];
if fit==1
  X=[1,1];
  Options = optimset('TolFun',.0001);
  LL=[];
  UL=[];
  pc=lsqcurvefit('powerb',X,darray,alpha(maxstresspivot,:),LL,UL,Options); %Curve fit alpha
end


ForceAverage=average(F);

cfparam=[R,K1,K2,K3,average_phi,average_phis,xi];

configparam=[alphamax,pivot,changepivot,average_Beta,fp,dN];

dd=d*100;
d=dd;
```

B.1.4 *UserModel* Code

```
%This is the user interface for the CFORIGINAL model.  The model can also be accessed through
%the optdes interface
%function usermodel
clear all;
close all;
%User Inputs
matprop(1)=1;               %E%E
matprop(2)=1;%Sy   %Sy
matprop(3)=matprop(2)/matprop(1);%Sy/E
K3=0;
R=0.395;
K1=.1906;
K2=0;
cfparam(2)=K1;
cfparam(3)=K2;
```

```
ltot=1;
k1=.60106;
b=1;
geoparam(1,1)=b;
geoparam(2,1)=b;
geoparam(3,1)=b;
pivotparam(1,4)=k1;
r4=0;
r4type=0;          %0==> User input      1 ==> Orthoplaner
di=0;              %0..1
d=16;              %percent displacement (0..100)  +--> percent of ri to displace  - -->percent of (r2+r3-ri) to displace
ds=0;              %Percent of rest length to preload spring
%Pin joint types   1=pin  2=small  3=long
pivotparam(1,1)=2;
pivotparam(2,1)=3;
pivotparam(3,1)=1;
%Pin Joint reference links for long length segments
%Should only matter for pivot 2    Can be either link 2 or link 3
pivotparam(2,2)=3;
%Initial angles can be inputed through the pivot parameters. The defaults for
%the normal slider crank are as follows:
%Initial wind up on springs -->  pos. # is a counter clockwise rotation  results in negative torque
%With no pre-load, the springs will be at rest in rest posistion (theta#i)
pivotparam(1,3)=0;
pivotparam(2,3)=0;
pivotparam(3,3)=0;
fit=0;
cfparam(1)=R;
cfparam(4)=K3;
[lengths,cfparam,configparam,pivotparam,geoparam,deltax,force,di,d,SF,pc,alpha,Beta,fp,phi,ka,C,DesignPara
    m]=cfmmodel(ltot,r4type,r4,di,d,ds,geoparam,pivotparam,cfparam,matprop,fit);
%Plot Force output
figure(1)
plot(deltax,force);
axis([0,max(deltax),0,max(force)*1.1]);
%Plot mechanism in initial and fully deflected position
figure(2)
hold on;
r2=lengths(2);
axis equal;
theta2i=pivotparam(1,5);
theta3i=pivotparam(2,5);
r2ix=cos(theta2i)*r2;
r2iy=sin(theta2i)*r2;
x=[0,r2ix];
y=[0,r2iy];
r3=lengths(3);
r3ix=r2ix+cos(pivotparam(2,5))*r3;
r3iy=r2iy+sin(pivotparam(2,5))*r3;
plot(x,y,'g');
x=[r2ix,r3ix];
y=[r2iy,r3iy];
plot(x,y,'b');
x=[r3ix,r3ix];
y=[r3iy,0];
plot(x,y,'r');
if r2iy > r3ix
  range = r2iy+1;
else
  range = r3ix+1;
end
theta2final=pivotparam(1,6);
theta3final=pivotparam(1,6);
```

```
r2ix=cos(theta2final)*r2;
r2iy=sin(theta2final)*r2;
x=[0,r2ix];
y=[0,r2iy];
r3ix=r2ix+cos(pivotparam(2,6))*r3;
r3iy=r2iy+sin(pivotparam(2,6))*r3;
plot(x,y,'g-.');
x=[r2ix,r3ix];
y=[r2iy,r3iy];
plot(x,y,'b-.');
x=[r3ix,r3ix];
y=[r3iy,0];
plot(x,y,'r-.');
hold off;
%if r2iy > r3ix & r2iy>range
%   range = r2iy+1;
%elseif r3ix>range
%   range = r3ix+1;
%end
%axis([0 range 0 range]);%
%plotmech(2,r2,r3,theta2i,theta3i,theta2final,theta3final);
%plot(deltax,cfparam(5))
%postprocess2(r2,r3,percentage,pivotparam,matprop,cfparam,deltax,phi,force)
```

B.1.5 *OptdesModel* Code

```
function optdesmodel(x)

%Preps model to be used with OptdesX
clear all;
close all;
format long;

% Data file order
% E Sy ltot k1 b
% R K1 K2 K3  %deflectioninitial %deflection of total %deflec of spring
% pintype1 pintype2 pintype3 r4type r4
%0   Reference for caculating pivot 2 flexible member length 0
%theta2prewind   theta3prewind  theta4prewind


load cfc_Data1.txt;
matprop(1)=cfc_Data1(1,1);
matprop(2)=cfc_Data1(1,2);
matprop(3)=matprop(2)/matprop(1);

ltot=cfc_Data1(1,3);
pivotparam(1,4)=cfc_Data1(1,4);
geoparam(1,1)=cfc_Data1(1,5);

cfparam(1)=cfc_Data1(2,1);
cfparam(2)=cfc_Data1(2,2);
cfparam(3)=cfc_Data1(2,3);
cfparam(4)=cfc_Data1(2,4);

di=cfc_Data1(2,5);
d=cfc_Data1(2,6);
ds=cfc_Data1(2,7);  %Percent of rest length to preload spring


%Pin joint types   1=pin  2=small  3=long
```

```
pivotparam(1,1)=cfc_Data1(3,1);
pivotparam(2,1)=cfc_Data1(3,2);
pivotparam(3,1)=cfc_Data1(3,3);
r4type=cfc_Data1(3,4);
r4=cfc_Data1(3,5);

%Pin Joint reference links for long length segments
%Should only matter for pivot 2    Can be either link 2 or link 3
pivotparam(2,2)=cfc_Data1(4,2);

%Initial angles can be inputed through the pivot parameters. The defaults for
%the normal slider crank are as follows:
%Initial wind up on springs -->  pos. # is a counter clockwise rotation  results in negative torque
%With no pre-load, the springs will be at rest in rest posistion (theta#i)


pivotparam(1,3)=cfc_Data1(5,1);
pivotparam(2,3)=cfc_Data1(5,2);
pivotparam(3,3)=cfc_Data1(5,3);
fit=cfc_Data1(6,1);



[lengths,cfparam,configparam,pivotparam,geoparam,deltax,force,di,d,SF,pc,alpha,Beta,fp,phi,ka,C,DesignPara
    m]=cfmmodel(ltot,r4type,r4,di,d,ds,geoparam,pivotparam,cfparam,matprop,fit);

averageforce=average(force)

save cfc_Results.txt lengths geoparam pivotparam cfparam configparam averageforce di d SF pc ka C Design-
    Param -ASCII

%Result File Setup
%ri r2 r3 r4
%b1 h1 l1
%b2 h2 l2
%b3 h3 l3
%pinjoint1 0 theta2pre k1 theta2i theta2final
%pinjoint2 Reference theta3pre k2 theta3i theta3final
%pinjoint3 0 theta4pre k3 0 0
%0 0 0 ks 0 0
%R K1 K2 K3 phi phis xi
%alphamax pivot changepivot average_Beta fp dN
%averageforce
%di
%d
%SF
%m,n
%ka1 ka2 ka3
%C1 C2 C3
%hparam1 bparam1 D1 Area1
%hparam2 bparam2 D2 Area2
%hparam3 bparam3 D3 Area3
```

B.2 Optimization Code

The optimization is performed by OptdesX. This software contains built in optimization routines. It is necessary to construct a C file called *anasubC*. This file establishes the analysis variables, analysis functions, and the model or links to the model. The variable names in the anasubC code are mapped to the given parameter names in Table B.1

B.2.1 *anasubC* Code

```
#include "supportC.h"
#include  "math.h"
#include  "stdlib.h"
#include  "string.h"
#include  <stdio.h>

double ri,r2,r3,r4,r4type,d,L,di,ds,E,Sy,SF,rtot;
  double pivotparam[6][6];
  double hp1,bp1,D1,Area1,hp2,bp2,D2,Area2,hp3,bp3,D3,Area3;
  double AA1,BB1,CC1,DD1,AA2,BB2,CC2,DD2,AA3,BB3,CC3,DD3;
  double geoparam[3][3];
  double cfparam[7];
  double lengths[4];
  double configparam[5];
  double C1,C2,C3;
  double R,K1,K2,xi,averageforce,m,n,ka1,ka2,ka3,dN;
  double k1,k2,k3,ks,averagephi,averagephis;
  double alphamax, pivot, changepivot,averagebeta,fp,ltot;
  double fit,b1,h1,b2,h2,b3,h3,l1,l2,l3;
  int hold;

/*============================================================================
   Function anapreC
      Preprocessing Function
----------------------------------------------------------------------------*/
#ifdef __STDC__
void anapreC( char *modelName )
#else
void anapreC( modelName )
char *modelName;
#endif
{
  /* set model name (16 chars max) */
  strcpy( modelName, "Original CF" );
}

/*============================================================================
   Function anafunC
      Analysis Function
----------------------------------------------------------------------------*/
#ifdef __STDC__
void anafunC( void )
```

```
#else
void anafunC( )
#endif
{


  /* don't forget to declare your variables and functions to be
    double precision */


  /*File declarations for linking to other models  */
  FILE *out, * in, *flag;
  /* char str[80];*/


  /* get AV values from OptdesX (Variable names 16 chars max) */
  /* be sure to use the ADDRESS of the variables in the function calls */

  /*Checks to see if Hold existes  */
  flag=fopen("Hold.txt","r");
  if(flag!=NULL)
   {fclose(flag);
    system("rm Hold.txt");
   }
  fclose(flag);

  avdscaC(&E,"E");
  avdscaC(&Sy,"Sy");

  avdscaC(&ltot,"ltot");
  avdscaC(&pivotparam[0][3],"k1");
  avdscaC(&geoparam[0][0],"b");
  avdscaC(&cfparam[0],"R");
  avdscaC(&cfparam[1],"K1");
  avdscaC(&cfparam[2],"K2");
  avdscaC(&cfparam[3],"K3");
  avdscaC(&di,"% Defl. Intial");
  avdscaC(&d,"d");
  avdscaC(&ds,"% Spring Pre-load");



  avdscaC(&r4,"r4");
  avdscaC(&r4type,"r4 type");


  avdscaC(&pivotparam[0][0],"Pin 1 Type");
  avdscaC(&pivotparam[1][0],"Pin 2 Type");
  avdscaC(&pivotparam[2][0],"Pin 3 Type");

  avdscaC(&pivotparam[1][1],"Pin 2 Reference");

  avdscaC(&pivotparam[0][2],"Theta2 Preload");
  avdscaC(&pivotparam[1][2],"Theta3 Preload");
  avdscaC(&pivotparam[2][2],"Theta4 Preload");
  avdscaC(&fit,"Fit 1Yes 0No");




  /*Hold portion of program for linking to Matlab*/
```

```
 /*Checks to see if Hold existes  */
 flag=fopen("Hold.txt","r");
 if(flag!=NULL)
  {fclose(flag);
    system("rm Hold.txt");
  }
 fclose(flag);

 out = fopen("cfc_Data1.txt","w");

 /*Create Data file for input into Matlab  */
 fprintf(out,"%g %g %g %g %g -1 -1\n",E,Sy,ltot,pivotparam[0][3],geoparam[0][0]);
 fprintf(out,"%g %g %g %g %g %g %g\n",cfparam[0],cfparam[1],cfparam[2],cfparam[3],di,d,ds);
 fprintf(out,"%g %g %g %g %g -1 -1\n",pivotparam[0][0],pivotparam[1][0],pivotparam[2][0],r4type,r4);
 fprintf(out,"-1 %g -1 -1 -1 -1 -1\n",pivotparam[1][1]);
 fprintf(out,"%g %g %g -1 -1 -1 -1\n",pivotparam[0][2],pivotparam[1][2],pivotparam[2][2]);
 fprintf(out,"%g -1 -1 -1 -1 -1 -1\n",fit);


 fclose(out);  /*Close matlab data file   */
 hold=1;

 /*system("matlab ,main.m &");   */
 /*Force anasubC to hold till Matlab is finished*/

 flag=fopen("Stop.txt","w");
 fprintf(flag,"%g \n",1.00);
 fclose(flag);

 flag=NULL;

 while (flag==NULL)
   {
   flag= fopen("Hold.txt","r");
   }
 fclose(flag);
 system("rm Hold.txt");

/*Read in data from Result file*/
 in = fopen("cfc_Results.txt","r");
    /*variable=getValue(in,#));*/

fscanf(in,"%lf%lf%lf%lf%lf",&ri,&r2,&r3,&r4,&L);

fscanf(in,"%lf%lf%lf",&b1,&h1,&l1);
fscanf(in,"%lf%lf%lf",&b2,&h2,&l2);
fscanf(in,"%lf%lf%lf",&b3,&h3,&l3);


      fscanf(in,"%lf%lf%lf%lf%lf%lf",&pivotparam[0][0],&pivotparam[0][1],&pivotparam[0][2],&pivotparam[0][3],&p
      ivotparam[0][4],&pivotparam[0][5]);

      fscanf(in,"%lf%lf%lf%lf%lf%lf",&pivotparam[1][0],&pivotparam[1][1],&pivotparam[1][2],&pivotparam[1][3],&p
      ivotparam[1][4],&pivotparam[1][5]);

      fscanf(in,"%lf%lf%lf%lf%lf%lf",&pivotparam[2][0],&pivotparam[2][1],&pivotparam[2][2],&pivotparam[2][3],&p
      ivotparam[2][4],&pivotparam[2][5]);

      fscanf(in,"%lf%lf%lf%lf%lf%lf",&pivotparam[3][0],&pivotparam[3][1],&pivotparam[3][2],&pivotparam[3][3],&p
      ivotparam[3][4],&pivotparam[3][5]);

      fscanf(in,"%lf%lf%lf%lf%lf%lf%lf",&cfparam[0],&cfparam[1],&cfparam[2],&cfparam[3],&cfparam[4],&cfpara
      m[5],&cfparam[6]);
```

```
fscanf(in,"%lf%lf%lf%lf%lf%lf",&alphamax,&pivot,&changepivot,&averagebeta,&fp,&dN);
fscanf(in,"%lf",&averageforce);
fscanf(in,"%lf",&di);
fscanf(in,"%lf",&d);
fscanf(in,"%lf",&SF);
fscanf(in,"%lf%lf",&m,&n);
fscanf(in,"%lf%lf%lf",&ka1,&ka2,&ka3);
fscanf(in,"%lf%lf%lf",&C1,&C2,&C3);
fscanf(in,"%lf%lf%lf%lf",&hp1,&bp1,&D1,&Area1);
fscanf(in,"%lf%lf%lf%lf",&hp2,&bp2,&D2,&Area2);
fscanf(in,"%lf%lf%lf%lf",&hp3,&bp3,&D3,&Area3);

fclose(in);

 k1=pivotparam[0][3];
 k2=pivotparam[1][3];
 k3=pivotparam[2][3];
 ks=pivotparam[3][3];


 /* send functions to OptdesX (Function names 16 chars max) */
 afdscaC(averageforce, "Average Force" );
 afdscaC(cfparam[0], "R" );
 afdscaC(cfparam[1], "K1" );
 afdscaC(cfparam[2], "K2" );
 afdscaC(cfparam[3], "K3");
 afdscaC(cfparam[4], "Phi");
 afdscaC(cfparam[5], "Phi S");
 afdscaC(cfparam[6], "Xi" );
 afdscaC(dN,"dN");
 afdscaC(alphamax,"Max. Alpha");
 afdscaC(pivot,"max S P");
 afdscaC(changepivot,"pivot changes");
 afdscaC(averagebeta,"average Beta");
 afdscaC(fp,"f");
 afdscaC(k1,"k1");
 afdscaC(k2,"k2");
 afdscaC(k3,"k3");
 afdscaC(ks,"ks");

 afdscaC(pivotparam[0][4],"Theta2 initial");
 afdscaC(pivotparam[1][4],"Theta3 initial");

 afdscaC(pivotparam[0][5],"Theta2 final");
 afdscaC(pivotparam[1][5],"Theta3 final");

 afdscaC(ri,"r initial");
 afdscaC(r2,"r2");
 afdscaC(r3,"r3");
 afdscaC(r4,"r4");

 afdscaC(di,"% Defl. Initial");
 afdscaC(d,"d");
 afdscaC(ds,"% Spring Pre-Load");
 afdscaC(SF,"Safety Factor");
 afdscaC(m,"Power m");
 afdscaC(n,"Power n");
 afdscaC(L,"L");
 afdscaC(b1,"b1");
 afdscaC(h1,"h1");
 afdscaC(l1,"l1");
 afdscaC(b2,"b2");
 afdscaC(h2,"h2");
```

```
   afdscaC(l2,"l2");
   afdscaC(b3,"b3");
   afdscaC(h3,"h3");
   afdscaC(l3,"l3");
   afdscaC(ka1,"ka1");
   afdscaC(ka2,"ka2");
   afdscaC(ka3,"ka3");
   afdscaC(C1,"C1");
   afdscaC(C2,"C2");
   afdscaC(C3,"C3");

   afdscaC(hp1,"h param 1");
   afdscaC(bp1,"b param 1");
   afdscaC(D1,"D1");
   afdscaC(Area1,"Design Area 1");

   afdscaC(hp2,"h param 2");
   afdscaC(bp2,"b param 2");
   afdscaC(D2,"D2");
   afdscaC(Area2,"Design Area 2");

   afdscaC(hp3,"h param 3");
   afdscaC(bp3,"b param 3");
   afdscaC(D3,"D3");
   afdscaC(Area3,"Design Area 3");

   afdscaC(AA1,"AA 1");
   afdscaC(AA2,"AA 2");
   afdscaC(AA3,"AA 3");

   afdscaC(BB1,"BB 1");
   afdscaC(BB2,"BB 2");
   afdscaC(BB3,"BB 3");

   afdscaC(CC1,"CC 1");
   afdscaC(CC2,"CC 2");
   afdscaC(CC3,"CC 3");

   afdscaC(DD1,"DD 1");
   afdscaC(DD2,"DD 2");
   afdscaC(DD3,"DD 3");



/*==========================================================================
    Function anaposC
      Postprocessing Function
--------------------------------------------------------------------------*/
#ifdef __STDC__
void anaposC( void )
#else
void anaposC( )
#endif
{

 FILE *out, * in, *flag;

  out = fopen("cfc_postdata1.txt","w");
      /*variable=getValue(in,#));*/

      fprintf(out,"%lf %lf %lf %lf 0 0 0\n",geoparam[0][0],geoparam[0][1],geoparam[0][2],geoparam[0][3]);
```

```
    fprintf(out,"%lf %lf %lf %lf 0 0 0\n",geoparam[1][0],geoparam[1][1],geoparam[1][2],geoparam[1][3]);

    fprintf(out,"%lf %lf %lf %lf %lf %lf %lf\n",cfparam[0],cfparam[1],cfparam[2],cfparam[3],cfparam[4],cfparam[5],cfparam[6]);

    fprintf(out,"%lf %lf %lf 0 0 0 0\n",pivotparam[0][0],pivotparam[0][1],pivotparam[0][2]);
    fprintf(out,"%lf %lf %lf 0 0 0 0\n",pivotparam[1][0],pivotparam[1][1],pivotparam[1][2]);
    fprintf(out,"%lf %lf %lf 0 0 0 0\n",pivotparam[2][0],pivotparam[2][1],pivotparam[2][2]);
    fprintf(out,"%lf %lf %lf 0 0 0 0\n",pivotparam[3][0],pivotparam[3][1],pivotparam[3][2]);
    fprintf(out,"%lf %lf %lf 0 0 0 0\n",pivotparam[4][0],pivotparam[4][1],pivotparam[4][2]);

    fprintf(out,"%lf 0 0 0 0 0 0\n",averageforce);
    fprintf(out,"%lf 0 0 0 0 0 0\n",di);
    fprintf(out,"%lf 0 0 0 0 0 0\n",d);

   fclose(out);

   system("matlab <postprocess.m");
}
```

B.3 Optdes/Matlab Link

The Matlab model code and the OptdesX optimization package are linked together through "hand shaking" that occurs through data files. One piece of software signals the other piece of software that it is finished with its part of the problem by creating or editing a data file. Meanwhile, the software that is not currently doing anything in the problem waits for the other software to signal that it is finished. Ideally, the two programs would share a common database and have internal triggers. However, with the software being used, this is impossible.

The MatLab file that controls the hand shakes is as follows:

```
while 1

  stop=0;
  load Stop.txt
  while Stop == 0.0
    load Stop.txt
  end

  temp=1.0;
```

```
  temp2=0.000;
  save Stop.txt temp2 -ASCII;


  % Insert first function here
  x=1;
  optdesmodel(x);

  save Hold.txt temp -ASCII
end
```

Stop is a file that tells MatLab to wait. MatLab continues to read the file until the value in the file is no longer zero. This value is changed by anasubC upon once all data has been written to the data file.

The MatLab function *OptdesModel* is then called. Once all the data has been saved from MatLab to a data file, MatLab creates the file **Hold**. Meanwhile, *anasubC* is waiting for the file **Hold** to be created.

To run the linked models, it is necessary to start Matlab and run the *OptdesLink* function, as well as start OptdesX. The model runs fairly quickly. It is much faster than launching the MatLab application each time through a system command. Additionally, this set up allows for easy debugging and model changes. It is not necessary to terminate the optimization code. The matlab code can be stopped, the model altered, and *OptdesLink* restarted.

APPENDIX C OPTIMIZATION PLOTS

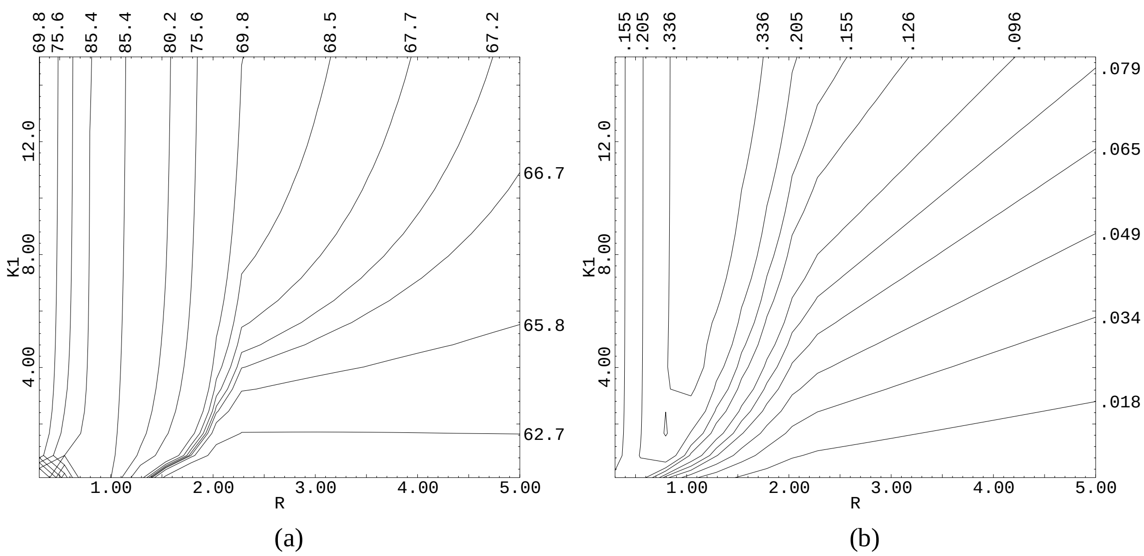

Figure C.1 2-D Explore plots for *slp*-b with R vs. K_1 and contours of (a) Ξ'_{ex} and (b) Ψ

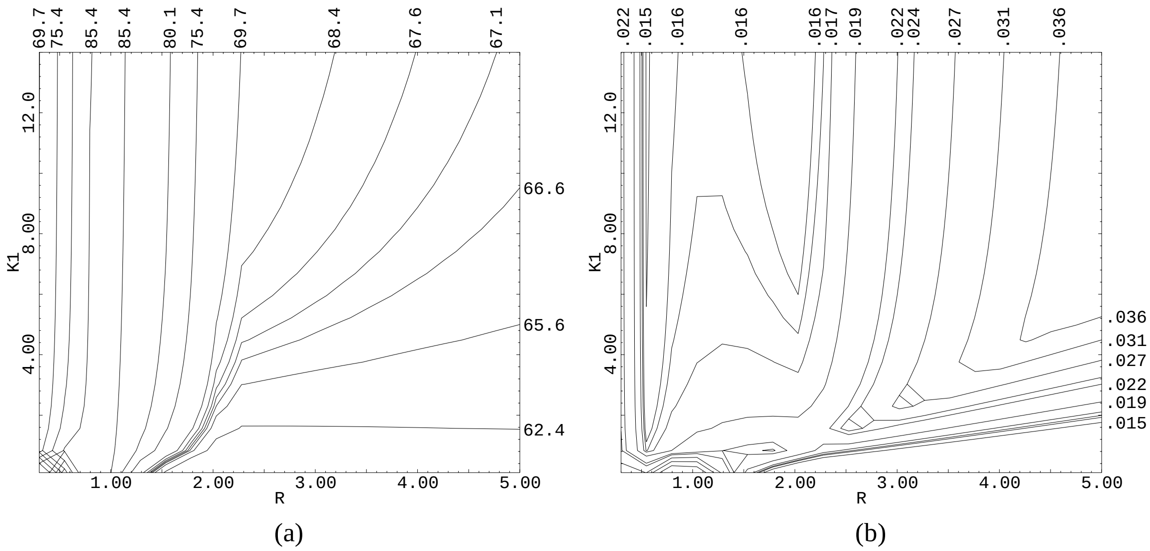

Figure C.2 2-D Explore plots for *ssp*-b with R vs. K_1 and contours of (a) Ξ'_{ex} and (b) Ψ

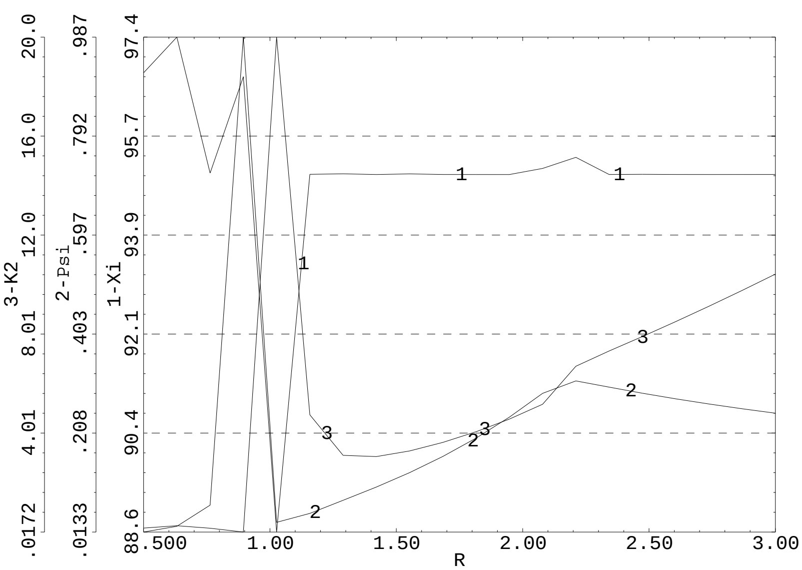

Figure C.3 Optimum plot for *lps*-b which shows Ξ'_{ex}, Ψ and optimal K_2 for given R value

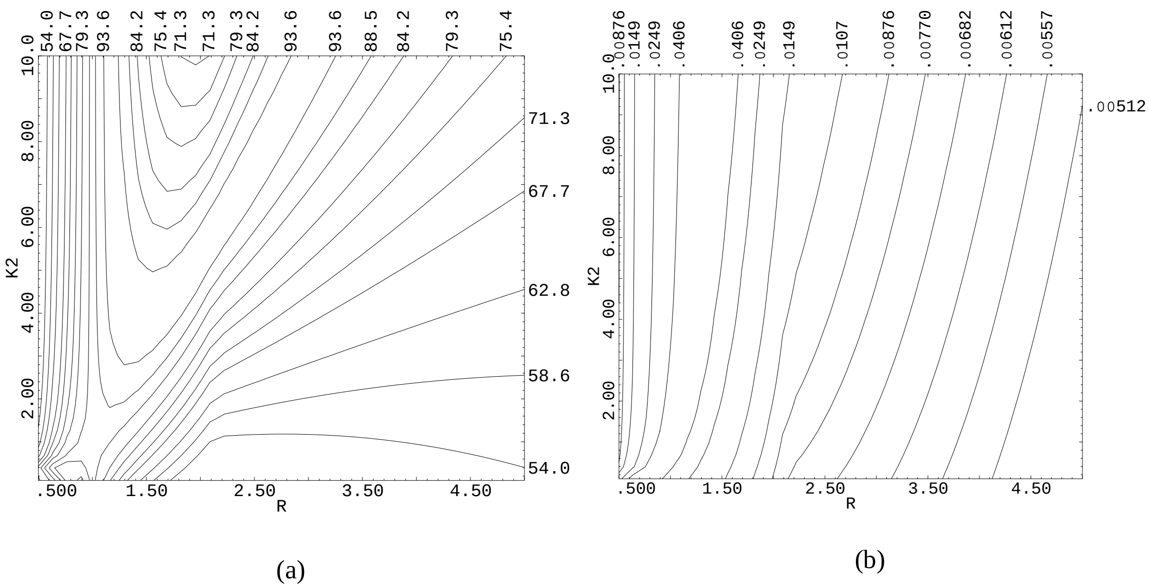

Figure C.4 2-D explore plots for *sps*-b with R vs. K_2 and contours of (a) Ξ'_{ex} and (b) Ψ

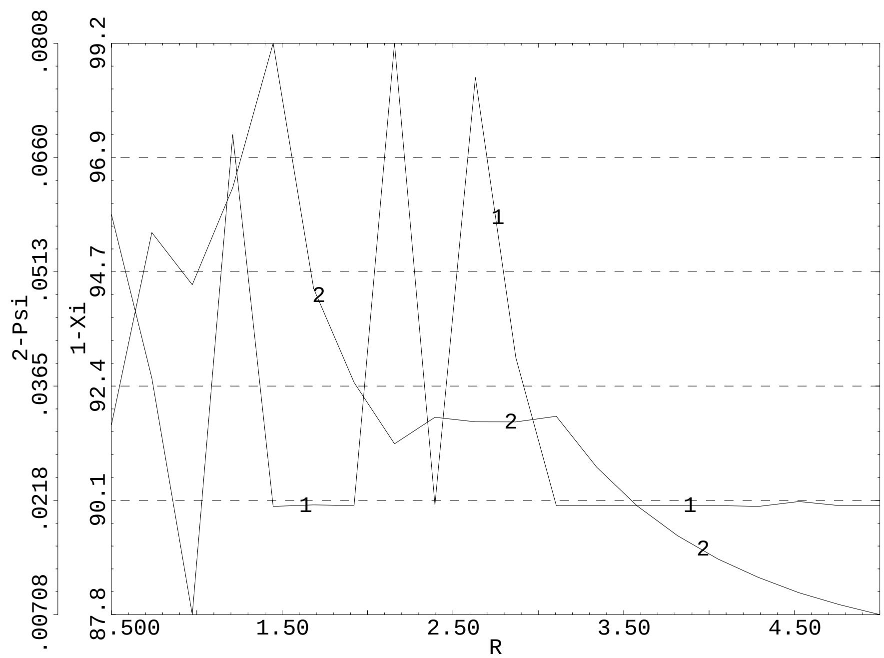

Figure C.5 Optimum plot of design variables K_1 and K_2 versus R for *sss*-b with curves of Ξ'_{ex} and Ψ

APPENDIX D

MECHANISM TABLES

The tables on the following pages summarize all of the new mechanisms along with their parameters. The *lpp*-a and *lpp*-b mechanisms are bolded in each graph so that they can be quickly found during design. Tables D.1 and D.2 list the mechanisms in the order in which they were presented. Tables D.3 and D.4 list all of the mechanisms sorted by M while Tables D.5 and D.6 tabulate all of the mechanisms sorted by Ψ. In the sorted tables, the mechanisms are separated into 16% (sub-class a) and 40% (sub-class b) deflection mechanisms.

Table D.1 Combined mechanism table

Configuration	Sub-Class	Primary Pivot	Ξ'_{ex}	R	K_1	K_2	κ_1	κ_2	κ_3	Φ	β	Ψ	λ	M	n
lpp	**a**	**1**	**99.7**	**0.8274**	**0**	**0**	**3.50**	**-**	**-**	**0.4537**	**2.901**	**1.000**	**1.097**	**0.4501**	**0.5004**
	a99	1	99.0	0.8018	0	0	3.45	-	-	0.4439	2.759	1.046	1.098	0.4373	0.4994
	a95	1	95.0	0.7106	0	0	3.28	-	-	0.4067	2.279	1.239	1.103	0.3923	0.4952
	a90	1	90.0	0.6185	0	0	3.10	-	-	0.3653	1.832	1.492	1.109	0.3479	0.4898
lpp	**b**	**1**	**97.6**	**0.8853**	**0**	**0**	**3.61**	**-**	**-**	**0.4773**	**3.248**	**1.002**	**1.094**	**0.4788**	**0.5033**
	b95	1	95.0	0.8595	0	0	3.56	-	-	0.4630	3.065	1.052	1.095	0.4683	0.5000
	b90	1	90.0	0.8226	0	0	3.49	-	-	0.4421	2.812	1.129	1.097	0.4535	0.4949
spp	a	1	99.7	0.8274	0	0	18.27	-	-	0.4537	15.152	0.039	1.027	2.3511	0.5004
	a99	1	99.0	0.8018	0	0	18.02	-	-	0.4439	14.412	0.041	1.028	2.2841	0.4994
	a95	1	95.0	0.7104	0	0	17.10	-	-	0.4066	11.895	0.049	1.029	2.0482	0.4951
	a90	1	90.0	0.6187	0	0	16.19	-	-	0.3654	9.576	0.059	1.031	1.8177	0.4898
spp	b	1	97.6	0.8853	0	0	18.85	-	-	0.4773	16.964	0.039	1.027	2.5006	0.5033
	b95	1	95.0	0.8595	0	0	18.60	-	-	0.4630	16.010	0.041	1.027	2.4460	0.5000
	b90	1	90.0	0.8226	0	0	18.23	-	-	0.4421	14.686	0.044	1.027	2.3687	0.4949
psp	a	2	94.6	1	1	0	-	20.00	-	2.0560	82.242	0.015	1.000	5.6291	0.5062
psp	b	2	86.3	1	1	0	-	20.00	-	2.1500	86.000	0.016	1.000	5.4974	0.5164
plp	a	2	94.6	1	1	0	-	3.83	-	2.0561	15.747	0.378	1.088	1.0777	0.5062
	a90	2	90.0	0.4387	1	0	-	2.75	-	3.4511	13.677	0.644	1.123	0.8380	0.5115
	a85	2	85.0	0.3170	1	0	-	2.52	-	4.4878	14.904	0.698	1.134	0.8214	0.5176
	a80	2	80.0	0.2529	1	0	-	2.40	-	5.4987	16.527	0.710	1.141	0.8272	0.5239
plp	b	2	86.3	1	1	0	-	3.83	-	2.1501	16.466	0.409	1.088	1.0525	0.5164
	b85	2	85.0	0.7919	1	0	-	3.43	-	2.4473	15.046	0.500	1.098	0.9468	0.5178
	b80	2	80.0	0.6043	1	0	-	3.07	-	2.9399	14.487	0.596	1.110	0.8593	0.5233
slp	aIo	2	99.8	0.3950	0.1906	0	13.95	6.76	-	0.9573	18.628	0.145	1.086	2.0988	0.5132
	a99IO	2	99.0	0.5057	0.2640	0	15.06	5.70	-	1.1290	25.595	0.219	1.092	1.6933	0.5097
	a95Io	1	95.0	0.8237	1.6370	0	18.24	4.24	-	4.1829	139.117	0.338	1.107	2.3414	0.5002
	a90I	1	93.3	1.5278	15.0000	0	25.28	3.17	-	26.3159	1681.489	0.534	1.126	4.3532	0.5175
	a90IO	2	97.7	0.5437	0.3521	0	15.44	5.44	-	1.3688	32.622	0.233	1.095	1.5975	0.5090
slp	bIO	2	99.4	0.4323	0.2237	0	14.32	6.34	-	1.0467	21.473	0.181	1.088	1.8373	0.5341
	b95IO	1	96.2	0.6248	0.3924	0	16.25	4.98	-	1.4438	38.116	0.294	1.099	1.9768	0.4578
	b90Io	1	90.0	0.7267	0.8283	0	17.27	4.55	-	2.5248	75.281	0.331	1.103	2.1734	0.4794
ssp	aIo	2	99.8	0.3950	0.1906	0	13.95	20.00	-	0.9573	18.628	0.017	1.036	6.2080	0.5132
	a99I	2	99.0	0.7864	0.1000	0	17.86	20.00	-	0.6718	21.440	0.042	1.028	5.6676	0.5066
	a95I	2	96.2	0.9182	0.1000	0	19.18	20.00	-	0.7015	25.810	0.048	1.026	5.6339	0.5062
	a95IO	2	95.0	0.9563	0.5113	0	19.56	20.00	-	1.5750	60.277	0.022	1.026	5.6304	0.5062
	a90IO	2	90.0	1.4688	0.4050	0	24.69	20.00	-	1.3429	81.851	0.028	1.020	5.7279	0.5073
ssp	bIo	2	99.4	0.4323	0.2237	0	14.32	20.00	-	1.0467	21.473	0.019	1.035	5.7929	0.5341
	b94I	2	94.1	0.3000	0.1000	0	13.00	20.00	-	0.6423	10.854	0.030	1.038	6.3534	0.5372
	b90IO	2	90.0	0.8714	0.5343	0	18.71	20.00	-	1.7057	59.736	0.022	1.027	5.5051	0.5168
	b90o	2	91.2	0.9323	0.1000	0	19.32	20.00	-	0.7255	27.087	0.052	1.026	5.4994	0.5165
lps	aIo	3	93.1	0.7591	0	1.0029	3.37	-	23.17	1.2248	7.257	0.026	1.122	3.7184	0.5137
	a99I	3	99.0	2.5750	0	6.4256	6.84	-	13.88	1.4238	34.840	0.241	1.085	1.2616	0.4656
	a95I	3	95.0	2.4052	0	4.3688	6.52	-	14.16	1.2692	28.177	0.253	1.087	1.3261	0.4699
	a90	1	90.0	2.0960	0	2.0313	5.93	-	14.77	1.0408	19.101	0.287	1.091	1.1869	0.5256
	a99IO	3	99.0	2.1623	0	5.1740	6.05	-	14.62	1.4476	27.717	0.173	1.090	1.4370	0.4761
	a95IO	3	95.0	2.1623	0	3.6510	6.05	-	14.62	1.2475	23.885	0.211	1.090	1.4370	0.4761
	a90IO	3	90.8	2.1623	0	2.4156	6.05	-	14.62	1.0851	20.776	0.278	1.090	1.4370	0.4761
lps	bIo	3	83.7	0.8441	0	1.0230	3.53	-	21.85	1.2126	7.895	0.035	1.119	3.1623	0.5331
	b99IO	3	99.0	1.9336	0	4.9463	5.62	-	15.17	1.5344	25.282	0.222	1.093	1.7882	0.4250
	b95IO	3	95.0	1.9339	0	4.5230	5.62	-	15.17	1.4816	24.419	0.235	1.093	1.7881	0.4249
	b90IO	3	90.0	1.9292	0	3.9830	5.61	-	15.18	1.4161	23.263	0.252	1.093	1.7902	0.4254
	b95I	1	95.0	0.8561	0	0.0100	3.55	-	21.68	0.4683	3.089	1.053	1.118	0.4670	0.4995
	b90I	1	90.0	0.8178	0	0.0100	3.48	-	22.23	0.4472	2.829	1.137	1.120	0.4516	0.4942
sps	aIO	3	93.1	0.7591	0	1.0029	17.59	-	23.17	1.2248	37.901	0.028	1.050	3.7183	0.5137
	a99I	1	99.3	0.7328	0	0.1845	17.33	-	23.65	0.5711	17.147	0.063	1.050	2.1056	0.4963
	a90IO	3	94.6	1.0000	0	1.0022	20.00	-	20.00	1.0292	41.166	0.057	1.050	2.8145	0.5062
sps	bIo	3	83.7	0.8441	0	1.0235	18.44	-	21.85	1.2129	41.247	0.037	1.050	3.1623	0.5331
	b98Io	3	98.4	0.6528	0	0.2549	16.53	-	25.32	0.6380	17.429	0.031	1.050	3.9715	0.5572
	b86IO	3	86.3	1.0000	0	1.0000	20.00	-	20.00	1.0750	43.001	0.062	1.050	2.7487	0.5164
sss	a	1	100.0	2.6633	1.0000	12.6700	36.63	20.00	13.75	3.4016	456.482	0.020	1.050	8.2162	0.5324
	a99	1	99.4	1.4903	0.3497	8.3820	24.90	20.00	16.71	3.4388	213.264	0.079	1.050	4.2382	0.5168
	a95IO	2	95.0	1.3464	1.7047	2.9708	23.46	20.00	17.43	4.6011	253.313	0.021	1.050	5.6882	0.5068
	a95I	3	95.6	1.6573	0.4140	15.3423	26.57	20.00	16.03	4.6831	330.679	0.084	1.050	1.7796	0.4888
	a90IO	2	91.1	1.5518	0.3970	0.6459	25.52	20.00	16.44	1.4903	97.043	0.031	1.050	5.7582	0.5076
sss	b	1	99.5	2.0821	1.0000	9.3816	30.82	20.00	14.80	3.6285	344.684	0.029	1.050	5.2859	0.5883
	b99	1	99.0	1.8709	0.6930	7.1497	28.71	20.00	15.34	3.0645	252.583	0.033	1.050	4.7814	0.5768
	b90I	3	96.3	1.2420	0.3330	5.4510	22.42	20.00	18.05	3.1967	160.686	0.076	1.050	2.3326	0.4923
	b88IO	2	88.4	1.1990	1.8187	3.3349	21.99	20.00	18.34	5.4789	264.926	0.024	1.050	5.5108	0.5172
Configuration	Sub-Class	Primary Pivot	Ξ'_{ex}	R	K_1	K_2	κ_1	κ_2	κ_3	Φ	β	Ψ	λ	M	n

Table D.2 Combined mechanism table

Configuration	Sub-Class	d_{Nmax}	C_1	C_2	C_3	D_{1equal}	D_{2equal}	D_{3equal}	D_{1min}	D_{2min}	D_{3min}	Sub-Class	Configuration
lpp	**a**	26.96										**a**	***lpp***
	a99	26.90										a99	
	a95	26.57										a95	
	a90	26.04										a90	
lpp	**b**	39.79										**b**	***lpp***
	b95	39.68										b95	
	b90	39.47										b90	
spp	a	26.96										a	*spp*
	a99	26.90										a99	
	a95	26.57										a95	
	a90	26.04										a90	
spp	b	39.79										b	*spp*
	b95	39.68										b95	
	b90	39.47										b90	
psp	a	27.13										a	*psp*
psp	b	40.00										b	*psp*
plp	a	27.13										a	*plp*
	a90	24.03										a90	
	a85	21.34										a85	
	a80	19.11										a80	
plp	b	40.00										b	*plp*
	b85	39.24										b85	
	b80	36.46										b80	
slp	aIo	23.23	1.71	1.00	-	2.54	1.00	-	0.51	1.00	-	aIo	*slp*
	a99IO	24.97	1.13	1.00	-	1.43	1.00	-	1.00	1.00	-	a99IO	
	a95Io	26.95	1.00	1.92	-	1.00	7.04	-	1.00	1.00	-	a95Io	
	a90I	26.28	1.00	4.82	-	1.00	119.69	-	1.00	1.07	-	a90I	
	a90IO	25.39	1.00	1.00	-	1.00	1.00	-	1.00	1.00	-	a90IO	
slp	bIO	30.18	1.47	1.00	-	1.98	1.00	-	0.63	1.00	-	bIO	*slp*
	b95IO	36.92	1.00	1.09	-	1.00	1.28	-	1.00	1.00	-	b95IO	
	b90Io	38.58	1.00	1.47	-	1.00	3.14	-	1.00	1.00	-	b90Io	
ssp	aIo	23.23	5.07	1.00	-	7.52	1.00	-	0.06	1.00	-	aIo	*ssp*
	a99I	26.85	2.54	1.00	-	11.20	1.00	-	0.68	1.00	-	a99I	
	a95I	27.09	2.18	1.00	-	10.43	1.00	-	1.01	1.00	-	a95I	
	a95IO	27.12	2.09	1.00	-	2.00	1.00	-	0.22	1.00	-	a95IO	
	a90IO	26.43	1.33	1.00	-	2.00	1.00	-	0.84	1.00	-	a90IO	
ssp	bIo	30.18	4.63	1.00	-	6.24	1.00	-	0.06	1.00	-	bIo	*ssp*
	b94I	23.08	6.67	1.00	-	15.38	1.00	-	0.05	1.00	-	b94I	
	b90IO	39.74	2.30	1.00	-	2.00	1.00	-	0.17	1.00	-	b90IO	
	b90o	39.93	2.15	1.00	-	10.35	1.00	-	1.05	1.00	-	b90o	
lps	aIo	26.77	9.07	-	1.00	6.86	-	1.00	0.01	-	1.00	aIo	*lps*
	a99I	23.10	0.68	-	1.00	0.32	-	1.00	1.00	-	1.00	a99I	
	a95I	23.63	0.79	-	1.00	0.50	-	1.00	1.00	-	1.00	a95I	
	a90	24.60	1.00	-	0.84	1.00	-	0.82	1.00	-	1.37	a90	
	a99IO	24.39	1.00	-	1.00	0.47	-	1.00	0.47	-	1.00	a99IO	
	a95IO	24.39	1.00	-	1.00	0.66	-	1.00	0.66	-	1.00	a95IO	
	a90IO	24.39	1.00	-	1.00	1.00	-	1.00	1.00	-	1.00	a90IO	
lps	bIo	39.60	7.33	-	1.00	6.05	-	1.00	0.02	-	1.00	bIo	*lps*
	b99IO	33.91	0.99	-	1.00	0.55	-	1.00	0.56	-	1.00	b99IO	
	b95IO	33.91	0.99	-	1.00	0.60	-	1.00	0.61	-	1.00	b95IO	
	b90IO	33.95	1.00	-	1.00	0.68	-	1.00	0.68	-	1.00	b90IO	
	b95I	39.66	1.00	-	0.13	1.00	-	0.00	1.00	-	0.73	b95I	
	b90I	39.44	1.00	-	0.12	1.00	-	0.00	1.00	-	0.98	b90I	
sps	aIO	26.77	1.74	-	1.00	1.31	-	1.00	0.25	-	1.00	aIO	*sps*
	a99I	26.67	1.00	-	0.52	1.00	-	0.14	1.00	-	0.98	a99I	
	a90IO	27.13	1.00	-	1.00	1.00	-	1.00	1.00	-	1.00	a90IO	
sps	bIo	39.60	1.40	-	1.00	1.16	-	1.00	0.42	-	1.00	bIo	*sps*
	b98Io	37.47	2.35	-	1.00	6.01	-	1.00	0.46	-	1.00	b98Io	
	b86IO	40.00	1.00	-	1.00	1.00	-	1.00	1.00	-	1.00	b86IO	
sss	a	22.82	1.000	1.332	7.099	1.000	1.832	33.744	1.000	0.775	0.094	a	*sss*
	a99	26.37	1.000	0.745	2.222	1.000	0.435	12.492	1.000	1.052	1.139	a99	
	a95IO	26.71	1.462	1.000	2.693	0.500	1.000	2.000	0.160	1.000	0.102	a95IO	
	a95I	25.93	0.340	0.289	1.000	0.039	0.022	1.000	0.997	0.895	1.000	a95I	
	a90IO	26.21	1.260	1.000	3.104	1.974	1.000	1.979	0.986	1.000	0.066	a90IO	
sss	b	32.44	1.000	1.041	4.338	1.000	1.541	19.533	1.000	1.365	0.239	b	*sss*
	b99	34.51	1.000	0.936	3.502	1.000	0.995	13.377	1.000	1.215	0.311	b99	
	b90I	39.35	0.589	0.381	1.000	0.148	0.055	1.000	0.724	0.996	1.000	b90I	
	b88IO	39.54	1.610	1.000	2.398	0.500	1.000	2.000	0.120	1.000	0.145	b88IO	
Configuration	Sub-Class	d_{Nmax}	C_1	C_2	C_3	D_{1equal}	D_{2equal}	D_{3equal}	D_{1min}	D_{2min}	D_{3min}	Sub-Class	Configuration

Table D.3 Combined mechanism table sorted by M

Configuration	Sub-Class	Primary Pivot	Ξ'_{ex}	R	K_1	K_2	κ_1	κ_2	κ_3	Φ	β	Ψ	λ	***M***	n
lpp	a90	1	90.0	0.6185	0	0	3.10	-	-	0.3653	1.832	1.492	1.109	**0.3479**	0.4898
lpp	a95	1	95.0	0.7106	0	0	3.28	-	-	0.4067	2.279	1.239	1.103	**0.3923**	0.4952
lpp	a99	1	99.0	0.8018	0	0	3.45	-	-	0.4439	2.759	1.046	1.098	**0.4373**	0.4994
lpp	**a**	**1**	**99.7**	**0.8274**	**0**	**0**	**3.50**	**-**	**-**	**0.4537**	**2.901**	**1.000**	**1.097**	**0.4501**	**0.5004**
pl p	a85	2	85.0	0.3170	1	0	-	2.52	-	4.4878	14.904	0.698	1.134	**0.8214**	0.5176
pl p	a80	2	80.0	0.2529	1	0	-	2.40	-	5.4987	16.527	0.710	1.141	**0.8272**	0.5239
pl p	a90	2	90.0	0.4387	1	0	-	2.75	-	3.4511	13.677	0.644	1.123	**0.8380**	0.5115
pl p	a	2	94.6	1	1	0	-	3.83	-	2.0561	15.747	0.378	1.088	**1.0777**	0.5062
lps	a90	1	90.0	2.0960	0	2.0313	5.93	-	14.77	1.0408	19.101	0.287	1.091	**1.1869**	0.5256
lps	a99I	3	99.0	2.5750	0	6.4256	6.84	-	13.88	1.4238	34.840	0.241	1.085	**1.2616**	0.4656
lps	a95I	3	95.0	2.4052	0	4.3688	6.52	-	14.16	1.2692	28.177	0.253	1.087	**1.3261**	0.4699
lps	a90IO	3	90.8	2.1623	0	2.4156	6.05	-	14.62	1.0851	20.776	0.278	1.090	**1.4370**	0.4761
lps	a95IO	3	95.0	2.1623	0	3.6510	6.05	-	14.62	1.2475	23.885	0.211	1.090	**1.4370**	0.4761
lps	a99IO	3	99.0	2.1623	0	5.1740	6.05	-	14.62	1.4476	27.717	0.173	1.090	**1.4370**	0.4761
slp	a90IO	2	97.7	0.5437	0.3521	0	15.44	5.44	-	1.3688	32.622	0.233	1.095	**1.5975**	0.5090
slp	a99IO	2	99.0	0.5057	0.2640	0	15.06	5.70	-	1.1290	25.595	0.219	1.092	**1.6933**	0.5097
sss	a95I	3	95.6	1.6573	0.4140	15.3423	26.57	20.00	16.03	4.6831	330.679	0.084	1.050	**1.7796**	0.4888
spp	a90	1	90.0	0.6187	0	0	16.19	-	-	0.3654	9.576	0.059	1.031	**1.8177**	0.4898
spp	a95	1	95.0	0.7104	0	0	17.10	-	-	0.4066	11.895	0.049	1.029	**2.0482**	0.4951
slp	aIo	2	99.8	0.3950	0.1906	0	13.95	6.76	-	0.9573	18.628	0.145	1.086	**2.0988**	0.5132
sps	a99I	1	99.3	0.7328	0	0.1845	17.33	-	23.65	0.5711	17.147	0.063	1.050	**2.1056**	0.4963
spp	a99	1	99.0	0.8018	0	0	18.02	-	-	0.4439	14.412	0.041	1.028	**2.2841**	0.4994
slp	a95Io	1	95.0	0.8237	1.6370	0	18.24	4.24	-	4.1829	139.117	0.338	1.107	**2.3414**	0.5002
spp	a	1	99.7	0.8274	0	0	18.27	-	-	0.4537	15.152	0.039	1.027	**2.3511**	0.5004
sps	a90IO	3	94.6	1.0000	0	1.0022	20.00	-	20.00	1.0292	41.166	0.057	1.050	**2.8145**	0.5062
sps	aIO	3	93.1	0.7591	0	1.0029	17.59	-	23.17	1.2248	37.901	0.028	1.050	**3.7183**	0.5137
lps	aIo	3	93.1	0.7591	0	1.0029	3.37	-	23.17	1.2248	7.257	0.026	1.122	**3.7184**	0.5137
sss	a99	1	99.4	1.4903	0.3497	8.3820	24.90	20.00	16.71	3.4388	213.264	0.079	1.050	**4.2382**	0.5168
slp	a90I	1	93.3	1.5278	15.0000	0	25.28	3.17	-	26.3159	1681.489	0.534	1.126	**4.3532**	0.5175
psp	a	2	94.6	1	1	0	-	20.00	-	2.0560	82.242	0.015	1.000	**5.6291**	0.5062
ssp	a95IO	2	95.0	0.9563	0.5113	0	19.56	20.00	-	1.5750	60.277	0.022	1.026	**5.6304**	0.5062
ssp	a95I	2	96.2	0.9182	0.1000	0	19.18	20.00	-	0.7015	25.810	0.048	1.026	**5.6339**	0.5062
ssp	a99I	2	99.0	0.7864	0.1000	0	17.86	20.00	-	0.6718	21.440	0.042	1.028	**5.6676**	0.5066
sss	a95IO	2	95.0	1.3464	1.7047	2.9708	23.46	20.00	17.43	4.6011	253.313	0.021	1.050	**5.6882**	0.5068
ssp	a90IO	2	90.0	1.4688	0.4050	0	24.69	20.00	-	1.3429	81.851	0.028	1.020	**5.7279**	0.5073
sss	a90IO	2	91.1	1.5518	0.3970	0.6459	25.52	20.00	16.44	1.4903	97.043	0.031	1.050	**5.7582**	0.5076
ssp	aIo	2	99.8	0.3950	0.1906	0	13.95	20.00	-	0.9573	18.628	0.017	1.036	**6.2080**	0.5132
sss	a	1	100.0	2.6633	1.0000	12.6700	36.63	20.00	13.75	3.4016	456.482	0.020	1.050	**8.2162**	0.5324
Configuration	Sub-Class	Primary Pivot	Ξ'_{ex}	R	K_1	K_2	κ_1	κ_2	κ_3	Φ	β	Ψ	λ	***M***	n
lps	b90I	1	90.0	0.8178	0	0.0100	3.48	-	22.23	0.4472	2.829	1.137	1.120	**0.4516**	0.4942
lpp	b90	1	90.0	0.8226	0	0	3.49	-	-	0.4421	2.812	1.129	1.097	**0.4535**	0.4949
lps	b95I	1	95.0	0.8561	0	0.0100	3.55	-	21.68	0.4683	3.089	1.053	1.118	**0.4670**	0.4995
lpp	b95	1	95.0	0.8595	0	0	3.56	-	-	0.4630	3.065	1.052	1.095	**0.4683**	0.5000
lpp	**b**	**1**	**97.6**	**0.8853**	**0**	**0**	**3.61**	**-**	**-**	**0.4773**	**3.248**	**1.002**	**1.094**	**0.4788**	**0.5033**
pl p	b80	2	80.0	0.6043	1	0	-	3.07	-	2.9399	14.487	0.596	1.110	**0.8593**	0.5233
pl p	b85	2	85.0	0.7919	1	0	-	3.43	-	2.4473	15.046	0.500	1.098	**0.9468**	0.5178
pl p	b	2	86.3	1	1	0	-	3.83	-	2.1501	16.466	0.409	1.088	**1.0525**	0.5164
lps	b95IO	3	95.0	1.9339	0	4.5230	5.62	-	15.17	1.4816	24.419	0.235	1.093	**1.7881**	0.4249
lps	b99IO	3	99.0	1.9336	0	4.9463	5.62	-	15.17	1.5344	25.282	0.222	1.093	**1.7882**	0.4250
lps	b90IO	3	90.0	1.9292	0	3.9830	5.61	-	15.18	1.4161	23.263	0.252	1.093	**1.7902**	0.4254
slp	bIO	2	99.4	0.4323	0.2237	0	14.32	6.34	-	1.0467	21.473	0.181	1.088	**1.8373**	0.5341
slp	b95IO	1	96.2	0.6248	0.3924	0	16.25	4.98	-	1.4438	38.116	0.294	1.099	**1.9768**	0.4578
slp	b90Io	1	90.0	0.7267	0.8283	0	17.27	4.55	-	2.5248	75.281	0.331	1.103	**2.1734**	0.4794
sss	b90I	3	96.3	1.2420	0.3330	5.4510	22.42	20.00	18.05	3.1967	160.686	0.076	1.050	**2.3326**	0.4923
spp	b90	1	90.0	0.8226	0	0	18.23	-	-	0.4421	14.686	0.044	1.027	**2.3687**	0.4949
spp	b95	1	95.0	0.8595	0	0	18.60	-	-	0.4630	16.010	0.041	1.027	**2.4460**	0.5000
spp	b	1	97.6	0.8853	0	0	18.85	-	-	0.4773	16.964	0.039	1.027	**2.5006**	0.5033
sps	b86IO	3	86.3	1.0000	0	1.0000	20.00	-	20.00	1.0750	43.001	0.062	1.050	**2.7487**	0.5164
lps	bIo	3	83.7	0.8441	0	1.0230	3.53	-	21.85	1.2126	7.895	0.035	1.119	**3.1623**	0.5331
sps	bIo	3	83.7	0.8441	0	1.0235	18.44	-	21.85	1.2129	41.247	0.037	1.050	**3.1623**	0.5331
sps	b98Io	3	98.4	0.6528	0	0.2549	16.53	-	25.32	0.6380	17.429	0.031	1.050	**3.9715**	0.5572
sss	b99	1	99.0	1.8709	0.6930	7.1497	28.71	20.00	15.34	3.0645	252.583	0.033	1.050	**4.7814**	0.5768
sss	b	1	99.5	2.0821	1.0000	9.3816	30.82	20.00	14.80	3.6285	344.684	0.029	1.050	**5.2859**	0.5883
psp	b	2	86.3	1	1	0	-	20.00	-	2.1500	86.000	0.016	1.000	**5.4974**	0.5164
ssp	b90o	2	91.2	0.9323	0.1000	0	19.32	20.00	-	0.7255	27.087	0.052	1.026	**5.4994**	0.5165
ssp	b90IO	2	90.0	0.8714	0.5343	0	18.71	20.00	-	1.7057	59.736	0.022	1.027	**5.5051**	0.5168
sss	b88IO	2	88.4	1.1990	1.8187	3.3349	21.99	20.00	18.34	5.4789	264.926	0.024	1.050	**5.5108**	0.5172
ssp	bIo	2	99.4	0.4323	0.2237	0	14.32	20.00	-	1.0467	21.473	0.019	1.035	**5.7929**	0.5341
ssp	b94I	2	94.1	0.3000	0.1000	0	13.00	20.00	-	0.6423	10.854	0.030	1.038	**6.3534**	0.5372
Configuration	Sub-Class	Primary Pivot	Ξ'_{ex}	R	K_1	K_2	κ_1	κ_2	κ_3	Φ	β	Ψ	λ	***M***	n

Table D.4 Combined mechanism table sorted by M

Configuration	Sub-Class	d_{Nmax}	C_1	C_2	C_3	D_{1equal}	D_{2equal}	D_{3equal}	D_{1min}	D_{2min}	D_{3min}	Sub-Class	Configuration
lpp	a90	26.04										a90	*lpp*
lpp	a95	26.57										a95	*lpp*
lpp	a99	26.90										a99	*lpp*
lpp	**a**	**26.96**										**a**	***lpp***
pl p	a85	21.34										a85	*pl p*
pl p	a80	19.11										a80	*pl p*
pl p	a90	24.03										a90	*pl p*
pl p	a	27.13										a	*pl p*
lps	a90	24.60	1.00	-	0.84	1.00	-	0.82	1.00	-	1.37	a90	*lps*
lps	a99I	23.10	0.68	-	1.00	0.32	-	1.00	1.00	-	1.00	a99I	*lps*
lps	a95I	23.63	0.79	-	1.00	0.50	-	1.00	1.00	-	1.00	a95I	*lps*
lps	a90IO	24.39	1.00	-	1.00	1.00	-	1.00	1.00	-	1.00	a90IO	*lps*
lps	a95IO	24.39	1.00	-	1.00	0.66	-	1.00	0.66	-	1.00	a95IO	*lps*
lps	a99IO	24.39	1.00	-	1.00	0.47	-	1.00	0.47	-	1.00	a99IO	*lps*
slp	a90IO	25.39	1.00	1.00	-	1.00	1.00	-	1.00	1.00	-	a90IO	*slp*
slp	a99IO	24.97	1.13	1.00	-	1.43	1.00	-	1.00	1.00	-	a99IO	*slp*
sss	a95I	25.93	0.340	0.289	1.000	0.039	0.022	1.000	0.997	0.895	1.000	a95I	*sss*
spp	a90	26.04										a90	*spp*
spp	a95	26.57										a95	*spp*
slp	aIo	23.23	1.71	1.00	-	2.54	1.00	-	0.51	1.00	-	aIo	*slp*
sps	a99I	26.67	1.00	-	0.52	1.00	-	0.14	1.00	-	0.98	a99I	*sps*
spp	a99	26.90										a99	*spp*
slp	a95Io	26.95	1.00	1.92	-	1.00	7.04	-	1.00	1.00	-	a95Io	*slp*
spp	a	26.96										a	*spp*
sps	a90IO	27.13	1.00	-	1.00	1.00	-	1.00	1.00	-	1.00	a90IO	*sps*
sps	aIO	26.77	1.74	-	1.00	1.31	-	1.00	0.25	-	1.00	aIO	*sps*
lps	aIo	26.77	9.07	-	1.00	6.86	-	1.00	0.01	-	1.00	aIo	*lps*
sss	a99	26.37	1.000	0.745	2.222	1.000	0.435	12.492	1.000	1.052	1.139	a99	*sss*
slp	a90I	26.28	1.00	4.82	-	1.00	119.69	-	1.00	1.07	-	a90I	*slp*
psp	a	27.13										a	*psp*
ssp	a95IO	27.12	2.09	1.00	-	2.00	1.00	-	0.22	1.00	-	a95IO	*ssp*
ssp	a95I	27.09	2.18	1.00	-	10.43	1.00	-	1.01	1.00	-	a95I	*ssp*
ssp	a99I	26.85	2.54	1.00	-	11.20	1.00	-	0.68	1.00	-	a99I	*ssp*
sss	a95IO	26.71	1.462	1.000	2.693	0.500	1.000	2.000	0.160	1.000	0.102	a95IO	*sss*
ssp	a90IO	26.43	1.33	1.00	-	2.00	1.00	-	0.84	1.00	-	a90IO	*ssp*
sss	a90IO	26.21	1.260	1.000	3.104	1.974	1.000	1.979	0.986	1.000	0.066	a90IO	*sss*
ssp	aIo	23.23	5.07	1.00	-	7.52	1.00	-	0.06	1.00	-	aIo	*ssp*
sss	a	22.82	1.000	1.332	7.099	1.000	1.832	33.744	1.000	0.775	0.094	a	*sss*
Configuration	Sub-Class	d_{Nmax}	C_1	C_2	C_3	D_{1equal}	D_{2equal}	D_{3equal}	D_{1min}	D_{2min}	D_{3min}	Sub-Class	Configuration
lps	b90I	39.44	1.00	-	0.12	1.00	-	0.00	1.00	-	0.98	b90I	*lps*
lpp	b90	39.47										b90	*lpp*
lps	b95I	39.66	1.00	-	0.13	1.00	-	0.00	1.00	-	0.73	b95I	*lps*
lpp	b95	39.68										b95	*lpp*
lpp	**b**	**39.79**										**b**	***lpp***
pl p	b80	36.46										b80	*pl p*
pl p	b85	39.24										b85	*pl p*
pl p	b	40.00										b	*pl p*
lps	b95IO	33.91	0.99	-	1.00	0.60	-	1.00	0.61	-	1.00	b95IO	*lps*
lps	b99IO	33.91	0.99	-	1.00	0.55	-	1.00	0.56	-	1.00	b99IO	*lps*
lps	b90IO	33.95	1.00	-	1.00	0.68	-	1.00	0.68	-	1.00	b90IO	*lps*
slp	bIO	30.18	1.47	1.00	-	1.98	1.00	-	0.63	1.00	-	bIO	*slp*
slp	b95IO	36.92	1.00	1.09	-	1.00	1.28	-	1.00	1.00	-	b95IO	*slp*
slp	b90Io	38.58	1.00	1.47	-	1.00	3.14	-	1.00	1.00	-	b90Io	*slp*
sss	b90I	39.35	0.589	0.381	1.000	0.148	0.055	1.000	0.724	0.996	1.000	b90I	*sss*
spp	b90	39.47										b90	*spp*
spp	b95	39.68										b95	*spp*
spp	b	39.79										b	*spp*
sps	b86IO	40.00	1.00	-	1.00	1.00	-	1.00	1.00	-	1.00	b86IO	*sps*
lps	bIo	39.60	7.33	-	1.00	6.05	-	1.00	0.02	-	1.00	bIo	*lps*
sps	bIo	39.60	1.40	-	1.00	1.16	-	1.00	0.42	-	1.00	bIo	*sps*
sps	b98Io	37.47	2.35	-	1.00	6.01	-	1.00	0.46	-	1.00	b98Io	*sps*
sss	b99	34.51	1.000	0.936	3.502	1.000	0.995	13.377	1.000	1.215	0.311	b99	*sss*
sss	b	32.44	1.000	1.041	4.338	1.000	1.541	19.533	1.000	1.365	0.239	b	*sss*
psp	b	40.00										b	*psp*
ssp	b90o	39.93	2.15	1.00	-	10.35	1.00	-	1.05	1.00	-	b90o	*ssp*
ssp	b90IO	39.74	2.30	1.00	-	2.00	1.00	-	0.17	1.00	-	b90IO	*ssp*
sss	b88IO	39.54	1.610	1.000	2.398	0.500	1.000	2.000	0.120	1.000	0.145	b88IO	*sss*
ssp	bIo	30.18	4.63	1.00	-	6.24	1.00	-	0.06	1.00	-	bIo	*ssp*
ssp	b94I	23.08	6.67	1.00	-	15.38	1.00	-	0.05	1.00	-	b94I	*ssp*
Configuration	Sub-Class	d_{Nmax}	C_1	C_2	C_3	D_{1equal}	D_{2equal}	D_{3equal}	D_{1min}	D_{2min}	D_{3min}	Sub-Class	Configuration

Table D.5 Combined mechanism table sorted by Ψ

Configuration	Sub-Class	Primary Pivot	Ξ'_{ex}	R	K_1	K_2	κ_1	κ_2	κ_3	Φ	β	Ψ	λ	M	n
lpp	a90	1	90.0	0.6185	0	0	3.10	-	-	0.3653	1.832	**1.492**	1.109	0.3479	0.4898
lpp	a95	1	95.0	0.7106	0	0	3.28	-	-	0.4067	2.279	**1.239**	1.103	0.3923	0.4952
lpp	a99	1	99.0	0.8018	0	0	3.45	-	-	0.4439	2.759	**1.046**	1.098	0.4373	0.4994
lpp	**a**	**1**	**99.7**	**0.8274**	**0**	**0**	**3.50**	**-**	**-**	**0.4537**	**2.901**	**1.000**	**1.097**	**0.4501**	**0.5004**
pl p	a80	2	80.0	0.2529	1	0	-	2.40	-	5.4987	16.527	**0.710**	1.141	0.8272	0.5239
pl p	a85	2	85.0	0.3170	1	0	-	2.52	-	4.4878	14.904	**0.698**	1.134	0.8214	0.5176
pl p	a90	2	90.0	0.4387	1	0	-	2.75	-	3.4511	13.677	**0.644**	1.123	0.8380	0.5115
slp	a90I	1	93.3	1.5278	15.0000	0	25.28	3.17	-	26.3159	1681.489	**0.534**	1.126	4.3532	0.5175
pl p	a	2	94.6	1	1	0	-	3.83	-	2.0561	15.747	**0.378**	1.088	1.0777	0.5062
slp	a95Io	1	95.0	0.8237	1.6370	0	18.24	4.24	-	4.1829	139.117	**0.338**	1.107	2.3414	0.5002
lps	a90	1	90.0	2.0960	0	2.0313	5.93	-	14.77	1.0408	19.101	**0.287**	1.091	1.1869	0.5256
lps	a90IO	3	90.8	2.1623	0	2.4156	6.05	-	14.62	1.0851	20.776	**0.278**	1.090	1.4370	0.4761
lps	a95I	3	95.0	2.4052	0	4.3688	6.52	-	14.16	1.2692	28.177	**0.253**	1.087	1.3261	0.4699
lps	a99I	3	99.0	2.5750	0	6.4256	6.84	-	13.88	1.4238	34.840	**0.241**	1.085	1.2616	0.4656
slp	a90IO	2	97.7	0.5437	0.3521	0	15.44	5.44	-	1.3688	32.622	**0.233**	1.095	1.5975	0.5090
slp	a99IO	2	99.0	0.5057	0.2640	0	15.06	5.70	-	1.1290	25.595	**0.219**	1.092	1.6933	0.5097
lps	a95IO	3	95.0	2.1623	0	3.6510	6.05	-	14.62	1.2475	23.885	**0.211**	1.090	1.4370	0.4761
lps	a99IO	3	99.0	2.1623	0	5.1740	6.05	-	14.62	1.4476	27.717	**0.173**	1.090	1.4370	0.4761
slp	aIo	2	99.8	0.3950	0.1906	0	13.95	6.76	-	0.9573	18.628	**0.145**	1.086	2.0988	0.5132
sss	a95I	3	95.6	1.6573	0.4140	15.3423	26.57	20.00	16.03	4.6831	330.679	**0.084**	1.050	1.7796	0.4888
sss	a99	1	99.4	1.4903	0.3497	8.3820	24.90	20.00	16.71	3.4388	213.264	**0.079**	1.050	4.2382	0.5168
sps	a99I	1	99.3	0.7328	0	0.1845	17.33	-	23.65	0.5711	17.147	**0.063**	1.050	2.1056	0.4963
spp	a90	1	90.0	0.6187	0	0	16.19	-	-	0.3654	9.576	**0.059**	1.031	1.8177	0.4898
sps	a90IO	3	94.6	1.0000	0	1.0022	20.00	-	20.00	1.0292	41.166	**0.057**	1.050	2.8145	0.5062
spp	a95	1	95.0	0.7104	0	0	17.10	-	-	0.4066	11.895	**0.049**	1.029	2.0482	0.4951
ssp	a95I	2	96.2	0.9182	0.1000	0	19.18	20.00	-	0.7015	25.810	**0.048**	1.026	5.6339	0.5062
ssp	a99I	2	99.0	0.7864	0.1000	0	17.86	20.00	-	0.6718	21.440	**0.042**	1.028	5.6676	0.5066
spp	a99	1	99.0	0.8018	0	0	18.02	-	-	0.4439	14.412	**0.041**	1.028	2.2841	0.4994
spp	a	1	99.7	0.8274	0	0	18.27	-	-	0.4537	15.152	**0.039**	1.027	2.3511	0.5004
sss	a90IO	2	91.1	1.5518	0.3970	0.6459	25.52	20.00	16.44	1.4903	97.043	**0.031**	1.050	5.7582	0.5076
sps	aIO	3	93.1	0.7591	0	1.0029	17.59	-	23.17	1.2248	37.901	**0.028**	1.050	3.7183	0.5137
ssp	a90IO	2	90.0	1.4688	0.4050	0	24.69	20.00	-	1.3429	81.851	**0.028**	1.020	5.7279	0.5073
lps	aIo	3	93.1	0.7591	0	1.0029	3.37	-	23.17	1.2248	7.257	**0.026**	1.122	3.7184	0.5137
ssp	a95IO	2	95.0	0.9563	0.5113	0	19.56	20.00	-	1.5750	60.277	**0.022**	1.026	5.6304	0.5062
sss	a95IO	2	95.0	1.3464	1.7047	2.9708	23.46	20.00	17.43	4.6011	253.313	**0.021**	1.050	5.6882	0.5068
sss	a	1	100.0	2.6633	1.0000	12.6700	36.63	20.00	13.75	3.4016	456.482	**0.020**	1.050	8.2162	0.5324
ssp	aIo	2	99.8	0.3950	0.1906	0	13.95	20.00	-	0.9573	18.628	**0.017**	1.036	6.2080	0.5132
psp	a	2	94.6	1	1	0	-	20.00	-	2.0560	82.242	**0.015**	1.000	5.6291	0.5062
Configuration	Sub-Class	Primary Pivot	Ξ'_{ex}	R	K_1	K_2	κ_1	κ_2	κ_3	Φ	β	Ψ	λ	M	n
lps	b90I	1	90.0	0.8178	0	0.0100	3.48	-	22.23	0.4472	2.829	**1.137**	1.120	0.4516	0.4942
lpp	b90	1	90.0	0.8226	0	0	3.49	-	-	0.4421	2.812	**1.129**	1.097	0.4535	0.4949
lps	b95I	1	95.0	0.8561	0	0.0100	3.55	-	21.68	0.4683	3.089	**1.053**	1.118	0.4670	0.4995
lpp	b95	1	95.0	0.8595	0	0	3.56	-	-	0.4630	3.065	**1.052**	1.095	0.4683	0.5000
lpp	**b**	**1**	**97.6**	**0.8853**	**0**	**0**	**3.61**	**-**	**-**	**0.4773**	**3.248**	**1.002**	**1.094**	**0.4788**	**0.5033**
pl p	b80	2	80.0	0.6043	1	0	-	3.07	-	2.9399	14.487	**0.596**	1.110	0.8593	0.5233
pl p	b85	2	85.0	0.7919	1	0	-	3.43	-	2.4473	15.046	**0.500**	1.098	0.9468	0.5178
pl p	b	2	86.3	1	1	0	-	3.83	-	2.1501	16.466	**0.409**	1.088	1.0525	0.5164
slp	b90Io	1	90.0	0.7267	0.8283	0	17.27	4.55	-	2.5248	75.281	**0.331**	1.103	2.1734	0.4794
slp	b95IO	1	96.2	0.6248	0.3924	0	16.25	4.98	-	1.4438	38.116	**0.294**	1.099	1.9768	0.4578
lps	b90IO	3	90.0	1.9292	0	3.9830	5.61	-	15.18	1.4161	23.263	**0.252**	1.093	1.7902	0.4254
lps	b95IO	3	95.0	1.9339	0	4.5230	5.62	-	15.17	1.4816	24.419	**0.235**	1.093	1.7881	0.4249
lps	b99IO	3	99.0	1.9336	0	4.9463	5.62	-	15.17	1.5344	25.282	**0.222**	1.093	1.7882	0.4250
slp	bIO	2	99.4	0.4323	0.2237	0	14.32	6.34	-	1.0467	21.473	**0.181**	1.088	1.8373	0.5341
sss	b90I	3	96.3	1.2420	0.3330	5.4510	22.42	20.00	18.05	3.1967	160.686	**0.076**	1.050	2.3326	0.4923
sps	b86IO	3	86.3	1.0000	0	1.0000	20.00	-	20.00	1.0750	43.001	**0.062**	1.050	2.7487	0.5164
ssp	b90o	2	91.2	0.9323	0.1000	0	19.32	20.00	-	0.7255	27.087	**0.052**	1.026	5.4994	0.5165
spp	b90	1	90.0	0.8226	0	0	18.23	-	-	0.4421	14.686	**0.044**	1.027	2.3687	0.4949
spp	b95	1	95.0	0.8595	0	0	18.60	-	-	0.4630	16.010	**0.041**	1.027	2.4460	0.5000
spp	b	1	97.6	0.8853	0	0	18.85	-	-	0.4773	16.964	**0.039**	1.027	2.5006	0.5033
sps	bIo	3	83.7	0.8441	0	1.0235	18.44	-	21.85	1.2129	41.247	**0.037**	1.050	3.1623	0.5331
lps	bIo	3	83.7	0.8441	0	1.0230	3.53	-	21.85	1.2126	7.895	**0.035**	1.119	3.1623	0.5331
sss	b99	1	99.0	1.8709	0.6930	7.1497	28.71	20.00	15.34	3.0645	252.583	**0.033**	1.050	4.7814	0.5768
sps	b98Io	3	98.4	0.6528	0	0.2549	16.53	-	25.32	0.6380	17.429	**0.031**	1.050	3.9715	0.5572
ssp	b94I	2	94.1	0.3000	0.1000	0	13.00	20.00	-	0.6423	10.854	**0.030**	1.038	6.3534	0.5372
sss	b	1	99.5	2.0821	1.0000	9.3816	30.82	20.00	14.80	3.6285	344.684	**0.029**	1.050	5.2859	0.5883
sss	b88IO	2	88.4	1.1990	1.8187	3.3349	21.99	20.00	18.34	5.4789	264.926	**0.024**	1.050	5.5108	0.5172
ssp	b90IO	2	90.0	0.8714	0.5343	0	18.71	20.00	-	1.7057	59.736	**0.022**	1.027	5.5051	0.5168
ssp	bIo	2	99.4	0.4323	0.2237	0	14.32	20.00	-	1.0467	21.473	**0.019**	1.035	5.7929	0.5341
psp	b	2	86.3	1	1	0	-	20.00	-	2.1500	86.000	**0.016**	1.000	5.4974	0.5164
Configuration	Sub-Class	Primary Pivot	Ξ'_{ex}	R	K_1	K_2	κ_1	κ_2	κ_3	Φ	β	Ψ	λ	M	n

Table D.6 Combined mechanism table sorted by Ψ

Configuration	Sub-Class	d_{Nmax}	C_1	C_2	C_3	D_{1equal}	D_{2equal}	D_{3equal}	D_{1min}	D_{2min}	D_{3min}	Sub-Class	Configuration
lpp	a90	26.04										a90	*lpp*
lpp	a95	26.57										a95	*lpp*
lpp	a99	26.90										a99	*lpp*
lpp	**a**	**26.96**										**a**	***lpp***
pl p	a80	19.11										a80	*pl p*
pl p	a85	21.34										a85	*pl p*
pl p	a90	24.03										a90	*pl p*
slp	a90I	26.28	1.00	4.82	-	1.00	119.69	-	1.00	1.07	-	a90I	*slp*
pl p	a	27.13										a	*pl p*
slp	a95Io	26.95	1.00	1.92	-	1.00	7.04	-	1.00	1.00	-	a95Io	*slp*
lps	a90	24.60	1.00	-	0.84	1.00	-	0.82	1.00	-	1.37	a90	*lps*
lps	a90IO	24.39	1.00	-	1.00	1.00	-	1.00	1.00	-	1.00	a90IO	*lps*
lps	a95I	23.63	0.79	-	1.00	0.50	-	1.00	1.00	-	1.00	a95I	*lps*
lps	a99I	23.10	0.68	-	1.00	0.32	-	1.00	1.00	-	1.00	a99I	*lps*
slp	a90IO	25.39	1.00	1.00	-	1.00	1.00	-	1.00	1.00	-	a90IO	*slp*
slp	a99IO	24.97	1.13	1.00	-	1.43	1.00	-	1.00	1.00	-	a99IO	*slp*
lps	a95IO	24.39	1.00	-	1.00	0.66	-	1.00	0.66	-	1.00	a95IO	*lps*
lps	a99IO	24.39	1.00	-	1.00	0.47	-	1.00	0.47	-	1.00	a99IO	*lps*
slp	aIo	23.23	1.71	1.00	-	2.54	1.00	-	0.51	1.00	-	aIo	*slp*
sss	a95I	25.93	0.340	0.289	1.000	0.039	0.022	1.000	0.997	0.895	1.000	a95I	*sss*
sss	a99	26.37	1.000	0.745	2.222	1.000	0.435	12.492	1.000	1.052	1.139	a99	*sss*
sps	a99I	26.67	1.00	-	0.52	1.00	-	0.14	1.00	-	0.98	a99I	*sps*
spp	a90	26.04										a90	*spp*
sps	a90IO	27.13	1.00	-	1.00	1.00	-	1.00	1.00	-	1.00	a90IO	*sps*
spp	a95	26.57										a95	*spp*
ssp	a95I	27.09	2.18	1.00	-	10.43	1.00	-	1.01	1.00	-	a95I	*ssp*
ssp	a99I	26.85	2.54	1.00	-	11.20	1.00	-	0.68	1.00	-	a99I	*ssp*
spp	a99	26.90										a99	*spp*
spp	a	26.96										a	*spp*
sss	a90IO	26.21	1.260	1.000	3.104	1.974	1.000	1.979	0.986	1.000	0.066	a90IO	*sss*
sps	aIO	26.77	1.74	-	1.00	1.31	-	1.00	0.25	-	1.00	aIO	*sps*
ssp	a90IO	26.43	1.33	1.00	-	2.00	1.00	-	0.84	1.00	-	a90IO	*ssp*
lps	aIo	26.77	9.07	-	1.00	6.86	-	1.00	0.01	-	1.00	aIo	*lps*
ssp	a95IO	27.12	2.09	1.00	-	2.00	1.00	-	0.22	1.00	-	a95IO	*ssp*
sss	a95IO	26.71	1.462	1.000	2.693	0.500	1.000	2.000	0.160	1.000	0.102	a95IO	*sss*
sss	a	22.82	1.000	1.332	7.099	1.000	1.832	33.744	1.000	0.775	0.094	a	*sss*
ssp	aIo	23.23	5.07	1.00	-	7.52	1.00	-	0.06	1.00	-	aIo	*ssp*
psp	a	27.13										a	*psp*
Configuration	Sub-Class	d_{Nmax}	C_1	C_2	C_3	D_{1equal}	D_{2equal}	D_{3equal}	D_{1min}	D_{2min}	D_{3min}	Sub-Class	Configuration
lps	b90I	39.44	1.00	-	0.12	1.00	-	0.00	1.00	-	0.98	b90I	*lps*
lpp	b90	39.47										b90	*lpp*
lps	b95I	39.66	1.00	-	0.13	1.00	-	0.00	1.00	-	0.73	b95I	*lps*
lpp	b95	39.68										b95	*lpp*
lpp	**b**	**39.79**										**b**	***lpp***
pl p	b80	36.46										b80	*pl p*
pl p	b85	39.24										b85	*pl p*
pl p	b	40.00										b	*pl p*
slp	b90Io	38.58	1.00	1.47	-	1.00	3.14	-	1.00	1.00	-	b90Io	*slp*
slp	b95IO	36.92	1.00	1.09	-	1.00	1.28	-	1.00	1.00	-	b95IO	*slp*
lps	b90IO	33.95	1.00	-	1.00	0.68	-	1.00	0.68	-	1.00	b90IO	*lps*
lps	b95IO	33.91	0.99	-	1.00	0.60	-	1.00	0.61	-	1.00	b95IO	*lps*
lps	b99IO	33.91	0.99	-	1.00	0.55	-	1.00	0.56	-	1.00	b99IO	*lps*
slp	bIO	30.18	1.47	1.00	-	1.98	1.00	-	0.63	1.00	-	bIO	*slp*
sss	b90I	39.35	0.589	0.381	1.000	0.148	0.055	1.000	0.724	0.996	1.000	b90I	*sss*
sps	b86IO	40.00	1.00	-	1.00	1.00	-	1.00	1.00	-	1.00	b86IO	*sps*
ssp	b90o	39.93	2.15	1.00	-	10.35	1.00	-	1.05	1.00	-	b90o	*ssp*
spp	b90	39.47										b90	*spp*
spp	b95	39.68										b95	*spp*
spp	b	39.79										b	*spp*
sps	bIo	39.60	1.40	-	1.00	1.16	-	1.00	0.42	-	1.00	bIo	*sps*
lps	bIo	39.60	7.33	-	1.00	6.05	-	1.00	0.02	-	1.00	bIo	*lps*
sss	b99	34.51	1.000	0.936	3.502	1.000	0.995	13.377	1.000	1.215	0.311	b99	*sss*
sps	b98Io	37.47	2.35	-	1.00	6.01	-	1.00	0.46	-	1.00	b98Io	*sps*
ssp	b94I	23.08	6.67	1.00	-	15.38	1.00	-	0.05	1.00	-	b94I	*ssp*
sss	b	32.44	1.000	1.041	4.338	1.000	1.541	19.533	1.000	1.365	0.239	b	*sss*
sss	b88IO	39.54	1.610	1.000	2.398	0.500	1.000	2.000	0.120	1.000	0.145	b88IO	*sss*
ssp	b90IO	39.74	2.30	1.00	-	2.00	1.00	-	0.17	1.00	-	b90IO	*ssp*
ssp	bIo	30.18	4.63	1.00	-	6.24	1.00	-	0.06	1.00	-	bIo	*ssp*
psp	b	40.00										b	*psp*
Configuration	Sub-Class	d_{Nmax}	C_1	C_2	C_3	D_{1equal}	D_{2equal}	D_{3equal}	D_{1min}	D_{2min}	D_{3min}	Sub-Class	Configuration

APPENDIX E GLOSSARY OF TERMS AND VARIABLES

α	The *stress factor,* a non-dimensionalized parameter where $\alpha = \frac{\gamma\zeta K_{\theta}\Delta\theta}{\rho}$. This parameter is used in the stress feasibility equation.
β	Non-Dimensionalized parameter in force feasibility equation where $\beta = \frac{\gamma K_{\theta}(R+1)^2\Phi}{\rho}$
Δy	Deflection normal to the CFM input displacement.
γ	PRBM characteristic radius factor
κ	Parameter used to relate moments of inertias between the different flexible segments. $\left(\kappa_i = \frac{\gamma_i\zeta_i K_{\theta_i}}{\rho_i}\right)$

λ	Length parameter used to calculate the actual length from the PRBM length where $l_{tot} = \lambda r_{tot}$. This parameter is mechanism dependent.
μ	Ratio of the small-length flexural pivot length over the associated PRBM length
Ω	A material parameter in the stress feasibility equation where $\Omega = \frac{S_y}{E}$
ψ	(Stiffness Intensity Factor) This parameter summarizes the stiffness at a given primary pivot stress level and mechanism size. This allows for comparisons in maximum stiffnesses between mechanisms.
Ψ	(Normalized Stiffness Intensity Factor) This parameter divides the stiffness intensity factor by the stiffness intensity factor of the *lpp* mechanims for the given sub-class. This normalizes the values with 1 being the highest.
ρ	Is either $\frac{1}{\gamma}$ for fixed-pinned beams or μ for small-length flexural pivots

ζ	Defines the ratio between the total PRBM length r_{tot} and a link length
Ξ	The original percent constant-force where the maximum force is divided by the minimum force.
Ξ'	Percent constant-force using the minimum and maximum known forces (no extrapolation).
Ξ'_{ex}	The extrpolated percent constant-force calculated by dividing the extraoplated force at zero displacement by the maximum force at full displacement.
A	A geometeric parameter in the stress feasibility equation where $A = \frac{c}{r_{tot}}$
C	Ratio of a flexible segment thickness to the primary pivot thickness.
CFEC	Constant-force electrical contact
CFM	Constant-force mechanism
Classification Varaibles	Those variables that dependent on the mechanism and are looked up in tables.

Configuration	Distiguishes between different possible flexible segment configurations.
Constraint Variable Value	Those variable values that are constrained by the design requirments.
Coupled Variables	Those variables that are shared between tow or more of the principal design equations.
D_{equal}	Ratio of a flexible segment width and the primary pivot width when thicknesses are equal.
D_{min}	Ratio of a flexible segment width and the primary pivot width when thicknesses are maximized.
d_{Nmax}	The maximum normal displacement percentage which allows for quick calculations of the maximum normal deflection.
Displacement Equaiton	Main equation used to determine the percent displacement when doing design of CFMs.
Force Design Equation	Main equation used to calculate the force of a CFM. Knowledge of the PRBM is not required to use this equation.

Force Feasibility	$F = \frac{\beta E I_1}{r_{tot}^2}$ Equation used to quickly calculate the force knowing only the cross section of the first flexible segment, the material properties, the configuraiton, and the total PRBM length.
Force Feasible Mechanism	Those mechanisms that are guaranteed to produce the needed force without violating the stress requirments. However, no guarantee is given that the flexible segment thicknesses will satisfy the design constraints.
Guaranteed Stress Feasbile	Those mechanisms that are guaranteed to procude the desired displacement in any part of the design space. However, no guarantee is given that the need force can be achieved.
In-plane Orientation	In this orientation, all motion takes place in the plane of fabrication. This requires that all link and flexible segment widths be the same.
Isolated Varaibles	Those variables that occur only in one of the three equations.
K_θ	PRBM stiffness coefficient
Known Variable Value	A variable value that is set by the design requirements.

M	Multiplier in the power curve fit of α.
n	Power in the power curve fit of α.
Out-of-plane Orientation	All motion is normal to the plane of fabrication. This requires that all link and flexible segment thicknesses be the same.
Principal Equations	The three primary equations required to design CFMs. These equations are combinations of the stress feasibility equation, force feasibility equation, and other equations developed.
Primary Pivot	The flexible pivot in the CFM with the highest stress.
Stress Design Equation	Main equation used to determine the stress within a CFM. Knowledge of the PRBM is not required to use this equation.
Stress Feasibility	$\alpha A \leq \frac{\Omega}{SF}$ Equation used to determine the stress feasibility of a given design.
Stress Feasible Mechanism	Those mechanisms that are capable of producing the desired displacement in part of the design space, but not capable in

	other parts of the design space. However, no guarantee is given that the need force can be achieved.
Sub-class	Distinguishes between different sets of constant-force parameters within a given class and configuration thus specifying a specific mechanism.
Unknown Variable Value	Those variables values that have no information given by the design requirements.